(2)

FINAL

Annual Report to the Air Force Office of Scientific Research

Nov. 1, 1990 - Jan. 31, 1992

DYNAMICS AND CONTROL OF TETHERED ANTENNAS/ REFLECTORS IN ORBIT

Contract No. F49620-90C-0009

Principal Investigator: Peter M. Bainum
Distinguished Professor of Aerospace Engineering
Dept. of Mechanical Engineering

Visiting Scholar: Tan Zhao Zhi
Dept. of Mechanical Engineering

Graduate Research Assistants: Li Zhong
Ph.D. Student
Dept. of Mechanical Engineering

Xiong Xiao Ou
Masters Student
Dept. of Mechanical Engineering

Howard University
School of Engineering
Washington, D.C. 20059

February 1992

Annual Report to the Air Force Office of Scientific Research

Nov. 1, 1990 - Jan. 31, 1992

DYNAMICS AND CONTROL OF TETHERED ANTENNAS/ REFLECTORS IN ORBIT

Contract No. F49620-90C-0009

Principal Investigator: Peter M. Bainum
Distinguished Professor of
Aerospace Engineering
Dept. of Mechanical Engineering

Visiting Scholar: Tan Zhao Zhi
Dept. of Mechanical Engineering

Graduate Research Assistants: Li Zhong
Ph.D. Student
Dept. of Mechanical Engineering

Xiong Xiao Ou
Masters Student
Dept. of Mechanical Engineering

Howard University
School of Engineering
Washington, D.C. 20059

February 1992

REPORT DOCUMENTATION PAGE

Form Approved
OMB No. 0704-0188

1. AGENCY USE ONLY (Leave blank)	2. REPORT DATE	3. REPORT TYPE AND DATES COVERED
	January 1992	Annual Report Nov. 1, 1990 - Jan. 31, 1992

4. TITLE AND SUBTITLE
Dynamics and Control of Tethered Antennas/Reflectors in Orbit

5. FUNDING NUMBERS
C-F49 620-90C-0009
2302/AS

6. AUTHOR(S)
Peter M. Bainum, Tan ZhaoZhi, Li Zhong, and Xiong Xiao Ou

7. PERFORMING ORGANIZATION NAME(S) AND ADDRESS(ES)
Howard University
Dept. of Mechanical Engineering
Washington, D.C. 20059

8. PERFORMING ORGANIZATION REPORT NUMBER

9. SPONSORING MONITORING AGENCY NAME(S) AND ADDRESS(ES)
Air Force Office of Scientific Research
AFSC/NA
Bolling Air Force Base, D.C. 20332- 6448

10. SPONSORING MONITORING AGENCY REPORT NUMBER

11. SUPPLEMENTARY NOTES

12a DISTRIBUTION AVAILABILITY STATEMENT
Approved for public release; distribution is unlimited.

12b. DISTRIBUTION CODE

13. ABSTRACT *(Maximum 200 words)*
A momentum exchange controller where the time rate of change of the flexible momentum relative to the rigid body motion is used as a part of a feedback control law for maneuvers and flexible vibration suppression is introduced. This control concept is applied to: (1) a model of a rigid hub (based) with a cantilevered flexible appendage undergoing a single axis maneuver; and (2) as a component of an adaptive feedback control strategy for the retrieval of an orbiting tethered antenna/reflector system. The optimal linear quadratic Gaussian (LQG) digital control of the orbiting tethered antenna/reflector system is analyzed. The flexibility of both the antenna and the tether are included in this high order system model. With eight point actuators optimally positioned together with tether tension modulation it is seen that the degree of controllability is very high. A method of measuring tether transverse motions is proposed and is required to guarantee system observability. An analytical formulation for the modelling of the solar radiation disturbance on the tethered antenna/reflector system is introduced. A control law based on tension modulation where the gains are based on the linear quadratic regulator theory is able to maintain satisfactory pointing accuracy for low and moderate altitude orbits under the influence of solar pressure. For the higher altitudes a combination of tether tension modulation together with active(actuator) control will be required.

14. SUBJECT TERMS	15. NUMBER OF PAGES
Dynamics and control; orbiting/reflector antenna systems; vibration suppression; solar pressure environmental disturbance torques	102
	16. PRICE CODE

17. SECURITY CLASSIFICATION OF REPORT	18. SECURITY CLASSIFICATION OF THIS PAGE	19. SECURITY CLASSIFICATION OF ABSTRACT	20. LIMITATION OF ABSTRACT
UNCLASSIFIED	UNCLASSIFIED	UNCLASSIFIED	UL

Summary

A momentum exchange controller where the time rate of change of the flexible momentum relative to the rigid body motion is used as a part of a feedback control law for maneuvers and flexible vibration suppression is introduced. This control concept is applied to: (1) a model of a rigid hub (base) with a cantilevered flexible appendage undergoing a single axis maneuver; and (2) as a component of an adaptive feedback control strategy for the retrieval of an orbiting tethered antenna/reflector system. The optimal linear quadratic Gaussian (LQG) digital control of the orbiting tethered antenna/reflector system is analyzed. The flexibility of both the antenna and the tether are included in this high order system model. With eight point actuators optimally positioned together with tether tension modulation it is seen that the degree of controllability is very high. A method of measuring tether transverse motions is proposed and is required to guarantee system observability. An analytical formulation for the modelling of the solar radiation disturbance on the tethered antenna/reflector system is introduced. A control law based on tension modulation where the gains are based on the linear quadratic regulator theory is able to maintain satisfactory pointing accuracy for low and moderate altitude orbits under the influence of solar pressure. For the higher altitudes a combination of tether tension modulation together with active (actuator) control will be required.

ACKNOWLEDGEMENT

This research has been conducted under the direction of Dr. Spencer Wu, Program Manager, Aerospace Sciences, Air Force Office of Scientific Research, Bolling AFB, Washington, D.C. Appreciation is expressed for the strong encouragement and useful comments provided by Dr. Wu during the course of this study. Thanks are also extended to Dr. Wu for making time available for an oral progress report by all participants during his visit to Howard University.

TABLE OF CONTENTS

1. INTRODUCTION

1.1 Feasibility of Concept based on Existing Work

In an earlier paper [1]* Yasaka suggested that a large Earth-oriented flexible orbiting antenna system culd be stabilized by using the gravity-gradient torques through the adjustment of the lengths of a series of tethers which would be connected between the feed panels and the reflector surface. The structural feasibility and a related stress analysis was presented. In a subsequent related treatment, Bainum and Kumar [2] investigated the dynamics and stability of an orbiting flexible shallow spherical shell with a dumbbell connected to the shell at its apex by a spring loaded double gimballed joint. In addition to providing a favorable composite moment of inertia distribution for gravitational stabilization, through the use of internal magnetics, (eddy current) passive damping can also be utilized. Subsequently, Bainum and Reddy [3] have considered the shape and orientation control of the shell antenna by including active control elements in addition to the passive damping. Numerical results verified the significant savings in fuel consumption that could be realized when the hybrid shell-dumbbell-actuator system is acting together as compared with the active thrusters operating alone.

In the first year's contractual effort [4] the basic equations of motion and related stability analyses for a tethered antenna

---

*For references sited in this report please refer to reference list at the end of ech chapter.

reflector system during station keeping were developed, and optimal tension control laws for inplane motion control were synthesized. It was concluded that additional types of control would be required for out-of-plane motion damping and also for providing shape control of the flexible antenna surface.

A comprehensive review of the literature related to the control of various classes of tethered satellite systems for deployment, station keeping, and retrieval was conducted. Both linear and nonlinear control laws were reviewed, with the conclusion that control laws based on optimal control theory offer the greatest potential for the proposed orbiting tethered reflector/antenna systems.[4]

The second year's research [5] concentrated on the use of active control thrusters to provide first order control for the roll/yaw motions of the shell and also the out-of-plane tether swing motion. Actuators would be positioned at the end of the rigid boom, through which the tether is deployed and connected to the shell, and also placed along the periphery of the shell. Additional thrusters mounted normal to the shell's largest surface could also be used in combination with tether tension modulation to ensure both orientation and antenna shape control.

Control laws were also developed that could be used for deployment of the tethered antenna system where the actual control gains could be adjusted in a piecewise adaptive manner depending on the difference between the commanded and true length and the mass of the deployed tether. A deployment strategy was also developed which could be adopted to an orbiting test scale model of the

system.[5] Finally, some preliminary results were presented for the defensive near-minimum time slewing maneuver of the antenna/reflector with the tether either fully retrieved or (assumed) separated. The two-point boundary value problem resulting from the application of Pontryagin's maximum principle was (numerically) solved by the quasilinearization algorithm.[5]

1.2 Relevance to SDI and Military Mutibeam Communications

Associated with the capability to orient a large flexible antenna/reflector type of device accurately while at the same time maintain the surface shape to within centimeters or even millimeters are many applications in both the military and civilian fields. For example, high energy beams can be generated by a power source and reflected from specific known points on the reflector surface to preselected targets. In the very important communications field, such an antenna surface can receive multibeam communication waves from electronic feed devices and transmit these to a variety of small mobile receivers to comprise strategic communication links during early, critical phases of an attack when larger, fixed land-based antennas would be far more vulnerable to observation/damage. Such devices could also be employed to transmit coded electronic mail rapidly over different communication channels.

1.3 Outline of the Research Reported

The second chapter introduces the concept of a momentum exchange controller where the time rate of change of the flexible

momentum of the system relative to the rigid body motion is used as a part of the feedback control law for maneuvers and vibration suppression. A particular example of a rigid central part connected to a pair of cantilevered flexible appendages, such as solar panels, is considered. Lyapunov stability techniques are used to obtain upper and lower bounds on the control law gains. With the presence of this type of feedback control, an additional independent control system acting on the flexible parts can be designed for further vibration suppression. A paper based on this research was presented at the AAS/AIAA Astrodynamics Specialist Conference, Durango, Co., Aug. 19-22, 1991.

The next chapter also uses the momentum exchange control technique as a part of an adaptive feedback control concept for the retrieval of the orbiting tether antenna/reflector system. The time rate of change of that part of the angular momentum due to the tether motion from the local vertical is used as a part of the feedback law for the antenna attitude control system. This is used in conjunction with an open-loop exponentially decreasing tether commanded length control during retrieval. The selection of the dimensionless control gains is based both on system stability considerations when the system is linearized about a given reference length, and on numerical simulation of the nonlinear time varying system. The feedback control gains are then adapted to the instantaneously changing tether length. This chapter is based on results presented in a paper at the Second Joint Japan/U.S.A. Conference on Adaptive Structures, Nagoya, Japan, Nov. 12-14, 1991.

Chapter 4 considers the optimal LQG (linear quadratic

Gaussian) digital control of the orbiting flexible tethered antenna system. The flexibility of both the tether as well as the antenna (shell) is included. A comprehensive computer simulation program is developed to also include the important effects of state measurement, plant and measurement noise, system controllability and observability. The LQG technique is employed to synthesize a controller with the Kalman filter to deal with measurement and plant noise in the presence of sampled data observations. The optimum number and location of the actuators are determined by means of the concept of degree of controllability and related numerical simulations. The results contained in Chapter 4 willl also be included in a paper accepted for presentation at the AAS/AIAA Space Flight Mechanics Meeting in Colorado Springs, Co., Feb. 24-26, 1992.

In the following chapter the effect of solar radiation pressure on the tethered antenna/reflector subsatellite system is considered. The solar radiation pressure is one of the dominant sources of disturbances, especially in the higher altitude orbits. One of the objectives of Chapter 5 is to develop the analytical formulations for the modelling of solar radiation disturbance torques on the tethered antenna subsatellite system. A second objective is to evaluate the effects of these disturbances (for station keeping operations) to determine at what altitude levels the tension control law is still able to maintain the required pointing accuracy, and to develop a hybrid compensation control strategy (involving tether tension plus some kind of actuators attached to the antenna) for the situations where the tension

modulation control alone can not meet the mission pointing accuracy. Papers based on this chapter (Chapter 5) have been offered for possible presentation at the 1992 AIAA/AAS Astrodynamics Conference, Hilton Head, S.C., Aug. 10-12, 1992 and also at The World Space Congress (IAF/COSPAR), Washington, D.C., Aug. 28-Sept. 5, 1992.

Chapter 6 summarizes some concluding remarks and suggestions for further continuing research.

Chapter 1 - References

1. Yasaka, Tetsuo, "The Structural Feasibility of a Gravity Stabilized Antenna," Acta Astronautica, Vol. 8, No. 5-6, 1981, pp. 689-701.

2. Kumar, V.K. and Bainum, P.M., "Motion of a Flexible Shallow Spherical Shell in Orbit," AIAA Journal, Vol. 20, No. 8, August, 1982, pp. 1113-1119.

3. Bainum, P.M. and Reddy, A.S.S.R., "On th Shape and Orientation Control of an Orbiting Shallow Spherical Shell Structure," IFAC/ESA Symposium on Automatic Control in Space, Noordwijkerhout, The Netherlands, July 5-9, 1982.

4. Bainum, Peter M., Liu Liangdong, Bai Jingwu and Li Zhong, "Dynamics and Control of Tethered Antennas/Reflectors in Orbit," Final Report: AFOSR Contract F 49620-89-C-002, Dept. of Mechanical Engineering, Howard University, Dec. 1989.

5. Bainum, Peter M., Liu Liangdong, Li Zhong, and Tan Zhao Zhi, "Dynamics and Control of Tethered Antennas/Reflectors in Orbit," Final Report AFOSR Contract F49620-90C-0009, Dept. of Mechanical Engineering, Howard University, Dec. 1990.

2. MOMENTUM EXCHANGE: FEEDBACK CONTROL OF FLEXIBLE SPACECRAFT MANEUVERS AND VIBRATION

The momentum exchange controller in which the time rate of change of the flexible momentum relative to the rigid body motion is used as a part of the feedback control law for maneuvers and vibration suppression of flexible systems is introduced. A particular model of a rigid hub (base) with a cantilevered flexible appendage undergoing a single-axis maneuver is considered. The feedback control on the hub includes the rigid body motion and the time rate of change of that part of the flexible momentum resulting from flexible vibration. The lower and upper bounds of the control law for system Lyapunov stability are obtained, and the relationship of the control law with the energy Lyapunov test function is established. With the presence of this feedback control, an additional independent flexible control system acting on the flexible parts can be designed for further vibration suppression. This hybrid control system can be applied to both stationkeeping and large angle maneuvers. Both analytical and numerical results are presented to show the theoretical and practical merit of this approach.

2.1 Introduction

The control of flexible systems usually requires the controller to provide the control effort for maneuvering or targeting of the flexible systems/subsystems (such as antennas and telerobots) with the simultaneous vibration suppression. For instance, one of the major problems with robotic manipulator systems is the assembly time lost while waiting for the vibration suppression of the end of the manipulator arm.

The mathematical modelling of flexible systems involves the coupling of finite and infinite ordered mathematical subsystems-the rigid body motions described by ordinary differential equations and the flexible motions described by partial differential equations. The control objective is to maneuver the rigid body and suppress the flexible vibration simultaneously for targeting, or to suppress both motions for stationkeeping. Most previous approaches to this problem resorted to the discretization of the continuous systems into finite dimensional systems as the first stage of the process for control law design. It is commonly recognized that the discretization procedure inevitably involves modeling errors and control spillover issues. Also, since the frequencies of the flexible vibration are usually much higher than those of rigid body motions, the coupling of these two motions will result in the stiffening of the system differential equations. As a consequence, the numerical solutions to the traditionally optimal approaches, such as minimizing a quadratic cost functional or minimum time bang-bang control, are usually difficult to solve because of the inherent nonlinearity and stiffness of the resulting differential equations. In addition, the algorithms and control laws are usually sensitive to modeling errors and may lack robustness.

In order to suppress the flexible vibrations, certain quantities that contain the information about the flexible motion of the distributed systems are needed for the feedback controller. What are these quantities for continuous mechanical systems? From the viewpoint of dynamics, the rigid body motion and the flexible motion interact with each other by means of momentum exchange during maneuvering; hence, that part of the flexible momentum resulting from the flexible motion is expected to contain the information about the flexible vibration and can be used as a part of the feedback law. The main purpose of the present paper is to introduce the so-called momentum exchange control concept which is illustrated by the application to a particular model of a rigid hub with a flexible appendage beam undergoing a single-axis maneuver. The proposed control acting on the hub includes the feedback of the rigid body motion and the time rate of change of the flexible momentum of the beam (combination of the flexible modes). We will strictly prove the stability of this control law by using a Lyapunov test function, and the lower and upper bounds of the control law for system Lyapunov stability will be obtained. Many interesting and important implications of this control concept will be demonstrated with the development.

Concerning the related research, attention should be directed to recent impressive work by Junkins, et al[1,2], in which the maneuver and vibration suppression of a rigid hub with flexible appendage beams was considered, and the proposed control law involved the feedback of the combination of the root shear and bending moment of the beam which theoretically was equivalent to the time rate of change of the angular momentum of the beam - rigid plus flexible momentum. The idea was innovative and the resulting control was easily implemented from the viewpoint of measurement; however, from the viewpoint of the present investigation, it appears that the inclusion of the rigid momentum of the beam into the feedback control law is redundant and may corrupt the information about the flexible vibration with possible degradation of the system performance. This argument is further supported by the fact that there is no finite upper bound limit of the control gains required for system stability in Ref.[1]. The correspond-

ing version of the development of Junkins' control law is given in Appendix A for the purpose of comparison.

Another aim of the present paper is to design an additional independent flexible feedback control system for further vibration control. Independent flexible feedback control means that the feedback of this control system does not depend either upon the open - loop rigid body maneuver strategy or on the precalculated reference flexible motion; the feedback depends only on the instantaneous flexible displacements and velocities. Baruh and Siverberg first suggested separating the maneuver and vibration control problem[3]. It was proposed to suppress the vibrations by the natural modal control which did not affect the rigid body maneuvers in the sense that the control forces conserve the linear and angular momentum of the rigid body motion.

Together with the presence of the control acting on the rigid hub in the current paper, additional natural modal control acting on the flexible beam for further vibration suppression will also be employed. This hybrid control system is said to be independent in the above sense, and it will be shown that the system stability is guaranteed as long as the flexible control forces or torques are energy-dissipating.

In summary, the objectives of this paper are to: (1) present a kind of momentum exchange feedback control concept and prove the system stability by the Lyapunov direct method; (2) design an additional independent flexible control system for further vibration control; (3) apply this hybrid control system to the large angle maneuver problem of the flexible system; and (4) demonstrate the feasibility and practical merit of this approach by numerical simulation.

2.2 Momentum Exchange Feedback Control

A rigid hub (base) with a cantilevered flexible appendage is considered. The appendage is considered to be a uniform flexible beam, and the shear deformation and distributed rotary inertia are neglected. The beam is assumed to undergo small deformations so that linear elastic theory can be applied. The axial deformation is also neglected. Motion is restricted to the horizontal plane, and, at this stage of development, only a control torque acting on the hub is considered.

With reference to Fig. 1, the position vector of a differential element, dm, in the undeformed body-fixed frame, can be expressed as

$$\underline{r} = x\,\underline{i} + y\,\underline{j} \qquad (1)$$

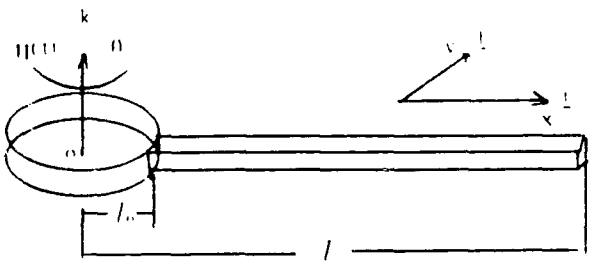

Fig. 1

The inertial velocity of dm can be obtained as:

$$\dot{\underline{r}} = -y\,\dot{\theta}\,\underline{i} + (x\,\dot{\theta} + \dot{y})\,\underline{j} \qquad (2)$$

Therefore, the total inertial angular momentum with respect to point O can be written as:

$$\underline{H} = I_h \dot{\theta}\, \underline{k} + \int_{l_0}^{l} [\, x(\dot{y} + x\dot{\theta}) + y(-\dot{\theta})\,]\, dm\, \underline{k}$$

$$= [\,(I_h + I_b)\dot{\theta} + \int_{l_0}^{l} \rho(x\dot{y} + y^2\dot{\theta})\, dx\,]\, \underline{k} \qquad (3)$$

where

I_h is the moment of inertia of the rigid hub w.r.t. the point O.

$I_b = \int_{l_0}^{l} \rho x^2\, dx$ is the moment of inertia of the undeformed beam.

That part of the angular momentum associated with the beam's flexible motion is denoted $H_f = \int_{l_0}^{l} \rho(x\dot{y} + y^2\dot{\theta})\, dx$, and is called the flexible momentum of the beam.

After applying the Euler-Newtonian equation of motion, one can obtain the rotational motion equation for the rigid body motion as:

$$(I_h + I_b)\ddot{\theta} + \frac{d}{dt} H_f = u(t) \qquad (4)$$

where u(t) is the control torque acting on the hub.

The partial differential equation governing the elastic vibration of the beam can be written as:

$$\rho\left(\frac{\partial^2 y}{\partial t^2} + x\frac{d^2\theta}{dt^2}\right) + EI\frac{\partial^4 y}{\partial x^4} = 0 + \text{H.O.T.} \qquad (5)$$

The H.O.T. denotes higher order terms which include other known effects [such as rotational stiffening ($y\dot{\theta}^2$) , shear deformation, etc.]. The fundamental development given here does not consider these higher order terms.

The boundary conditions on Eq.(5) are

$$\text{at } x = l_0 \qquad y(t, l_0) = \frac{\partial y}{\partial x}\Big|_{x=l_0} = 0$$

$$\text{at } x = l \qquad \frac{\partial^2 y}{\partial x^2}\Big|_{x=l} = \frac{\partial^3 y}{\partial x^3}\Big|_{x=l} = 0 \qquad (6)$$

A feedback control law for stationkeeping is introduced as:

$$u(t) = -k_1\theta - k_2\dot{\theta} - \gamma\frac{d}{dt} H_f \qquad (7)$$

The purpose of the first two feedback terms in (7) is straight-forward, providing the feedback control for the rigid body motion of the system; the last term in (7) is the feedback of the time rate of change of the flexible momentum of the beam and involves nonlinear output of the flexible motions.

Note that the form of this feedback control is different from that presented in Junkins, et al[1,2], where the control involved the feedback of both the root shear and bending moment of the beam, and the combination of these moments was equal to the time rate of change of the angular momentum of the beam: rigid plus flexible momentum.

However, the selection of the Lyapunov function for system stability here is similar to that in Ref.[1]; the slight difference lies in the first term of the Liapunov function. The Liapunov test function ("error energy") is taken as the following form:

$$V = \frac{1}{2} a_1 (I_h + I_b) \dot{\theta}^2 + \frac{1}{2} a_2 \theta^2 + \frac{1}{2} a_3 [\int_{l_a}^{l} \rho (\frac{\partial y}{\partial t} + x \dot{\theta})^2 dx + \int_{l_a}^{l} EI (\frac{\partial^2 y}{\partial x^2})^2 dx] \qquad (8)$$

The first term is the kinetic energy of the rigid body motion of the system; the second term $a_2 \theta^2$ "the torsional spring energy" is added to make the final state $(\theta, \dot{\theta}, y, \frac{\partial y}{\partial t})$ = (0,0,0,0) be the global minimum of V; the third term is the kinetic and potential energy of the beam. The weighting coefficients a_i are included to allow relative emphasis upon the three contributors to the "error energy" of the system.

It is obvious by inspection that imposing $a_i \geq 0$, guarantees that $V \geq 0$, and that the global minimum of V = 0 occurs only at the zero state. Differentiation, substitution of the equations of motion (5) and boundary conditions (6), and some calculus manipulations lead to

$$\dot{V} = a_1 (I_h + I_b) \dot{\theta} \ddot{\theta} + a_2 \theta \dot{\theta} + a_3 \dot{\theta} EI (l_a \frac{\partial^3 y}{\partial x^3} \Big|_{x=l_a} - \frac{\partial^2 y}{\partial x^2} \Big|_{x=l_a}) \qquad (9)$$

Furthermore, for the rigid hub, we have

$$I_h \ddot{\theta} = u - EI (l_a \frac{\partial^3 y}{\partial x^3} \Big|_{x=l_a} - \frac{\partial^2 y}{\partial x^2} \Big|_{x=l_a}) \qquad (10)$$

Upon substituting (4), (7), and (10) into (9), one can obtain

$$\dot{V} = \{ [a_2 - k_1 (a_1 + \frac{a_3 I_b}{I_h + I_b})] \theta - k_2 (a_1 + \frac{a_3 I_b}{I_h + I_b}) \dot{\theta} - [(a_1 - \frac{a_3 I_h}{I_h + I_b}) + \gamma (a_1 + \frac{a_3 I_b}{I_h + I_b})] \frac{d}{dt} H_f \} \dot{\theta} \qquad (11)$$

In order to meet the requirement that $\dot{V} \leq 0$ to guarantee stability, two of the coefficients in (11) are set to zero:

$$a_2 - k_1 (a_1 + \frac{a_3 I_b}{I_h + I_b}) = 0 \qquad (12)$$

$$(a_1 - \frac{a_3 I_h}{I_h + I_b}) + \gamma (a_1 + \frac{a_3 I_b}{I_h + I_b}) = 0 \qquad (13)$$

In this case, $\dot{V}$ becomes

$$\dot{V} = -k_2\left(a_1+\frac{a_3 I_b}{I_h+I_h}\right)\dot{\theta}^2 \le 0 \quad (\text{if } k_2 \ge 0) \tag{14}$$

Eqs.(12-14) lead to the following control gain requirements:

$$k_2 \ge 0 \tag{15}$$

$$k_1 = \frac{a_2(I_h+I_b)}{a_3 I_h + a_1(I_h+I_h)} \ge 0 \tag{16}$$

$$\gamma = \frac{a_3 I_h - a_1(I_h+I_b)}{a_3 I_b + a_1(I_h+I_h)} \tag{17}$$

Since $a_i \ge 0$, it can be easily proven that

$$-1 \le \gamma \le \frac{I_h}{I_b} \tag{18}$$

and $\gamma = -1$ when $a_3 = 0$; $\gamma = I_h / I_b$ when $a_1 = 0$.

Thus a finite lower and upper bound restricts the size of the control gain, ν. It should be noted that there was no such finite upper bound limit in Ref.[1,2]. Fig.2 shows γ as a function of a_3 / a_1.

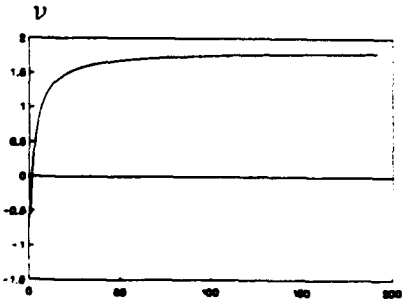

Fig. 2 ν as a function of a_3/a_1

Now attention is directed to the significant physical meaning of this feedback control law. According to Eq.(8), a_1/a_1 corresponds to the relative contribution of the flexible motion and the rigid body motion to the system error energy. When $a_1=0$ which corresponds to $\gamma=-1$, the " error energy " Lyapunov function does not contain the flexible energy term. In other words, the emphasis is totally put on the control of the rigid body motion. For the case where $\nu=-1$ it can be seen from Eqs.(4) and (7) that the effect of the flexible momentum, H_f, is removed from the closed-loop rigid body motion equation. Thus, the controller completely compensates for the flexible motion and the rigid body motion is not disturbed by the flexible vibration. Here a two-lumped mass beam model is used to approximate the continuous beam (Fig.3); however, the theoretical development and the validation of the results do not depend on the discretization procedure. Fig.4 and Fig.5 show the transient responses of the rigid body motion and the flexible motion, respectively, wherein the point 2 is the outermost lumped mass. The three cases considered are: $\nu=-1$, maximum emphasis on the rigid body motion (complete compensation for the flexible motion); $\nu=0$, no feedback of the flexible momentum; $\nu=I_h/I_b=1.83$, maximum emphasis on the flexible motion. It can be seen that with the increase of ν (larger relative emphasis on the suppression of the flexible motion) the dissipation of the flexible vibrations is better, and that the rigid body motion is subjected

to more disturbance, but the disturbance is not so large as to degrade the rigid body motion seriously. Therefore, in practical applications the control gain can be selected according to the requirement for the rigid body motion and the flexible vibration suppression, and it is a kind of trade-off. The selection of the control gain can be further enhanced by combining some optimum criteria.

Also, it should be noted that bounded restrictions for the gain ν are only sufficient conditions for system stability; however, from the present simulation, it is seen that these restrictions are close to the necessary conditions for system stability, especially the lower bound condition. Fig.6 and Fig.7 show that when the ν exceeds the lower bound the flexible motion becomes unstable and vice versa, when the ν exceeds the upper bound the rigid body motion diverges.

The system performance will generally depend on the ratio I_h / I_b. Fig. 8 and Fig. 9 show the system responses corresponding to three different ratios. It is seen that if this ratio increases, the flexible vibration will be usually easier to be suppressed and the rigid body motion will also decay more quickly with a little bit larger overshoot at the beginning. Also, from the simulation results, it is seen that this control law is robust in the presence of other unmodelled factors and modelling errors, and the robustness will degrade when the control gain ν approaches its boundaries.

2.3 Independent Flexible Control for Elastic Vibration

In Section II, it has been demonstrated that the feedback controller located on the rigid part of the spacecraft can perform the maneuver and simultaneous vibration suppression, and the system stability is guaranteed as long as the control law gains are within a certain range. However, it is of interest to further control and suppress the flexible vibration while the spacecraft is going through large angle rotations and large translations. To achieve this, another independent flexible control system acting on the flexible appendage is proposed.

Baruh and Silverberg[3] proposed a natural modal control for the independent elastic control system. They have proven that the natural control forces conserve the linear and angular momentum of the spacecraft and, therefore, do not appear on the right-hand side of the rigid body equations. However, the rigid body motion is still affected by the flexible motion via the kinematic and dynamic coupling which is sometimes very important. With the feedback control presented in Section II, it will be proved that the system stability is guaranteed as long as the elastic modal control system is an energy-dissipating system. To prove this, it is assumed that u_e is the feedback natural modal control on the flexible appendage; hence, u_e can be written as

$$u_e = \Sigma \phi_r f_r \qquad (19)$$

where ϕ_r is the rth natural modal shape corresponding to the flexible motion and f_r is the corresponding modal control force which can be designed in the modal space using various methods, such as optimal LQR, pole assignment, or velocity control.

In this case, Eq.(5) becomes

$$\rho\left(\frac{\partial^2 y}{\partial t^2} + x\frac{d^2\theta}{dt^2}\right) + EI\frac{\partial^4 y}{\partial x^4} = u_e \qquad (20)$$

The Lyapunov function is taken the same as (9). Using the orthogonality relation of the natural modal control (see details in Ref.[3]), and after similar manipulations, the derivative of V can be obtained as

$$\dot{V} = \text{right-hand side of Eq.(14)} + \int_0^l \rho \dot{y}\, u_e dx \qquad (21)$$

Therefore, if

$$\int_0^l \rho \dot{y}\, u_e\, dx \le 0 \qquad (22)$$

which means the control forces are energy-dissipating, then $\dot{V} \le 0$ and the system is stable.

Note that truncation of natural modes (finite control) does not change the discussion here. However, in reality it is almost impossible to obtain the exact natural mode shapes which are usually approximated by discretizing the continuous system model; the process of discretization inevitably introduces natural control errors. From the simulation results here, the momentum exchange control law is robust and can endure these errors induced from approximating the natural modal shapes. The simulation results show that the addition of this elastic control system further suppresses the elastic vibration and improves the system responses (Figs.10-11).

2.4 Large Angle Maneuvers

For large angle maneuvers, a reference open-loop rigid body maneuver is adopted, denoted by the subscripts as $\{\theta_r(t), \dot{\theta}_r(t), \ddot{\theta}_r(t), u_r(t)\}$ satisfying

$$(I_h + I_b)\ddot{\theta}_r = u_r(t) \qquad (23)$$

and the prescribed boundary conditions. The variables without subscripts represent the actual solutions to the system equations (4), (7), and (20).

The tracking control law takes the following form:

$$u(t) = u_r - k_1(\theta - \theta_r) - k_2(\dot{\theta} - \dot{\theta}_r) - \gamma\frac{d}{dt}H_r \qquad (24)$$

The "error energy" Lyapunov function is modified as

$$V = \frac{1}{2}a_1(I_h + I_b)(\dot{\theta} - \dot{\theta}_r)^2 + \frac{1}{2}a_2(\theta - \theta_r)^2 + \frac{1}{2}a_3\left\{\int_0^l \rho\left[\frac{\partial y}{\partial t} + x(\dot{\theta} - \dot{\theta}_r)\right]^2 dx + \int_0^l EI\left(\frac{\partial^2 y}{\partial x^2}\right)^2 dx\right\} \qquad (25)$$

The same manipulations as in Sect. II lead to

$$\dot{V} = \{[a_2 - k_1(a_1 + \frac{a_3 I_b}{I_h + I_b})](\theta - \theta_r) - k_2(a_1 + \frac{a_3 I_b}{I_h + I_b})(\dot{\theta} - \dot{\theta}_r)$$

$$-[(a_1 - \frac{a_3 I_h}{I_h + I_b}) + \nu(a_1 + \frac{a_3 I_b}{I_h + I_b})]\frac{d}{dt}H_f\}(\dot{\theta} - \dot{\theta}_r) + a_3\int \rho \dot{y}\, u_b\, dx - a_3\int \rho x \dot{y}\, dx\, \ddot{\theta}_r \qquad (26)$$

Again, the tracking control laws are subjected to the same requirements as in (15), (16), and (17). In this case,

$$\dot{V} = -k_2(a_1 + \frac{a_3 I_b}{I_h + I_b})(\dot{\theta} - \dot{\theta}_r)^2 + a_3\int \rho \dot{y}\, u_b\, dx - a_3\int \rho x \dot{y}\, dx\, \ddot{\theta}_r \qquad (27)$$

in which the first term is semi-negative definite; the second term is negative definite if the flexible control force is energy-dissipating; and the sign of the third term is generally varying. Therefore, as a whole, we cannot say the $\dot{V}$ is negative. In effect, the system has continuous inputs and the flexible vibration will be excited during large angle maneuvers. However, it is hoped that with this hybrid control the flexible vibration will be suppressed and that bounded-input/bounded-output viewpoint of stability can be established.

It is not the purpose to discuss the open-loop maneuver strategy here. A reveiew about this subject can be found in Ref.[4]. For the purpose of demonstration, a minimum-time maneuver strategy which is a bang--bang law is considered. It is recognized that a minimum-time maneuver bang--bang law will excite the flexible vibrations excessively, and it is intentionally used here to show the effectiveness of the proposed hybrid feedback control.

For quick large angle maneuvers, k_1 , k_2 are usually taken to be zero. Notice that in this case the remaining feedback term $(-\nu\frac{d}{dt}H_f)$ does not depend on the open-loop maneuver strategy and the precalculated corresponding reference flexible motion. The results of a 90 degree minimum-time maneuver are shown in Figs. 12-14. It is apparent from Fig. 14 that the deflection of the outermost lumped mass (point 2) is reduced by almost half when the flexible momentum is included as a feedback term in the tracking control law.

2.5 Conclusion

A kind of momentum exchange control law for maneuvers and vibration suppression of flexible systems, wherein the time rate of change of the flexible momentum is used as a part of the feedback control law, has been presented. The theoretical analysis for system stability by using a Lyapunov function is rigorous without resort to the disctretization of the continuous system, and the lower and upper bounds of the control gains for system stability have been obtained. For further vibration suppression, the natural

modal flexible control system is used in conjunction with the momentum exchange controller. This hybrid control system has also been applied to the large angle maneuver of the flexible system in which the minimum-time open-loop maneuver strategy is used. Simulation results have shown the effectiveness of this control system for both stationkeeping and minimum-time maneuvers.

This study is interesting and significant for understanding the behavior and control of distributed mechanical systems. It is noteworthy to see that just the single output feedback of the time rate of change of the flexible momentum contains enough information for the controller to suppress the vibration of continuous systems (infinite order systems). Also, the momentum exchange control law tends to be of a nonlinear form of the flexible displacements. This study has demonstrated the prospect and efficacy of using nonlinear control in some specific systems such as mechanical systems. Another key point is the usefulness of Lyapunov functions in the control problems of distributed systems.

References

1. J. L. Junkins, Z. Rahman, and H. Bang, "Near-Minimum-Time Maneuvers of Flexible Vehicles: A Liapunov Control Law Design Method". AIAA Aerospace Science Meeting, Reno, Nevada, January, 1990, AIAA 90-0663.

2. H. Bang and J. L. Junkins, "Liapunov Optimal Control Laws for Flexible Structures Maneuver and Vibration Control", AAS/AIAA Spaceflight Mechanics Meeting, Houston, Texas, February 11-13,1991, AAS 91-143.

3. H. Baruh and L. Silverberg, "Maneuver of Distributed Spacecraft", AIAA Guidance and Control Conference, Seattle, Washington, Aug. 1984, AIAA Paper 84-1952.

4. G. Singh, P. T. Kabamba, and N. H. McClamroch, "Planar, Time-Optimal, Rest-to-Rest Maneuvers of Flexible Spacecraft", Journal of Guidance and Control, Vol.12, No. 1, Jan-Feb. 1989, pp. 71-81.

Apendix A. A Comparison of Junkins' Control Law with the Present Law

In Ref. [1,2], Junkins, at el, presented a Liapunov control law design for the maneuver and vibration suppression of flexible systems. The model considered was a rigid hub with flexible appendage beams undergoing a single axis maneuver, and each beam had a finite tip mass. For easy comparison, only one appendage and no tip masses are adopted in the following development of Junkins' control law. In terms of the notations of Ref.[1], the system equations of motion are:

$$I_h \frac{d^2\theta}{dt^2} = u + (M_o - S_o l_o) \tag{28}$$

$$-(M_o - S_o l_o) = \int_{l_o}^{l} \rho x \left(\frac{\partial^2 y}{\partial t^2} + x \frac{d^2\theta}{dt^2} \right) dx \tag{29}$$

$$\rho \left(\frac{\partial^2 y}{\partial t^2} + x \frac{d^2\theta}{dt^2} \right) + EI \frac{\partial^4 y}{\partial x^4} = 0 \quad + HOT \tag{30}$$

where (M_o, S_o) denotes the bending moment and the shear force, at the root of the beam, respectively, and (30) satisfied the same boundary conditions as (6)

After substitution of (29) into (28), one can obtain

$$(I_h + I_b) \ddot{\theta} + \frac{d}{dt} H_f = u(t) \tag{31}$$

H_f is the flexible momentum of the beam.

The control law of Ref.[1] is taken as the form:

$$u = -[g_1 \theta + g_2 \dot{\theta} + g_3 (M_o - S_o l_o)] \tag{32}$$

After substitution of (29) into (32), the control law can be rewritten as

$$u = -[g_1 \theta + g_2 \dot{\theta} + g_3 (I_h \ddot{\theta} + \frac{d}{dt} H_f)] \tag{33}$$

Notice this control law is different from (7) in that the third term of (33) involves the extra time rate of change of the rigid momentum of the beam.

In order to show the difference, we use the same Lyapunov function (8) as the test function. In this case, the same manipulations as in Sect. II lead to the following requirements for the control gains:

$$g_2 \geq 0$$

$$g_1 = \frac{a_2[I_h + (1+g_3)I_b]}{a_3 I_h + a_4(I_h + I_b)}$$

$$g_3 = -1 + \frac{a_3 I_h}{a_4(I_h + I_b)} \qquad (34)$$

In this case, the derivative of the Lyapunov function

$$\dot{V} = -\frac{a_4(I_h + I_b)}{I_h}\dot{\theta}^2 \qquad (35)$$

From (34),

$$g_3 \geq -1 \quad \text{and without finite upper bound}$$

Also, from (34) and (35), it is seen that if a_4 is fixed and if a_3 is increased (means the increase of the relative contribution of the flexible motion to the error energy Lyapunov function), the gain g_3 will become large; however, the $\dot{V}$ is unchanged. This means physically that increasing the control gain g_3, unlike increasing the control gain g_2, will not automatically increase the suppression of the flexible motion. Therefore, it is concluded that the inclusion of the rigid momentum into the feedback control law is not necessary and may corrupt the feedback information with possible degradation of the system performance.

It is easily seen from Eq.(29) that the combination of the root shear and bending moment is equal to the time rate of change of the rigid momentum plus the flexible momentum of the beam. Therefore, the realization of the current proposed control law is not difficult; the flexible momentum feedback term can be realized by measuring the root shear force, root bending moment, and the angular acceleration of the hub.

Table 1 Spacecraft Dimensions, Appendage Material

Radius of the rigid central body, l_0	1.00 m
Length of the appendage, l	20.00 m
Appendage material stiffness, EI	1500.00 N-m ^{2}
Appendage material density, ρ	0.04096 kg/m
Mass of the rigid hub	400.00 kg
Total rotational inertia, I_h+I_b	309.1863 kg-m^2
Inertia ratio, I_h/I_b	1.83

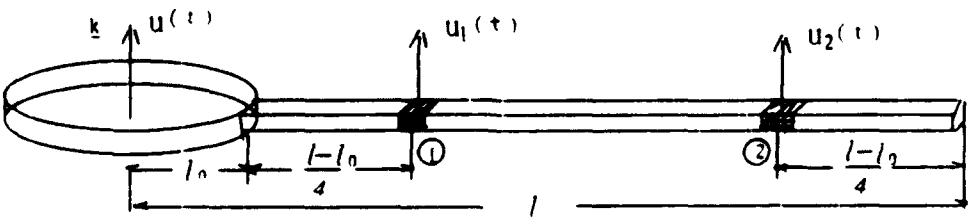

Fig. 3 Lumped-Mass Model for Numerical Simulations

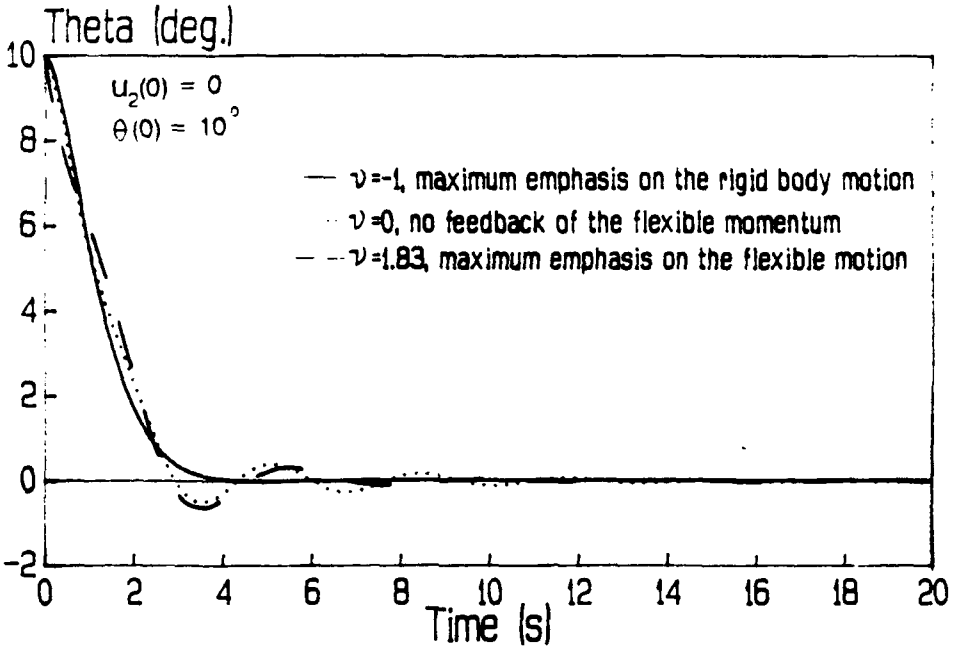

Fig. 4 Rigid Body Rotation Responses in Stationkeeping under Different Stable Control Laws

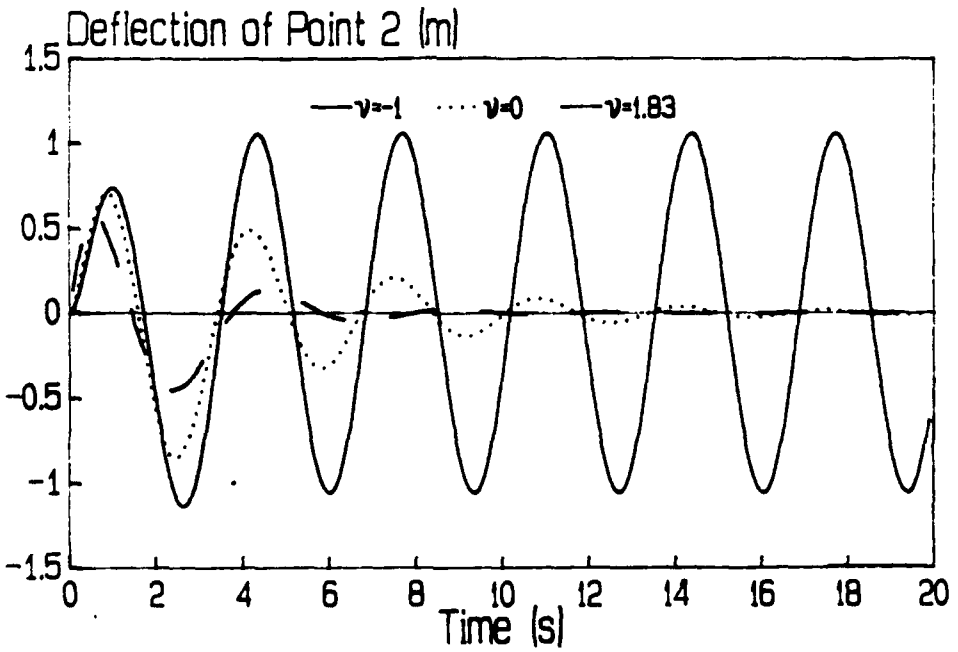

Fig. 5 Flexible Vibration Responses in Stationkeeping under Different Stable Control Laws (IC's the same as in Fig.4)

Note: $k_1 = 618$ and $k_2 = 773$ in Figs. 4–11 and $k_1 \sim k_2 = 0$ in Figs. 12–14.

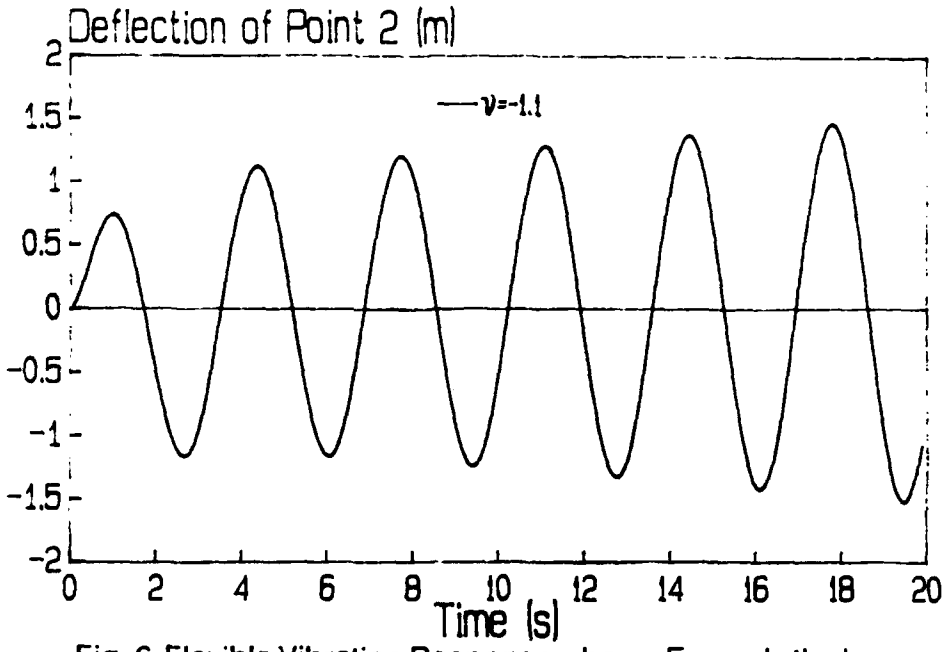

Fig. 6 Flexible Vibration Response when ν Exceeds the Lower Bound of Stability Range (IC's the same as in Fig 4)

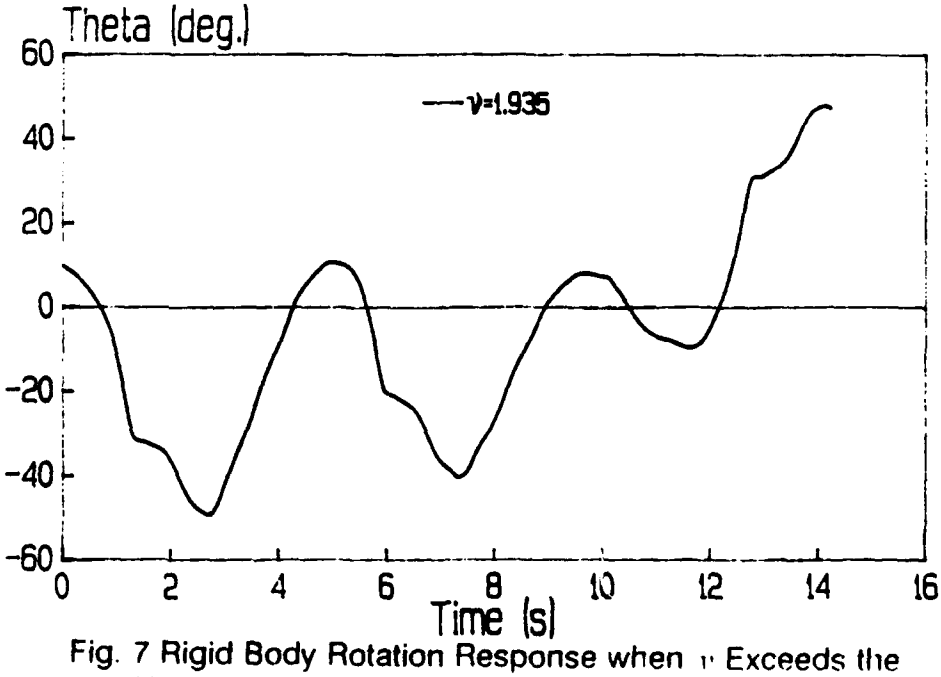

Fig. 7 Rigid Body Rotation Response when ν Exceeds the Upper Bound of Stability Range (IC's the same as in Fig 4)

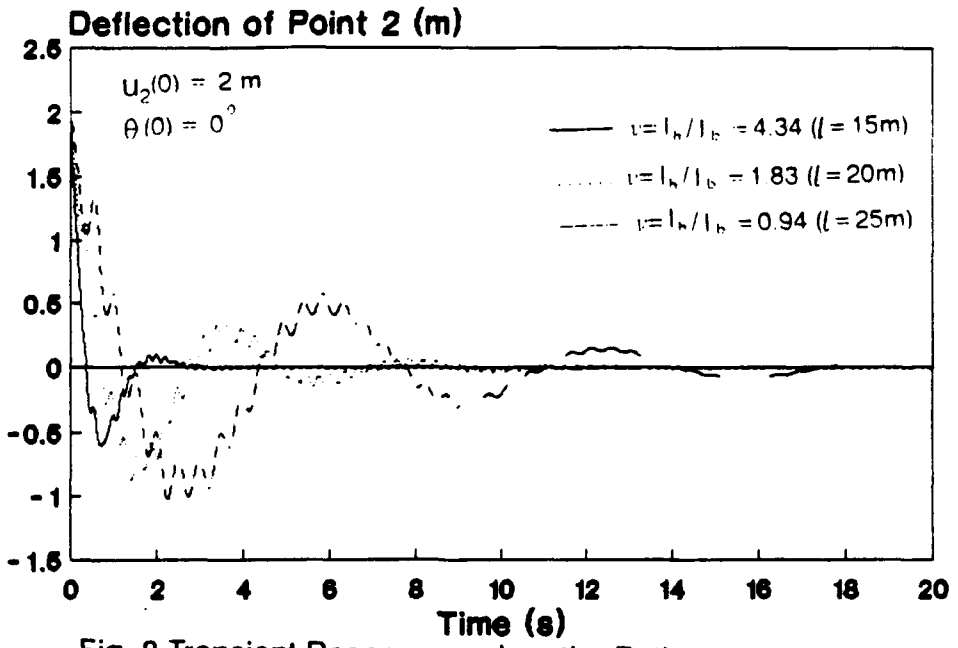

Fig. 8 Transient Responses when the Ratio I_h / I_b Changes

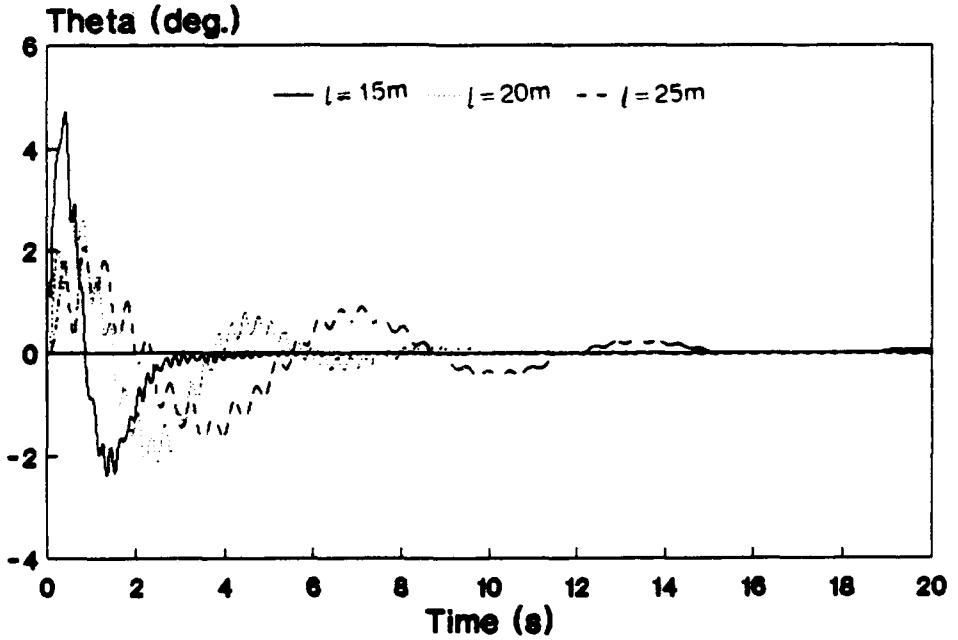

Fig. 9 Transient Responses when the Ratio I_h / I_b Changes
(IC's the same as in Fig.8)

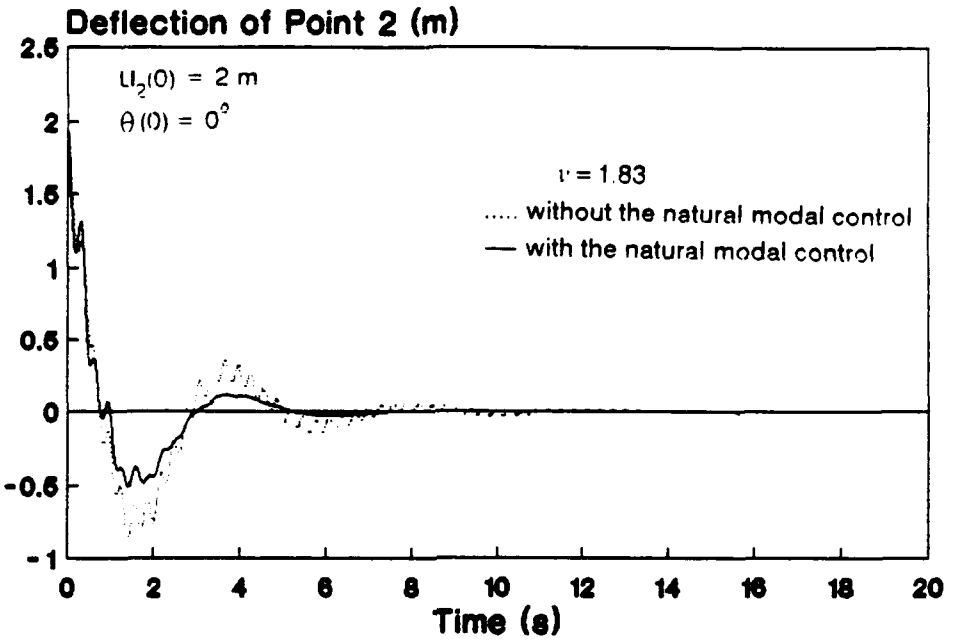

Fig. 10 Transient Responses with and without the Natural Modal Control

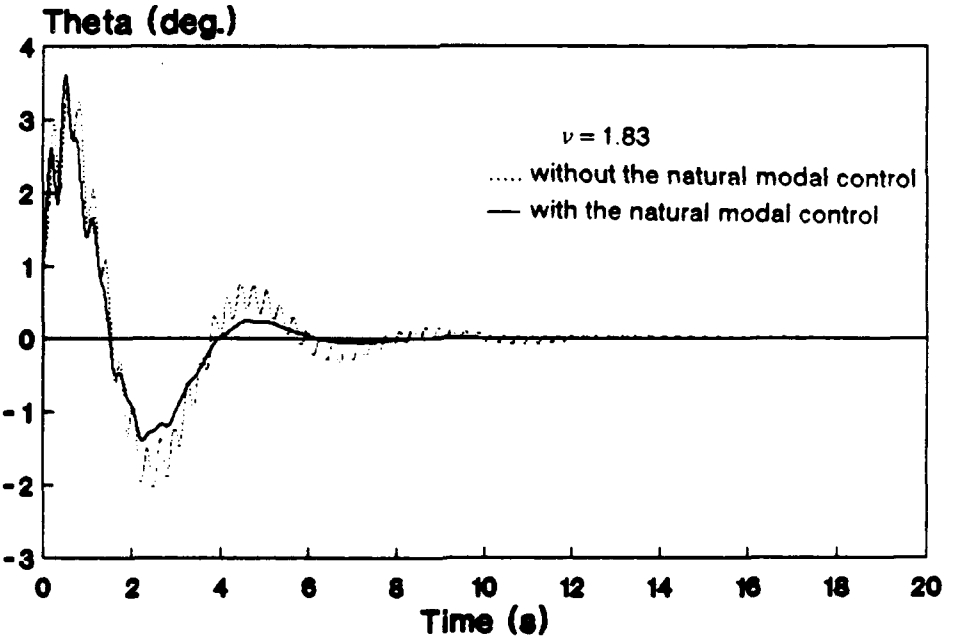

Fig. 11 Transient Responses with and without the Natural Modal Control (IC's the sme as in Fig. 10)

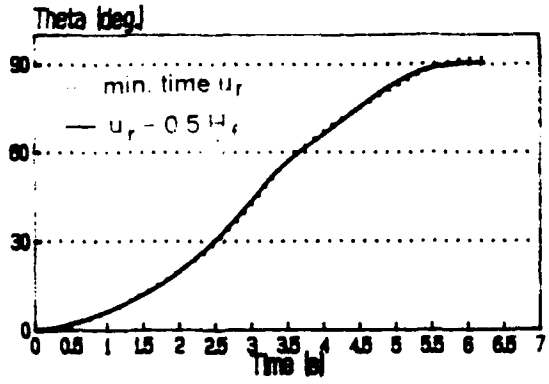

Fig. 12 90 Degree Angle Maneuver

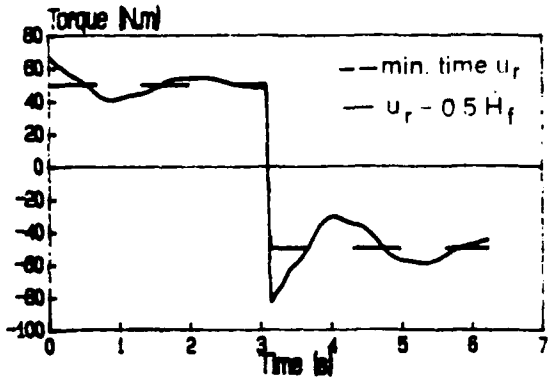

Fig. 13 90 Degree Angle Maneuver

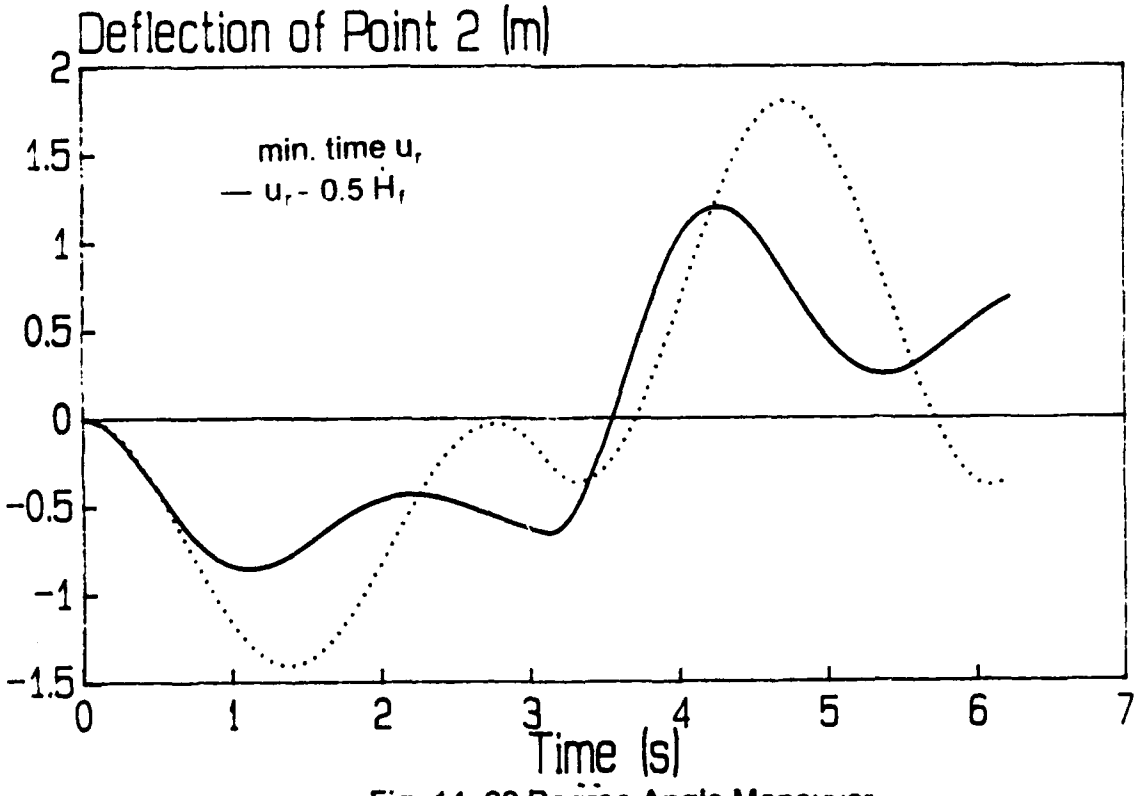

Fig. 14 90 Degree Angle Maneuver

3. Adaptive Feedback Control for the Retrieval of an Orbiting Tethered Antenna/Reflector System

ABSTRACT

An adaptive feedback control concept for the retrieval of an orbiting tether antenna/reflector system is introduced. In conjunction with an open-loop exponentially decreasing tether commanded length control, an attitude control system acting on the antenna is used for stabilizing the antenna as well as suppressing the tether swing librations through the control of the attitude motion of the antenna(base). The momentum exchange control technique wherein the time rate of change of the part of the angular momentum associated with the relative motion of the tether is used as a part of the feedback is applied to the control law design. The selection of the dimensionless control gains is based both on the consideration of the stability of the system linearized about a reference length, and on the numerical simulation of the actual nonlinear, time-varying system. The control gains are adapted to the instantaneously changing tether length. Numerical results are used to verify the control concept.

3.1 INTRODUCTION

Since the early 1970's a number of very large space antennas have been proposed for power transmission, astronautical research, and communications. The gravity stabilized configuration is particularly suited for very large flexible systems to alleviate the problems associated with the active attitude control of very large structures. An orbiting tethered antenna/reflector system has been proposed for possible communication or military use[1,2]. The subsatellite is nominally deployed below the antenna along the yaw axis at a sufficient distance (1km) to provide a favorable composite moment of inertia ratio for gravitational stabilization. It is assumed that the tether would be deployed through the end of a rigid boom attached to the shell(antenna) apex. The purpose of the present paper is to investigate the control strategy for the retrieval of the tethered antenna system.

It is well-known that retrieval is basically unstable because of the excitation of both in-plane and out-of-plane librations and insufficient tension during the terminal

phase. Many investigators have studied the tether deployment/retrieval problem. Most of the previous approaches on retrieval were based on modulation of the tether tension; however, tension control will not be effective for short tethers because of the low level of the gravity gradient, and it is found that the tension control without a constraint on the minimum tension level could easily lead to a slack tether.

Based on the momentum exchange control concept introduced in a recent paper[3], a new control strategy for suppression of the tether swing librations during retrieval is proposed in the present paper. It is proposed that together with an open-loop exponentially decreasing tether commanded length control an attitude feedback control acting on the antenna be utilized for stabilizing the antenna as well as suppressing the tether in-plane swing libration. The resulting feedback control law would include two components. One component involves the linear feedback of the antenna rigid body motions for the purpose of guaranteeing the stability and convergence of the antenna attitude motions. The dimensionless feedback gains of this part are adapted to the initial and final phases of the retrieval. The other component involves a feedback of the time rate of change of the part of the angular momentum associated with the in-plane motion of the tether relative to the local vertical. The purpose of this part of the feedback law is to provide the information about the tether in-plane swing motion for the controller to suppress the tether swing motion (momentum exchange control). The dimensionless gain for this part is selected based both on the consideration of the stability of the system linearized about a reference length and on the numerical simulation of the actual nonlinear, time-varying system. The gain is adapted to the instantaneously changing tether reference length. The possible practical advantage of this new approach over traditional tension control during retrieval is that the longitudinal vibration induced by this control method should be less than that induced by tension control; in general, tension control will directly excite the longitudinal vibration. It has been observed that longitudinal vibrations and wave propagation may present serious problems for tether operations, and the solution to these problems is being sought.

3.2 THE SYSTEM EQUATIONS OF MOTION

For system modelling the following assumptions are made:

- The shift of the center of mass of the system is neglected. The center of mass is assumed to lie at the same point as the center of mass of the antenna, and the center of mass of the system is moving in a circular orbit.
- The flexibility of the shell, boom, and tether is neglected and the tether is assumed uniform with a constant mass per length.
- The symmetry axis of the shell is nominally along the local vertical.
- The subsatellite is considered as a point mass.

The Newton-Euler method has been adopted to develop the system equations of motion. The coordinate systems used in the development of the system equations

of motion are shown in Fig.2. $O_pX_oY_oZ_o$ is an orbit-fixed reference frame centered at the center of mass of the shell, O_p, with O_pX_o along the local vertical and O_pY_o along the orbit normal opposite to the orbital angular velocity vector. $O_pX_pY_pZ_p$ is a shell-fixed reference frame, R_p , where O_pX_p , O_pY_p , O_pZ_p are the principal axes of the shell. OXYZ is the tether-fixed reference frame, R_t , with OX along the tether line, where O is the point from which the tether is deploying. The coordinates of point O in the shell frame, R_p , are (h_x , 0, 0)

The Euler angles, ψ, θ, ϕ, are the yaw, pitch , and roll angles of the shell, respectively. α, γ are in-plane and out-of-plane swing angles of the tether. Therefore, the whole system has the following degrees of freedom:

ψ, θ, ϕ ----- rigid body motion of the shell
α, γ -----librational motion of the subsatellite
l ----- length of the tether

The transformations from $O_pX_oY_oZ_o$ to $O_pX_pY_pZ_p$ and from $O_pX_pY_pZ_p$ to OXYZ are given by

$$\begin{bmatrix} X_p \\ Y_p \\ Z_p \end{bmatrix} = \begin{bmatrix} c\phi\, c\theta & s\phi\, c\psi + c\phi\, s\theta\, s\psi & s\phi\, s\psi - c\phi\, s\theta\, c\psi \\ -s\phi\, c\theta & c\phi\, c\psi - s\phi\, s\theta\, s\psi & c\phi\, s\psi + s\phi\, s\theta\, c\psi \\ s\theta & -c\theta\, s\psi & c\theta\, c\psi \end{bmatrix} \begin{bmatrix} X_o \\ Y_o \\ Z_o \end{bmatrix} \qquad (1)$$

$$[\, x\ y\ z\,]^T = T(\alpha\ \gamma)[\, x_p\ y_p\ z_p\,]^T$$

where

$$T(\alpha\ \gamma) = \begin{bmatrix} -c\gamma\, c\alpha & s\gamma & s\alpha\, c\gamma \\ s\gamma\, c\alpha & c\gamma & -s\alpha\, s\gamma \\ -s\alpha & 0 & -c\alpha \end{bmatrix} \qquad (2)$$

$$s \rightarrow \sin(\ )\ ;\quad c \rightarrow \cos(\ )$$

Consider an elemental mass, dm, whose instantaneous position vector from the center of the shell, O_p, is $\bar{r}$ (Fig.2). The equation of motion for dm can be written as

$$\bar{a}\, dm = \bar{f}\, dm + \bar{e}\, dm \qquad (3)$$

where

$\bar{a}$ = inertial acceleration of dm

$\bar{f}$ = gravitational force per unit mass

$\bar{e}$ = external forces acting per unit mass

The gravity force in the shell frame, R_p, is given by [4]

$$\bar{f} = \bar{f}_o + M\bar{r} \qquad (4)$$

where $\bar{f}_0$ is the gravity force at O_p expressed in the frame, R_p, and

$$M = \omega_c^2 \begin{bmatrix} 3C^2\phi C^2\theta - 1 & -3S\phi C\phi C^2\theta & 3C\phi S\theta C\theta \\ -3S\phi C\phi C^2\theta & 3S^2\phi C^2\theta - 1 & -3S\phi C\theta S\theta \\ 3C\phi S\theta C\theta & -3S\phi C\theta S\theta & 3S^2\theta - 1 \end{bmatrix} \qquad (5)$$

where ω_c is the orbital angular velocity.

The vector equation, (3) , can be written in the frame, R_p, as

$$[\bar{a}_o - \bar{f}_o + \ddot{\bar{r}} + 2\bar{\omega}x\dot{\bar{r}} + \bar{\omega}x(\bar{\omega}x\bar{r}) + \dot{\bar{\omega}}x\bar{r} - M\bar{r}]\,dm - \bar{e}\,dm = 0 \qquad (6)$$

where

$$\bar{\omega} = \begin{bmatrix} \omega_x \\ \omega_y \\ \omega_z \end{bmatrix} = \begin{bmatrix} \dot{\theta}S\phi + \dot{\psi}C\phi C\theta - \omega_c(S\phi C\psi + C\phi S\theta S\psi) \\ \dot{\theta}C\phi - \dot{\psi}S\phi C\theta - \omega_c(C\phi C\psi - S\phi S\theta S\psi) \\ \dot{\phi} + \dot{\psi}S\theta + \omega_c C\phi S\psi \end{bmatrix} \qquad (7)$$

The shift of the center of the mass of the entire system from the center of the antenna is neglected, that is, $\bar{f}_0 = \bar{a}_0$. After projecting equation (6) on the tether frame, R_t , the following is obtained

$$T[\ddot{\bar{r}} + 2\bar{\omega}x\dot{\bar{r}} + \bar{\omega}x(\bar{\omega}x\bar{r}) + \dot{\bar{\omega}}x\bar{r} - M\bar{r}]\,dm - \bar{e}|_t\,dm = 0 \qquad (8)$$

where $|_t$ indicates the projection onto the frame, R_t .

The expression for the $\bar{r}$ of the tether system is different from that of the shell due to the relative motion of the tether, so we consider the tethered subsatellite system and the shell system, separately.

TETHERED SUBSATELLITE SYSTEM

$$\bar{r} = T^{-1}\bar{r}_t + \bar{h} \qquad (9)$$

where $\bar{r}_t = (x, 0, 0)$ is the position vector of dm from O projected onto the frame. R_t. $\bar{h} = (h_x, 0, 0)$ is the position vector of point O from the shell's center of mass, O_s.

Hence,

$$\dot{\bar{r}} = T^{-1}\dot{\bar{r}}_t + \dot{T}^{-1}\bar{r}_t$$
$$\ddot{\bar{r}} = T^{-1}\ddot{\bar{r}}_t + 2\dot{T}^{-1}\dot{\bar{r}}_t + \ddot{T}^{-1}\bar{r}_t \qquad (10)$$

According to vector algebra

$$\dot{\bar{\omega}} \times \bar{r} + \bar{\omega} \times (\bar{\omega} \times \bar{r}) - M\bar{r} = [Q]\bar{r}$$
$$[Q] = [\dot{\bar{\omega}}] + [\bar{\omega}][\bar{\omega}] - [M] \qquad (11)$$

where

$$[\bar{\omega}] = \begin{bmatrix} 0 & -\omega_z & \omega_y \\ \omega_z & 0 & -\omega_x \\ -\omega_y & \omega_x & 0 \end{bmatrix}$$

After substitution of equations (10)–(11) into equation (8), there results

$$\bar{a}_t dm - \bar{e}|_t dm = 0 \qquad (12)$$

where

$$\bar{a}_t = \ddot{\bar{r}}_t + 2[T(\dot{T}^{-1}) + T[\omega]T^{-1}]\dot{\bar{r}}_t + [T(\ddot{T}^{-1}) + 2T[\omega](\dot{T}^{-1}) + T[Q]T^{-1}]\bar{r}_t + T[Q]\bar{h} \qquad (13)$$

Let

$$[T(\dot{T}^{-1}) + T[\omega]T^{-1}] = \begin{bmatrix} 0 & -\Omega_z & \Omega_y \\ \Omega_z & 0 & -\Omega_x \\ -\Omega_y & \Omega_x & 0 \end{bmatrix}$$

$$[T(\ddot{T}^{-1}) + 2T[\omega](\dot{T}^{-1}) + T[Q]T^{-1}] = \begin{bmatrix} \omega_{11} & \omega_{12} & \omega_{13} \\ \omega_{21} & \omega_{22} & \omega_{23} \\ \omega_{31} & \omega_{32} & \omega_{33} \end{bmatrix}$$

$$T[Q]\bar{h} = h_x \begin{bmatrix} g_1 \\ g_2 \\ g_3 \end{bmatrix}$$

The expressions for some terms are listed in Appendix A.

Also, let $$I_x = \int_{s,t} x\,dm \qquad H_{xx} = \int_{s,t} x^2\,dm$$

By projecting Eq.(12) along the X, Y, and Z axes and integrating the result over the subsatellite and tether, the translational equations of motion can be obtained as

$$\begin{aligned} &(m_s+m_t)\ddot{l} + I_x\omega_{11} + (m_s+m_t)h_x g_1 = F_{tx} \\ &2(m_s+m_t)\dot{l}\,\Omega_z + I_x\omega_{21} + (m_s+m_t)h_x g_2 = F_{ty} \\ &-2(m_s+m_t)\dot{l}\,\Omega_y + I_x\omega_{31} + (m_s+m_t)h_x g_3 = F_{tz} \end{aligned} \qquad (14)$$

where F_{tx}, F_{ty}, F_{tz} are three components of the force exerted on the tether by the shell. No other external forces acting on the tether and subsatellite are assumed. The equations of rotational motion of the tether can be obtained by the following operation:

$$\int_{s,t} \bar{r} \times [\text{Eq.}(12)] = 0 \qquad (15)$$

By projecting Eq.(15) along the Y and Z axes, respectively, the rotational equations for the in-plane and out-of-plane motions are obtained as

$$2I_x\Omega_y\dot{l} - H_{xx}\omega_{31} - h_x I_x g_3 = 0 \qquad (16)$$

$$2I_x\Omega_z\dot{l} + H_{xx}\omega_{21} + h_x I_x g_2 = 0 \qquad (17)$$

SHELL SYSTEM

The torques exerted on the shell are

$$\bar{L} = \bar{L}_G + \bar{L}_T \qquad (18)$$

where $\bar{L}_G$ is the gravitational torque and $\bar{L}_T$ the torque by the tether whose components in the shell body frame, R_b, can be obtained as

$$\bar{L}_G = 3\omega_c^2 \begin{bmatrix} s\theta c\theta s\phi (J_y - J_z) \\ -s\theta c\theta c\phi (J_z - J_x) \\ c^2\theta s\phi c\phi (J_x - J_y) \end{bmatrix} \qquad (19)$$

$$\bar{L}_T = h_x \begin{bmatrix} 0 \\ s\alpha c\gamma F_{tx} - s\alpha s\gamma F_{ty} - c\alpha F_{tz} \\ -s\gamma F_{tx} - c\gamma F_{ty} \end{bmatrix} \qquad (20)$$

where $J_{x,y,z}$ are the shell's principal moments of inertia. Upon applying the Euler–Newtonian equations, the equations of motion of the shell attitude motion can be obtained as

$$\begin{aligned}
&J_x\dot{\omega}_x - (J_y - J_z)\omega_y\omega_z = 3\omega_c^2 s\theta c\theta s\phi (J_y - J_z) + L_{ex} \\
&J_y\dot{\omega}_y - (J_z - J_x)\omega_z\omega_x = -3\omega_c^2 s\theta c\theta c\phi (J_z - J_x) + h_x(s\alpha c\gamma F_{tx} - s\alpha s\gamma F_{ty} - c\alpha F_{tz}) + L_{ey} \\
&J_z\dot{\omega}_z - (J_x - J_y)\omega_x\omega_y = 3\omega_c^2 c^2\theta s\phi c\phi (J_x - J_y) - h_x(s\gamma F_{tx} + c\gamma F_{ty}) + L_{ez} \qquad (21)
\end{aligned}$$

where the forces F_{tx}, F_{ty}, F_{tz} have already been obtained in Eq.(14) and L_{ex}, L_{ey}, L_{ez} are other external torques including the control torques. The system nonlinear equations of motion (16), (17), and (21) are used to obtain the system linearized equations and to simulate the closed-loop system.

SYSTEM QUASI-LINEARIZED EQUATIONS OF MOTION

In the case of retrieval the time rate of change of the tether length and its rate can be fast and, therefore, are treated as zero order terms (playing the same role as the constant terms in the stationkeeping case) in obtaining the system quasi-linearized equations of motion. The resulting quasi-linearized nondimensional system equations can be obtained as

$$\text{in-plane} \begin{cases} k_1\alpha'' + \theta'' + 3\alpha + 3\theta + k_1(\alpha' + \theta' - 1)\dfrac{l'}{l} = 0 \\ k_2\alpha'' + \theta'' - 3\Omega_y\theta + 2k_5(\alpha' + \theta' - 1)\dfrac{l'}{l} + k_5\alpha\dfrac{l''}{l} = U_\theta \end{cases} \qquad (22)$$

$$\text{out-of-plane} \begin{cases} k_1\gamma'' - \phi'' - 4\phi + (3 + k_1)\gamma + k_1(\gamma' - \phi' - \psi)\dfrac{l'}{l} = 0 \\ \psi'' - \Omega_x\psi - (1 + \Omega_x)\phi' = U_\psi \\ k_3\gamma'' - \phi'' + k_3\gamma - 4\Omega_z\phi - (1 - \Omega_z)\psi' + 2k_6(\gamma' - \phi' - \psi)\dfrac{l'}{l} + k_6\gamma\dfrac{l''}{l} = U_\phi \end{cases} \qquad (23)$$

where $()' = \dfrac{d}{d\tau}()$, $\tau = \omega_c t$. U_θ, U_ψ, and U_ϕ are pitch, yaw, and roll axis control torques, respectively, and no other external disturbance torques are assumed. The nondimensional parameters in Eqs. (22) and (23) are:

$$k_1=\frac{H_{xx}}{H_{xx}+hI_x}\ ;\ k_2=\frac{hI_x}{J_y^*}\ ;\ k_3=\frac{hI_x}{J_z^*}\ ;\ k_4=\frac{2I_x l}{H_{xx}+hI_x}\qquad (h=-h_x>0)$$

$$k_5=\frac{hm_{st}l}{J_y^*}\ ;\ k_6=\frac{hm_{st}l}{J_z^*}\ ;\ \Omega_x=\frac{J_z^*-J_y^*}{J_x^*}\ ;\ \Omega_y=\frac{J_x^*-J_z^*}{J_y^*}\ ;\ \Omega_z=\frac{J_y^*-J_x^*}{J_z^*}$$

$$J_x^*=J_x\ ;\ J_y^*=J_y+hI_x+m_{st}h^2\ ;\ J_z^*=J_z+hI_x+m_{st}h^2$$

It can be seen from the quasi-linearized equations that in the case of retrieval, $\frac{l'}{l}<0$, the in-plane and out-of-plane motions become unstable due to the divergent terms, such as $\alpha\frac{l'}{l}$, $\theta\frac{l'}{l}$, etc..

3.3 MOMENTUM EXCHANGE FEEDBACK CONTROL FOR SYSTEM IN-PLANE MOTION AT A FIXED TETHER REFERENCE LENGTH

In Ref.[3], Li and Bainum have introduced a new control concept called momentum exchange feedback control. The same control concept is applied to the current problem; that is, the time rate of change of that part of the angular momentum due to the tether deviation motion from the local vertical is used as a part of the feedback control law for suppressing the tether in-plane swing motion.

Let us first obtain the expression of the time rate of change of the tether angular momentum. From Eq.(20), the pitch torque exerted on the tether by the shell is

$$M_y=-h_x(s\alpha c\gamma F_{ix}-s\alpha s\gamma F_{iy}-c\alpha F_{iz}) \qquad (24)$$

After Eq.(24) is linearized about a fixed tether reference length, we obtain

$$M_y=-h_xI_x(\alpha''+\theta'')+m_{st}h_x^2\theta''-3h_x(I_x-m_{st}h_x)\theta \qquad (25)$$

Since $(\alpha+\theta)$ is the angle of the tether line from the local vertical in the linear sense, according to Newton's law, the linearized time rate of change of that part of the angular momentum due to the tether in-plane motion relative to the local vertical is

$$-h_xI_x(\alpha''+\theta'')$$

Therefore, applying the momentum exchange control concept, the nondimensional feedback control for the in-plane motion is introduced as

$$U_\theta=-g_1\theta-g_2\theta'-\gamma(k_2\alpha''+k_2\theta'') \qquad (26)$$

The first two terms in Eq.(26) are the linear feedback of the shell pitch angle and its rate; the last term is the feedback of the linearized time rate of change of the angular momentum due to the tether in-plane motion relative to the local vertical, for the purpose of exchanging the tether momentum with the shell and absorbing the tether swing motion energy by the control system.

The closed-loop system equations of the in-plane motion about a fixed tether reference length become

$$k_1\alpha'' + \theta'' + 3\alpha + 3\theta = 0$$

$$k_2\alpha'' + \theta'' - 3\Omega_v\theta = -g_1\theta - g_2\theta' - \gamma(k_2\alpha'' + k_2\theta'') \tag{27}$$

Note that the control goal is to suppress the angle θ and $(\alpha+\theta)$. After substitution of $\alpha=\beta-\theta$ into Eq.(27), one obtains

$$k_1\beta'' + (1-k_1)\theta'' + 3\beta = 0$$

$$(1+\gamma)k_2\beta'' + (1-k_2)\theta'' + g_2\theta' + (g_1-3\Omega_v)\theta = 0 \tag{28}$$

The characteristic equation of (28) is

$$f(\lambda) = [k_1 - k_2 - k_2(1-k_1)\gamma]\lambda^4 + k_1 g_2\lambda^3 + [3(1-k_2) + (g_1-3\Omega_v)k_1]\lambda^2$$

$$+3g_2\lambda + 3(g_1-3\Omega_v) \tag{29}$$

The Routh-Hurwitz criteria is applied and leads to following requirements for the control gains:

$$g_1 > 3\Omega_v \tag{30}$$

$$g_2 > 0 \tag{31}$$

$$-1 < \gamma < \frac{k_1-k_2}{k_2(1-k_1)} \tag{32}$$

3.4 RETRIEVAL

IN-PLANE MOTION CONTROL

The linear feedback control law (26) is applied to the retrieval where the system involves complex nonlinear and time-variant ordinary differential equations. However, it is expected that for a fairly moderate retrieval rate, the closed-loop system responses will be bounded when the control gain, ν, is within some range as indicated by (32). Numerical simulations are used to select the control gain ν which will generate bounded or convergent system responses. The system simulation parameters are shown in Table 1.

TABLE 1. SYSTEM SIMULATION PARAMETERS

m_p	m_s	m_t	l	h	a	ω_c
10000 kg	500 kg	8.35 kg	1 km	0.08 km	0.1 km	0.001178 rad/s

The decreasing commanded length is taken as the exponential form:

$$l = l_0 e^{-ct} \qquad l_0 = 1\,\text{km} \tag{33}$$

In general, the range of the control gain ν for bounded system responses will depend upon the retrieval rate c . For a particular retrieval rate $c = 3.45 \times 10^{-4} (s^{-1})$ for example, it is observed (based on numerical simulations) that the system is bounded when ν lies within the interval

$$1 < \nu < \frac{k_1 - k_2}{k_2 (1 - k_1)} \tag{34}$$

If the retrieval rate decreases, the interval will become larger with the same upper bound; or, vice versa, if the retrieval rate increases, the interval will become smaller with the same upper bound. However (also based on numerical simulations), there is a maximum retrieval rate c^* ; if the retrieval rate exceeds c^*, no control gain ν exists for bounded system responses. For these particular simulation parameters, it is found that c^* is approximately equal to $5.18 \times 10^{-4} (s^{-1})$.

Notice that in the case of retrieval the nondimensional parameters k_1, k_2 are changing with the instantaneous tether length. So is the upper bound of the control gain ν, shown in Fig. 3.

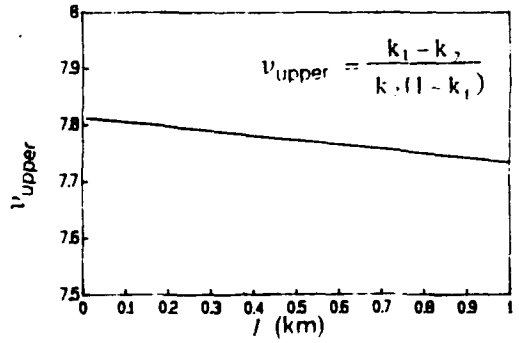

Fig.3 ν_{upper} as a Function of Tether Length

Also, the system configuration is more stable with the long tether length at the initiation phase of retrieval than with the short tether length at the final phase of retrieval. Therefore, the nondimensional gains, g_1 and g_2 , are selected to be adapted to the initial and final phase of retrieval for the purpose of saving control energy, that is,

$$\begin{aligned} g_1 &= g_{1i} \qquad g_2 = g_{2i} \quad ; \qquad 0.1 \text{ km} \le l \le 1 \text{ km} \\ g_1 &= g_{1f} \qquad g_2 = g_{2f} \quad ; \qquad 0.01 \text{ km} \le l < 0.1 \text{ km} \end{aligned} \tag{35}$$

OUT-OF-PLANE MOTION CONTROL

The system out-of-plane motion is coupled with the in plane motion and tether longitudinal translational motion, especially in the case of large swing angles and quick retrieval. Therefore, it is necessary to control the system out-of-plane motion during fast retrieval. To this end, it is proposed to control the shell yaw and pitch motion by linear feedback control law, that is

$$\begin{aligned} U_\psi &= g_{11}\psi + g_{12}\psi' + g_{13}\phi + g_{14}\phi' \\ U_\phi &= g_{21}\psi + g_{22}\psi' + g_{23}\phi + g_{24}\phi' \end{aligned} \tag{36}$$

The selection of the control gains g_{ij} is based on the shell linearized equations of motion without the tethered subsatellite system connected. The LQR or other methods can be used to design the control gains.

3.5 NUMERICAL RESULTS

First of all, it is shown that with the retrieval rate e^{-ct}, $c = 3.45 \times 10^{-4} (s^{-1})$ (Fig.4) and without any controls, the system responses diverge very quickly (Fig.5).

Fig.6 shows that with the addition of the three-axis attitude control on the shell (which, however, does not involve the momentum exchange feedback term), the shell attitude motions are subjected to a stable control, whereas the tether in-plane swing motion still diverges.

With the inclusion of the momentum exchange feedback term in the pitch control law, the pitch control law is then selected as:

$$U_\theta = -g_1\theta - g_2\theta' - \nu(k_2\alpha'' + k_2\theta'')$$

$$\nu = \frac{k_1 - k_2}{k_2(1-k_1)} - a \qquad a > 0$$

$$g_1 = 2.4 \quad g_2 = 2.3 \; ; \qquad 0.1 \text{ km} \le l \le 1 \text{ km}$$

$$g_1 = 5.4 \quad g_2 = 3.4 \; ; \qquad 0.01 \text{ km} \le l < 0.1 \text{ km}$$

Figs.7-9 show the system responses corresponding to the three cases: $a = 6$, $a = 4$, and $a = 1$. It can be seen that with the increase of the control gain ν (a decreases) the tether in-plane motion is better damped; however, the transient response of the pitch motion of the shell is subjected to a larger initial overshoot, but subsequently damps rapidly. This conclusion agrees with the physical explanation of the momentum exchange feedback control and the same results were observed in Ref.[3]. Therefore, the selection of the control gain ν is a kind of trade-off and the better system responses are usually achieved with the control gain ν close to the upper bound of the stability region.

Fig.10 shows the response of the tether out-of-plane swing motion. The tether out-of-plane motion will be disturbed by its coupling with the system in-plane motions and tether longitudinal translation. However, it can be seen that when the system in-plane motions are damped, the tether out-of-plane motion (not directly controlled) will not become too large, with a maximum swing angle of 20 degrees at the end of retrieval (for the selected control gains here).

Fig.11 shows the projection of the tether trajectory in the orbit plane.

Fig.12 shows the tether tension profile during retrieval. It can be seen that the change of tether tension is moderate and no slack tether occurs. This is one of the advantages of the current control method over tension control.

Fig.13 shows the requirement of the pitch control torque during retrieval for the selective control gains. The torque requirement is reasonable.

Although the control gain ν is selected in an adaptive manner, the fluctuation with the tether length is very small (Fig.2). It will be very interesting and of great practical value if a constant control gain ν can be applied with successful results. Fig.14 shows some typical system responses when a constant gain ν is used.

3.6 CONCLUSION

The retrieval dynamics of the orbiting tethered antenna/reflector system without active control is unstable. In the present paper, the control concept called momentum exchange and compensation has been applied to the retrieval of the tethered antenna/reflector system. The time rate of change of that part of the angular momentum due to the tether motion from the local vertical is used as a part of the feedback law in the antenna attitude control system. The tether retrieval commanded length is taken as a exponential form. The selection of the nondimensional control gains is based both on the consideration of the stability of the system linearized equations about a fixed reference length and on the numerical simulation for the real time-variant and nonlinear system. The numerical simulation results have shown the effectiveness of the current control method for the suppression of both the antenna and tether in-plane motions at relatively quick retrieval rates.

Another implication of this approach to tethered systems is that tether swing librations can be suppressed through the control of the motion of an attachment point or boom using this new methodology. This control concept provides an alternative technique for control of future possible tethered systems which may have some practical advantages such as: (1)avoiding excitation of the longitudinal vibrations and wave propagation of tethers induced by tension control and, (2)avoiding slack tethers.

Acknowledgment

This research was supported by the Air Force Office of Scientific Research Contract F 49620-90-C-009. Dr. Spencer Wu, Program Manager.

REFERENCES

1. Liu, Liangdong and Bainum, P.M , 1989, "Dynamics and Control of a Tethered Antenna/Reflector System in Orbit." The Journal of the Astronautical Sciences, Vol. 38, No. 3, 1990, pp. 247-268.

2. Li, Zhong and Bainum, P.M., 1990, "On the Development of Control Laws for an Orbiting Tethered Antenna/Reflector System Test Scale Model." the First U.S./Japan Conference on Adaptive Structures, Maui, Hawaii, Nov. 13-15, 1990.

3. Li, Zhong and Bainum, P.M., 1991, "Momentum Exchange: Feedback Control of Flexible Spacecraft Maneuvers and Vibration." AAS/AIAA Astrodynamics Specialist Conference, Durango, Colorado, August 19-22, 1991, Paper AAS 91-375.

4. Santini, P., 1976, "Stability of Flexible Spacecrafts." Acta Astronautica, Vol. 3, pp. 685-713.

APPENDIX A

$$\Omega_x = \sin\gamma\,\dot{\alpha} - \cos\alpha\cos\gamma\,\omega_x + \sin\gamma\,\omega_y + \sin\alpha\cos\gamma\,\omega_z$$

$$\Omega_y = \cos\gamma\,\dot{\alpha} + \cos\alpha\sin\gamma\,\omega_x + \cos\gamma\,\omega_y - \sin\alpha\sin\gamma\,\omega_z$$

$$\Omega_z = \dot{\gamma} - \sin\alpha\,\omega_x - \cos\alpha\,\omega_z$$

$$\omega_{11} = -\cos^2\gamma\,\dot{\alpha}^2 - \dot{\gamma}^2 - 2\dot{\alpha}(\cos\alpha\sin\gamma\cos\gamma\,\omega_x + \cos^2\gamma\,\omega_y - \sin\alpha\sin\gamma\cos\gamma\,\omega_z)$$
$$+ 2\dot{\gamma}(\sin\alpha\,\omega_x + \cos\alpha\,\omega_z) - (\sin^2\alpha\cos^2\gamma + \sin^2\gamma)\,\omega_x^2 - \cos^2\gamma\,\omega_y^2 - (\cos^2\alpha\cos^2\gamma + \sin^2\gamma)\,\omega_z^2$$
$$- 2\cos\alpha\sin\gamma\cos\gamma\,\omega_x\omega_y - 2\sin\alpha\cos\alpha\cos^2\gamma\,\omega_x\omega_z + 2\sin\alpha\sin\gamma\cos\gamma\,\omega_y\omega_z$$
$$- \omega_c^2\cos^2\alpha\cos^2\gamma(3\cos^2\phi\cos^2\theta - 1) - 6\,\omega_c^2\cos\alpha\sin\gamma\cos\gamma\sin\phi\cos\phi\cos^2\theta$$
$$+ 6\omega_c^2\sin\alpha\cos\alpha\cos^2\gamma\cos\phi\sin\theta\cos\theta - \omega_c^2\sin^2\gamma(3\sin^2\phi\cos^2\theta - 1)$$
$$+ 6\omega_c^2\sin\alpha\sin\gamma\cos\gamma\sin\phi\sin\theta\cos\theta - \omega_c^2\sin^2\alpha\cos^2\gamma(3\sin^2\theta - 1)$$

$$\omega_{21} = \ddot{\gamma} - \sin\alpha\,\dot{\omega}_x - \cos\alpha\,\dot{\omega}_z + \sin\gamma\cos\gamma\,\dot{\alpha}^2 - 2\dot{\alpha}(\cos\alpha\cos^2\gamma\,\omega_x - \sin\gamma\cos\gamma\,\omega_y - \sin\alpha\cos^2\gamma\,\omega_z)$$
$$- \cos^2\alpha\sin\gamma\cos\gamma\,\omega_x^2 + \sin\gamma\cos\gamma\,\omega_y^2 - \sin^2\alpha\sin\gamma\cos\gamma\,\omega_z^2 - \cos\alpha\cos2\gamma\,\omega_x\omega_y$$
$$+ 2\sin\alpha\cos\alpha\sin\gamma\cos\gamma\,\omega_x\omega_z + \sin\alpha\cos2\gamma\,\omega_y\omega_z + \omega_c^2\cos^2\alpha\sin\gamma\cos\gamma(3\cos^2\phi\cos^2\theta - 1)$$
$$- 3\omega_c^2\cos\alpha\cos2\gamma\sin\phi\cos\phi\cos^2\theta - 6\,\omega_c^2\sin\alpha\cos\alpha\sin\gamma\cos\gamma\cos\phi\sin\theta\cos\theta$$
$$- \omega_c^2\sin\gamma\cos\gamma(3\sin^2\phi\cos^2\theta - 1) + 3\omega_c^2\sin\alpha\cos2\gamma\sin\phi\sin\theta\cos\theta$$
$$+ \omega_c^2\sin^2\alpha\sin\gamma\cos\gamma(3\sin^2\theta - 1)$$

$$\omega_{31} = -\cos\gamma\,\ddot{\alpha} - \cos\alpha\sin\gamma\,\dot{\omega}_x - \cos\gamma\,\dot{\omega}_y + \sin\alpha\sin\gamma\,\dot{\omega}_z + 2\sin\gamma\,\dot{\alpha}\,\dot{\gamma}$$
$$- 2\dot{\gamma}(\cos\alpha\cos\gamma\,\omega_x - \sin\gamma\,\omega_y - \sin\alpha\cos\gamma\,\omega_z) + \sin\alpha\cos\alpha\cos\gamma(\omega_x^2 - \omega_z^2)$$
$$- \sin\alpha\sin\gamma\,\omega_x\omega_y + \cos2\alpha\cos\gamma\,\omega_x\omega_z - \cos\alpha\sin\gamma\,\omega_y\omega_z$$
$$- \omega_c^2\sin\alpha\cos\alpha\cos\gamma(3\cos^2\phi\cos^2\theta - 1) - 3\omega_c^2\cos2\alpha\cos\gamma\cos\phi\sin\theta\cos\theta$$
$$- 3\omega_c^2\sin\alpha\sin\gamma\sin\phi\cos\phi\cos^2\theta - 3\omega_c^2\cos\alpha\sin\gamma\sin\phi\sin\theta\cos\theta$$
$$+ \omega_c^2\sin\alpha\cos\alpha\cos\gamma(3\sin^2\theta - 1)$$

$$g_1 = -\sin\alpha\cos\gamma\,\dot{\omega}_y + \sin\gamma\,\dot{\omega}_z + \cos\alpha\cos\gamma\,(\omega_y^2 + \omega_z^2) + \sin\gamma\,\omega_x\omega_y + \sin\alpha\cos\gamma\,\omega_x\omega_z$$
$$+ \omega_c^2\cos\alpha\cos\gamma\,(3\cos^2\phi\cos^2\theta - 1) + 3\omega_c^2\sin\gamma\sin\phi\cos\phi\cos^2\theta$$
$$- 3\omega_c^2\sin\alpha\cos\gamma\cos\phi\sin\theta\cos\theta$$

$$g_2 = \sin\alpha\sin\gamma\,\dot{\omega}_y + \cos\gamma\,\dot{\omega}_z - \cos\alpha\sin\gamma\,(\omega_y^2 + \omega_z^2) + \cos\gamma\,\omega_x\omega_y - \sin\alpha\sin\gamma\,\omega_x\omega_z$$
$$- \omega_c^2\cos\alpha\sin\gamma(3\cos^2\phi\cos^2\theta - 1) + 3\omega_c^2\cos\gamma\sin\phi\cos\phi\cos^2\theta$$
$$+ 3\omega_c^2\sin\alpha\sin\gamma\cos\phi\sin\theta\cos\theta$$

$$g_3 = \cos\alpha\,\dot{\omega}_y + \sin\alpha\,(\omega_y^2 + \omega_z^2) - \cos\alpha\,\omega_x\omega_z + \omega_c^2\sin\alpha\,(3\cos^2\phi\cos^2\theta - 1)$$
$$+ 3\omega_c^2\cos\alpha\cos\phi\sin\theta\cos\theta$$

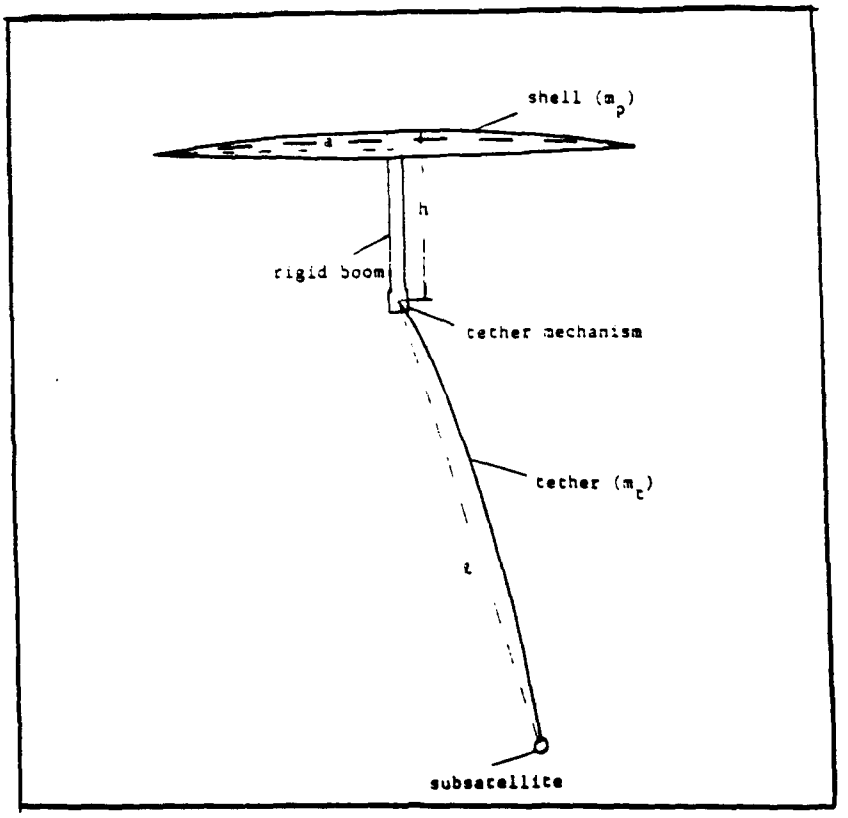

Fig. 1. Tethered Antenna/Reflector System

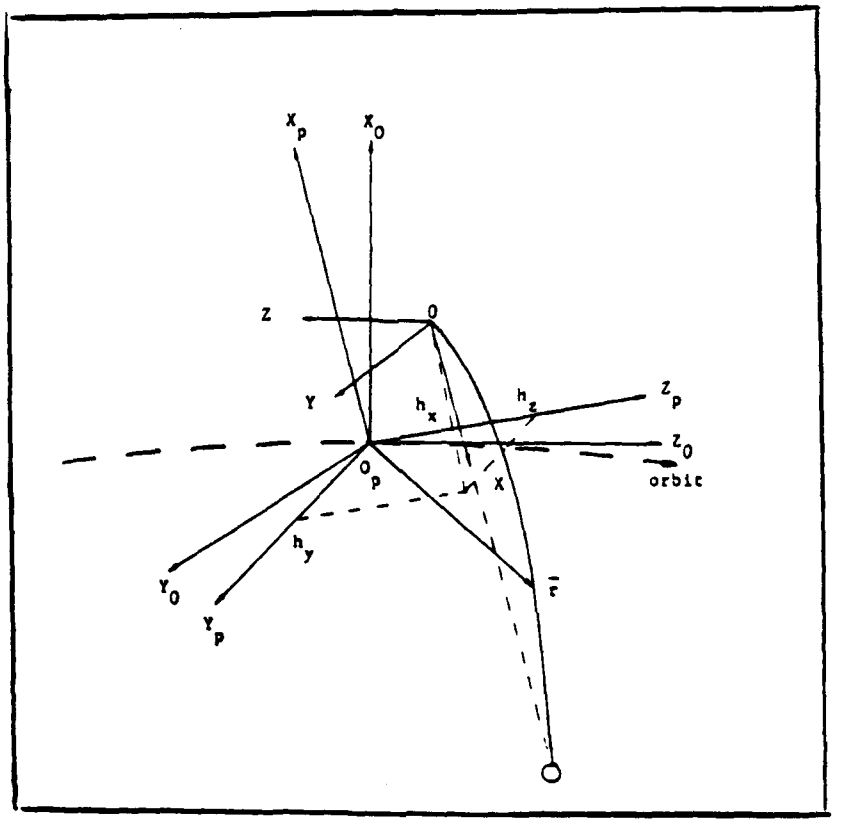

Fig. 2. Coordinate Systems

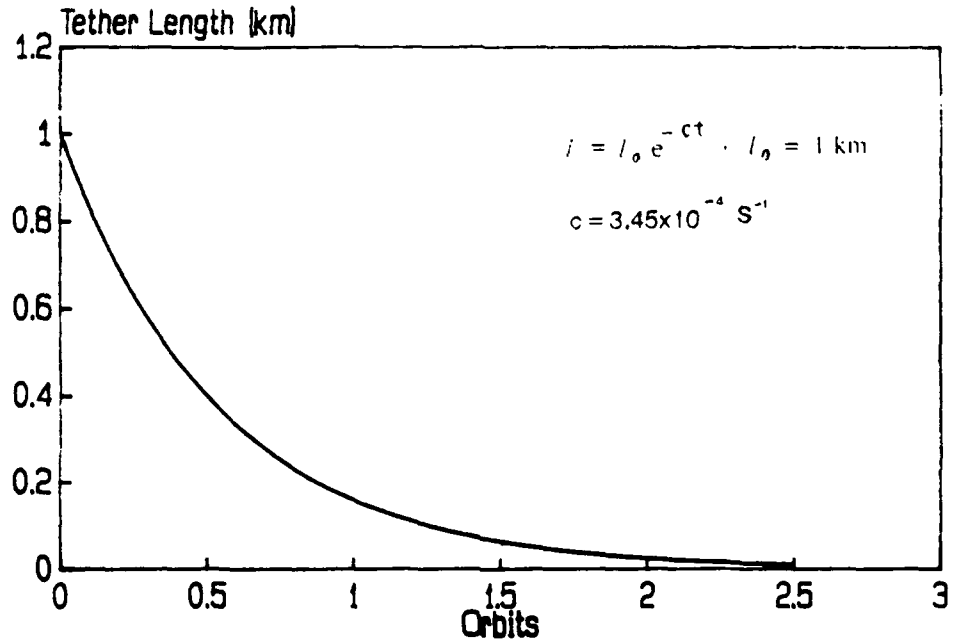

Fig.4 Tether Decreasing Commanded Length Profile

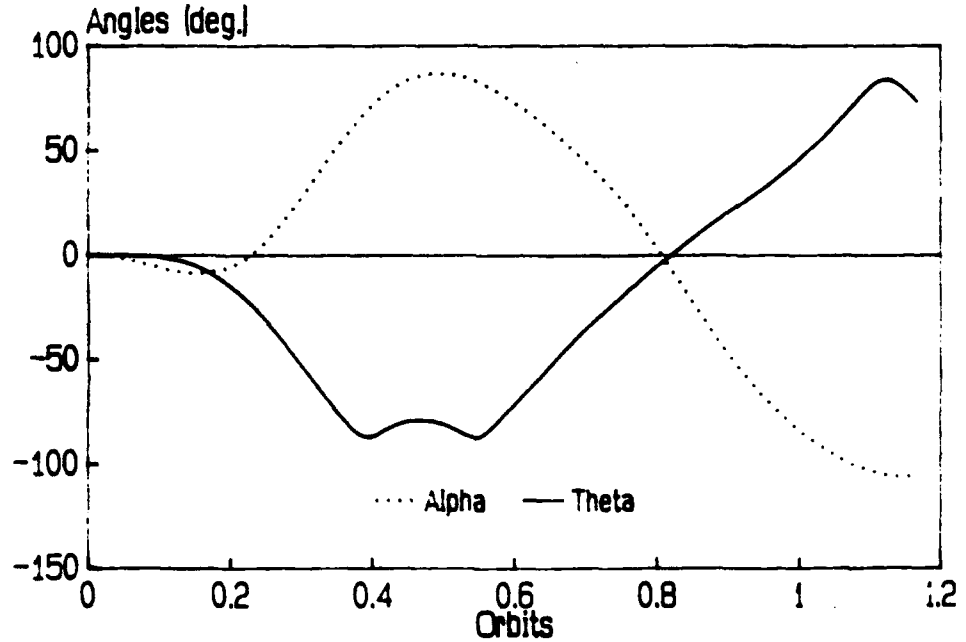

Fig.5 Typical System Responses without Active Shell Attitude Control

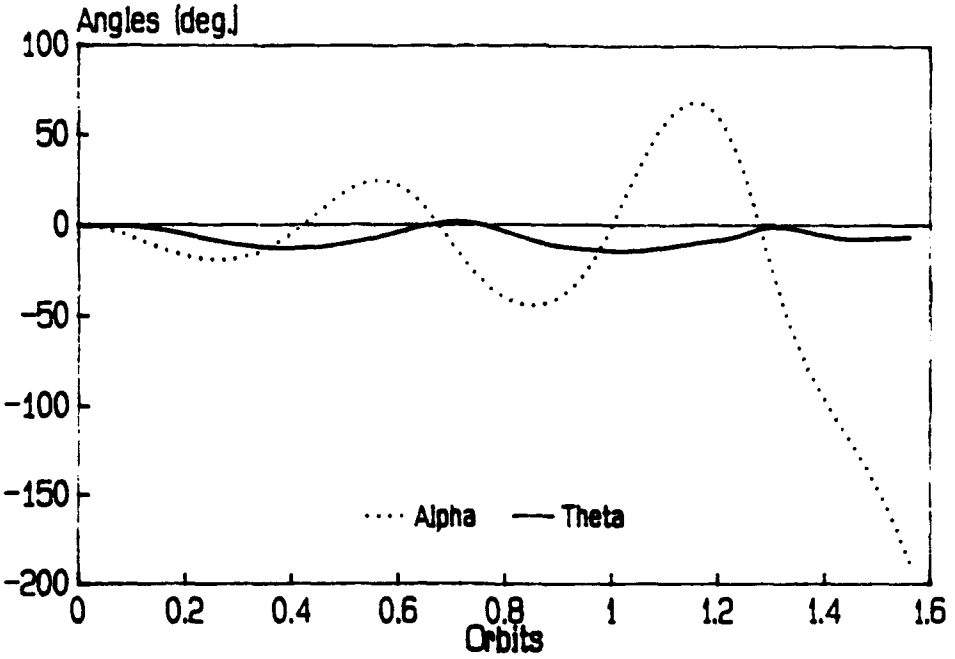

Fig.6 Typical System Responses when Shell Attitude Control is Applied (not Including Momentum Exchange Feedback Control Term)

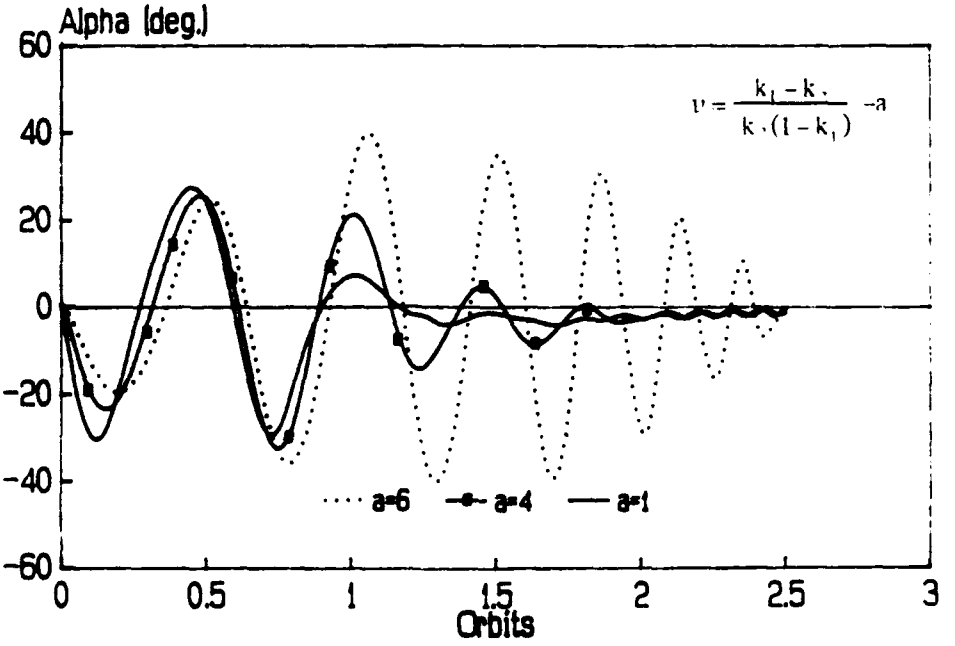

Fig.7 Tether In-Plane Swing Angle (Relative to Shell) Responses when Shell Attitude Control is Applied (Including Momentum Exchange Feedback Control Term)

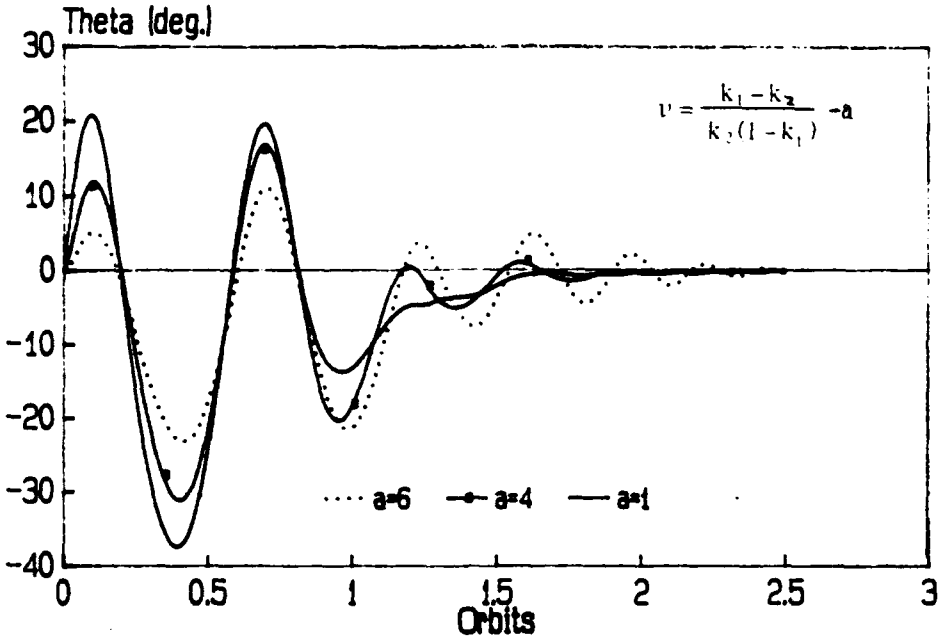

Fig.8 Shell Pitch Angle Responses when Attitude Control is Applied
(Including Momentum Exchange Feedback Control Term)

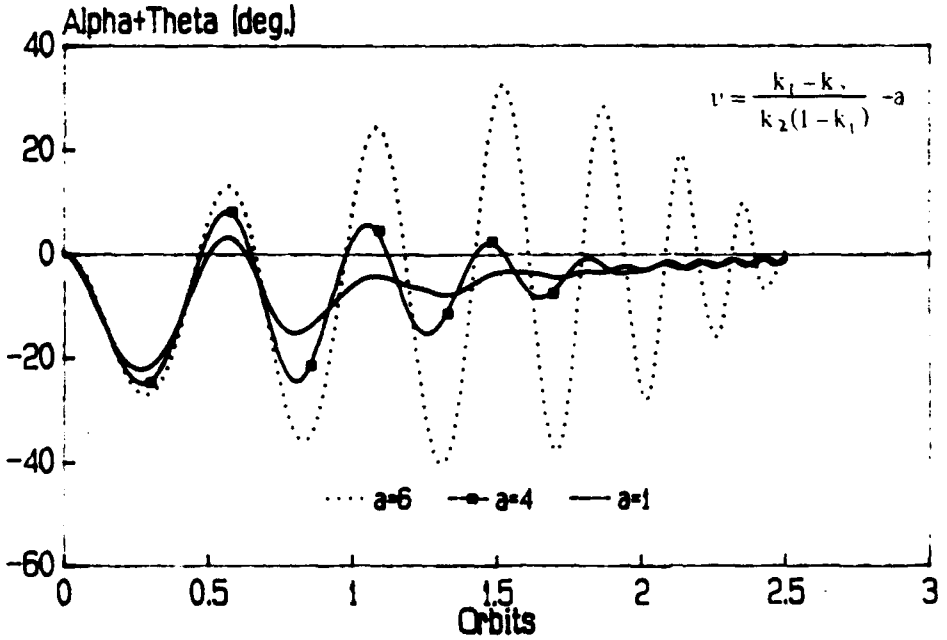

Fig.9 Tether In-Plane Swing Angle (Relative to Local Vertical)
Reponses when Attitude Control is Applied
(Including Momentum Exchange Feedback Control Term)

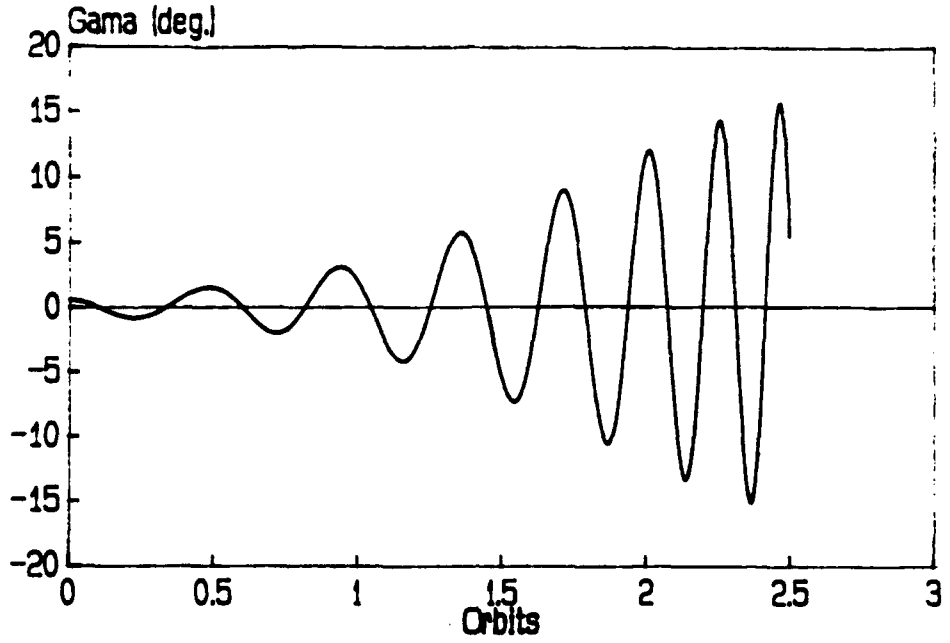

Fig.10 Tether Out-Of-Plane Swing Angle Response during Retrieval

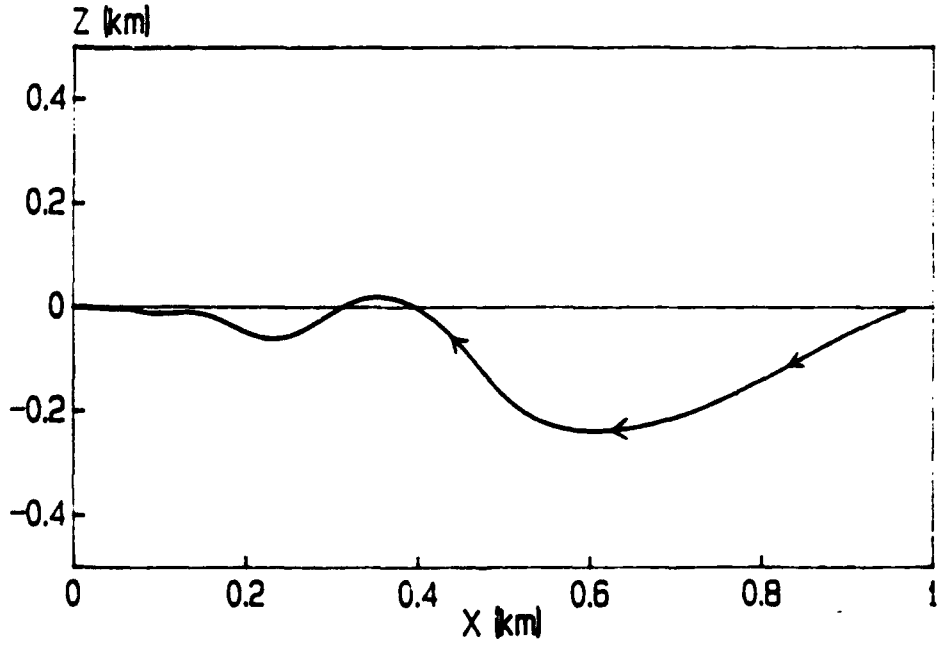

Fig.11 Projection of the Tether Trajectory in Orbit Plane

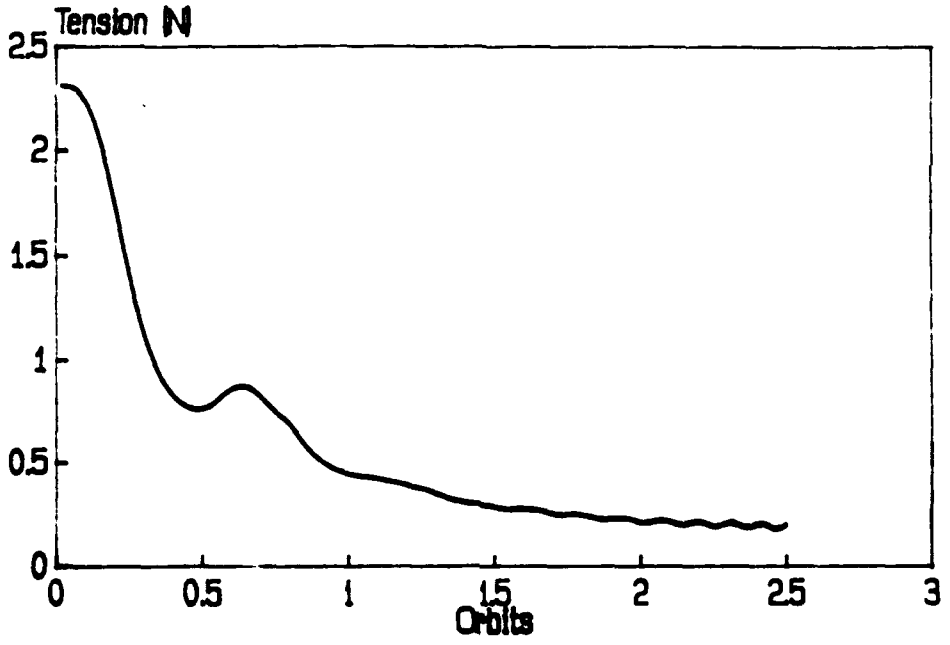

Fig.12 Tether Tension Profile during Retrieval

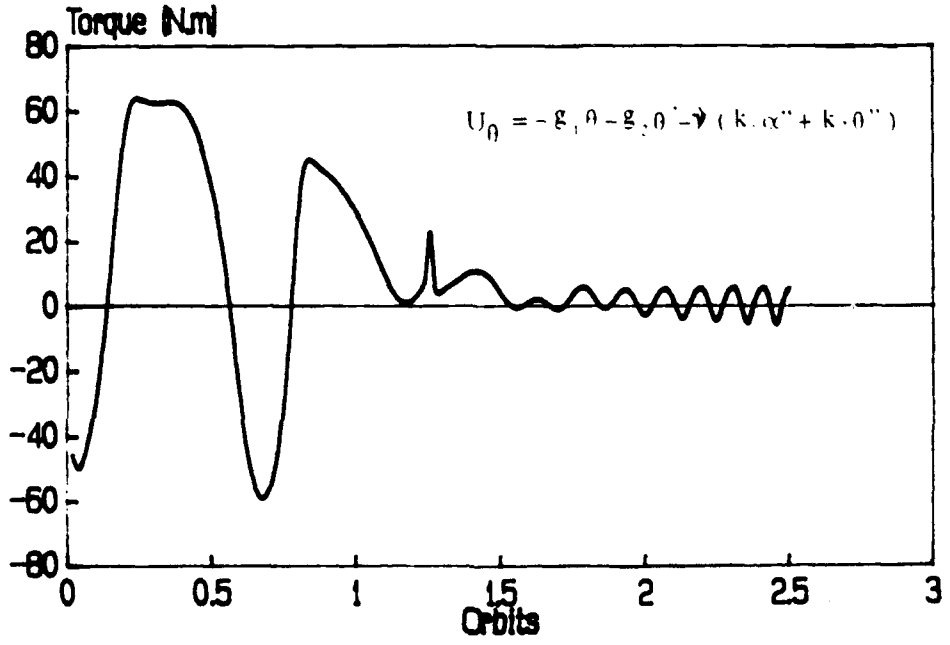

Fig.13 Pitch Torque Requirement during Retrieval

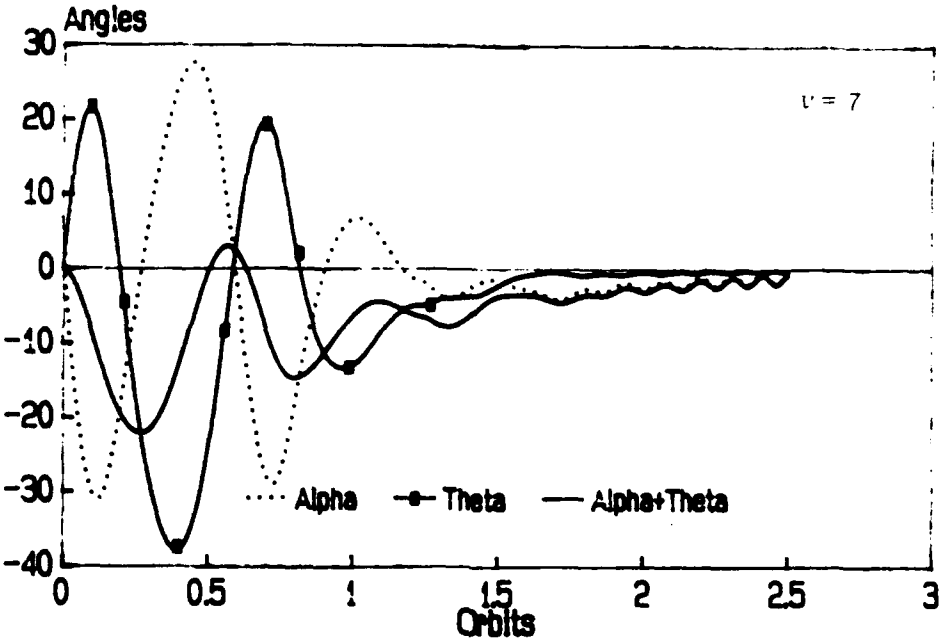

Fig. 14 Typical System Responses when a Constant Gain ν is Used

4. THE OPTIMAL LQG DIGITAL CONTROL OF AN ORBITING TETHERED ANTENNA/REFLECTOR SYSTEM†

The analysis and design of LQG optimal digital controllers and estimators are presented for an orbiting tethered shell system. Both the shell and tether are considered to be flexible. In this paper the emphasis is placed on: the mathematical models of the dynamics; the influence of the number of actuators and their locations; the methods of measurement of the state variables and design of LQG optimal digital controllers and observers.

Attitude and shape control is assumed to result from point actuators and tether tension. A symmetric design for the actuator locations is found by means of the concept of the degree of controllability and related simulations. To design a closed-loop control system, measurement is an important problem. If the tether transverse motion (swing and transverse vibration) is not directly measured, the system is not observable. One of the main contributions of this paper is a new practical method to measure the tether transverse motion. With the measurement of the tether transverse motion and several other properly placed sensors, the system will be completely observable.

The analysis and design of the optimal LQG digital control system for the tethered shell has been certified by simulation. For a system with joint bodies (a flexible shell and a flexible tether) the order of the system is very high. After maximizing the degrees of controllability and observability the best combination of the controller and observer pole locations is found by carefully selecting the wheighting matrices. Typical figures show transient responses under LQG synthesized control laws.

4.1 INTRODUCTION

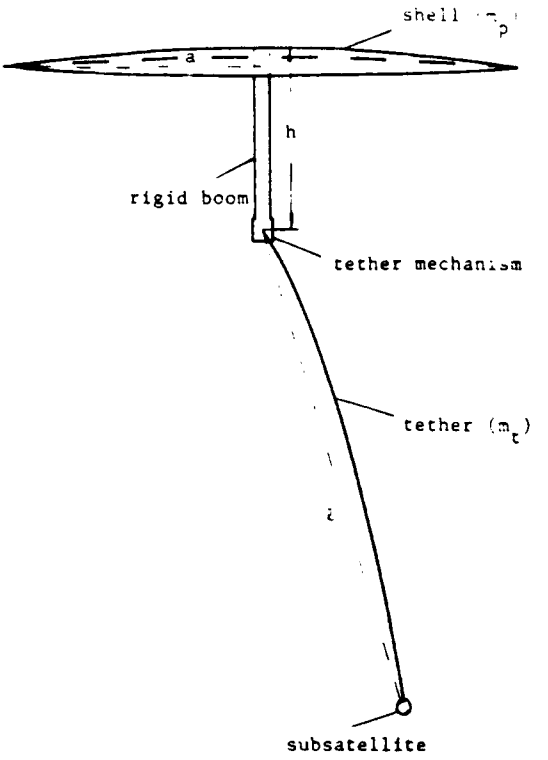

FIG. 1. Tethered Antenna/Reflector System.

Since the early 1970's very large space antennas have been proposed for power transmission, astronomical research and communications. The gravity stabilized configuration is particularly suited for large flexible systems to alleviate the problems associated with the active control of large structures. A tethered shell structure (Fig.1) to provide the favorable moment of inertia distribution for overall gravitational stabilization has been investigated by Liu and Bainum[1]. In their paper for a rigid shell and a flexible tether, the control problem, by using the continuous-time linear quadratic regulator (LQR) technique, has been solved. Because of the huge size and small mass, it is necessary for the future analysis to consider the shell to be flexible. The vibrations of the shell affect the tether motion and tension, and are coupled to the rotations of the shell. To control the shape and attitude of the shell and the tether, tether tension alone is not enough; therefore, it is suggested to add a few point actuators. The number and location of the actuators are determined by means of the concept of the degree of controllability. The state measurement is another important problem. In this paper it is shown that the system will be unobservable if the tether out-of-(orbit)plane swing motion or transverse vibration is not directly measured. A method to measure the tether transverse vibration and swing motion is developed in this paper; this method may be implemented in engineering practice, and can provide a high measurement accuracy. It can be used for any orbiting tethered system. With this method and a few properly placed sensors, it is

found that the system will have a satisfactory degree of observability.

In engineering practice a discrete time data system is more practical for the controller based on the on-board computer. Thus the technique of LQG (design of the optimal stochastic controller for a problem described in terms of linear system models, quadratic cost criteria, and Gaussian noise models) is employed to synthesize a controller with a Kalman filter to deal with the measurement noise and plant noise in the presence of sampled data observations.

4.2 MATHEMATICAL MODEL

Dynamical Equations

The mathematical model of a tethered shell system in orbit was developed in Ref. 1. The resulting linearized equations of motion were developed as:

1) shell attitude:

$$\psi'' - \Omega_x^* \psi - (1+\Omega_x^*)\,\phi' = (L_{Epx} + L_{epx}) / J_x \omega_c^2 \tag{1}$$

$$\theta'' - 3\Omega_y^* \theta - 2\sum_n I_1^{(n)} a e'_{Pn} / J_y^* - (h/J_y^*)\,[\sum_m I_{\phi_m}^* C_m'' + 2m_{st}^* (L' - u'_{Po}) + 2\sum_m I_{\phi_m}^* A_m' - I_x^* \alpha''] = (L_{Epy} + L_{epy}) / J_y^* \omega_c^2 \tag{2}$$

$$\phi'' + 4\Omega_z^* \phi + (1-\Omega_z^*)\,\psi' - h[(\gamma'' + \gamma) I_x^* + \sum_m I_{\phi_m}^* (B_m'' + B_m)] / J_z^* = -(L_{Epz} + L_{epz}) / J_z^* \omega_c^2 \tag{3}$$

2) tether longitude and swing motions:

$$\omega_c^2 [m_{st}^* (L'' - u_{p_o}'' + 3u_{p_o}) + \sum_m I_{\phi_m}^* (A_m'' - 3A_m) - 2\sum_m I_{\phi_m}^* C_m' + (2\alpha' + 2\theta' - 3) I_x^* - h m_{st}^* (3 - 2\theta')] = F_{tx} + (m_p E_{stx} - m_{st} E_{px}) / m_\Sigma \tag{4}$$

$$H_{xx}^* \alpha'' + (\theta'' + 3\alpha + 3\theta)(H_{xx}^* + h I_x^*) - \sum_m H_{x\phi_m}^* C_m'' - 3\sum_m (H_{x\phi_m}^* + h I_{\phi_m}^*) C_m - 2 I_x^* (L' - u'_{p_o}) - 2\sum_m H_{x\psi_m}^* A_m' = L_{ey} / \omega_c^2 \tag{5}$$

$$H_{xx}^* (\gamma'' + \gamma) - (H_{xx}^* + h I_x^*)(\phi'' + 4\phi - 3\gamma) + \sum_m H_{x\phi_m}^* (B_m'' + B_m) + 3\sum_m (H_{x\phi_m}^* + h I_{\phi_m}^*) B_m = L_{ez} / \omega_c^2 \tag{6}$$

3) tether and shell vibrations:

$$I^*_{\psi_n}(L''-u''_{p_o}+3u_{p_o})+\sum_m H^*_{\psi_n\psi_m}(A''_m-3A_m)-2\sum_m H_{\psi_n\phi_m}C'_m+(2\alpha'+2\theta' \quad (7n)$$
$$-3)H^*_{x\psi_n}+I^*_{\psi_n}h(2\theta'-3)+\sum_m K_{mn}A_m=H^{(n)}_{ex}$$

$$\sum_m H^*_{\phi_n\phi_m}C''_m+2I^*_{\phi_n}(L'-u'_{p_o})+2\sum_m H_{\phi_n\psi_m}A'_m-H^*_{x\phi_n}(\alpha''+\theta''+3\alpha+3\theta) \quad (8n)$$
$$-hI^*_{\phi_n}(\theta''+3\alpha+3\theta)+H_{\phi_n\phi_n}\omega_n^2C_n=H^{(n)}_{ez}$$

$$\sum_m H_{\phi_n\phi_m}(B''_m+B_m)+(\gamma''+4\gamma-\phi''-4\phi)H^*_{x\phi_n}-I^*_{\phi_n}(\phi''+4\phi-3\gamma)h \quad (9n)$$
$$+H_{\phi_n\phi_n}\omega_n^2B_n=H^{(n)}_{ey}$$

$$\epsilon''_{p_n}+(\Omega_n^2-3)\epsilon_{p_n}+2I_1^{(n)}\theta'/M_na=(3I_1^{(n)}+F_{p_x}\phi^o_p+E_n/\omega_c^2)/M_na \quad (10n)$$

ψ, θ, ϕ: yaw, pitch & roll angles of the shell, respectively;
J_x, J_y, J_z: inertial moments of the shell about the principal axes x, y and z, respectively;

$$\Omega^*_x=(J^*_z-J^*_y)/J_x \quad \Omega^*_y=(J_x-J^*_z)/J^*_y \quad \Omega^*_z=(J^*_y-J_x)/J^*_z$$

$$J^*_y=J_y+m^*_{st}h^2+I^*_xh \qquad J^*_z=J_z+m^*_{st}h^2+I^*_xh$$

m_p, m_t, m_s: masses of the shell, tether and subsatellite, respectively;

$$m_\Sigma=m_p+m_{st}; \quad m_{st}=m_s+m_t; \quad m^*_{st}=m_{st}\cdot m_p/m_\Sigma; \quad I_{(.)}=\int_{st}(.)\,dm$$

$$I^*_{(.)}=m_pI_{(.)}/m_\Sigma; \quad H_{(.)(*)}=\int_{st}(.)(*)\,dm; \quad H^*_{(.)(*)}=m_pH_{(.)(*)}/m_\Sigma$$

$\Psi_m = \sin(\beta_m/L)$, $\Phi_m=\sin(n\pi x/L)$ the m^{th} modal shape functions of the tether longitudinal and transverse vibrations, respectively;

L_{Epx}, L_{Epy}, L_{Epz}: the components of torque, produced by E_{st} and E_p, which appear in the tether force acting on the shell;

$$E_{st}=\int_{st}e\,dm; \quad E_p=\int_p e\,dm; \quad E=E_p+E_{st}; \quad \begin{bmatrix} e\text{: the external force} \\ \text{acting per unit mass} \end{bmatrix}$$

L_{epx}, L_{epy}, L_{epz}: the components of torque contributed by the external force acting on the shell;

h: the length of the boom;

$$\epsilon_{pn}=A_{pn}/a,$$

A_{pn}: the n^{th} modal amplitude of the shell;

a: the base radius of the shell;

ω_c: the orbital angular velocity;

M_n: the n^{th} modal mass;

$$\xi=r/a;$$

r: radial distance of a shell element from the symmetry axis;

$$I_1^{(n)}=\int_p x_p \Phi_{p_n} dm; \quad \begin{bmatrix} x_p\text{: coordinate of differential area on the} \\ \text{surface above the base plane of the shell} \end{bmatrix}$$

$$\Phi_{p_n}=A_{pj}[a^{p+4}C_{pj}\xi^p/(RD\lambda_{pj}^4)+J_p(\lambda_{pj}\xi)+D_{pj}I_p(\lambda_{pj}\xi)]\cos p(\beta_1+\beta_o)$$

the n^{th} modal shape function of shell vibration[2]

R: the radius of the shell curvature;

p, j: numbers of the nodal diameters (meridians) and nodal circles, respectively;

$J_p(.)$, $I_p(.)$: Bessel function and modified Bessel function, respectively, of the first kind and order p;

$$D=E_p h_p^3/12(1-\nu^2),$$

bending stiffness;

ν: Poisson's ratio;

E_p: Young's modulus of the shell;

h_p: wall thickness of the shell;

$$\Omega_n=\omega_{pn}/\omega_c,$$

ω_{pn}: shell frequency of the n^{th} mode,

E_n: generic force on the n^{th} mode;

F_{px}: component of the tether force acting on the shell along the shell symmetry axis;

Φ_p^o: shape function on the shell apex;

A_m, B_m & C_m: the amplitudes of the longitudinal, in-plane and out-of-plane components of the m^{th} mode of the tether;

u_{po} : the displacement of shell apex;

ω_n: the n^{th} mode natural frequency of tether transverse vibration,

$$\omega_n^2=n^2\pi^2(1+3m_s/m_t)-3/4;$$

F_{tx}: tether tension,

L_{ey} & L_{ez}: the torques produced by the external force;

α, γ: tether in-plane and out-of-plane swing angles, respectively;

H_{ex}, H_{ey} & H_{ez} result from the external force[3];

L : tether length;

$$K_{mn}=\begin{bmatrix} 0, & m\neq n \\ EA\beta_m^2(1+m_s\sin^2\beta_m/m_t)/2L & m=n \end{bmatrix}$$

E : Young's modulus of the tether;
A : the area of tether cross section;
$(\ )'=d(\ )/d\tau$, $\tau=\omega_c t$;

It is noted that only the modes without nodal diameters (p=0) are coupled to the rotation, so the first four of them (j=1, 2, 3 and 4) are considered. For the modes with one nodal diameter (p=1) whose amplitudes are quite large during the attitude adjusting, the first three of them (j=1, 2 and 3) are included. For the modes without nodal circles (j=0), the influence of the shell curvature remains insignificant. Since the frequencies for these modes are very nearly equal to the corresponding flat-plate frequencies, the frequencies are very low. The mode with two nodal diameters is taken as an example. For tether transverse vibration, six modes are taken, three for in-plane, three for out-of-plane. The following proposed numerical values of a tethered shell system are adopted here:

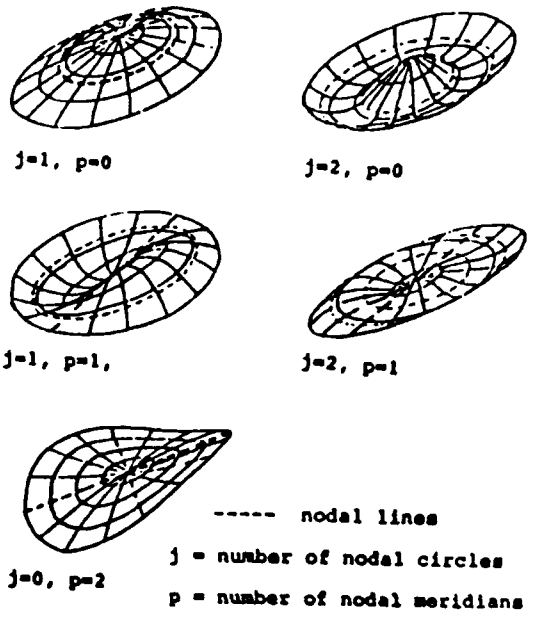

Fig.2 Several Modal Shapes of a Shell

a (shell base radius)=100 m. m_p (shell mass)=10000 kg.
R (shell curvature radius)=5 km. H (shell height)=1 m.
ν (shell Poisson's ratio)=1/3 h_p (shell thickness)=1 cm.
E_p (shell Young's modulus)=$8.4047*10^9$ N/m^2
m_s (subsatellite mass)=500 kg. m_t (tether mass)=8.35 kg.
L_c(commanded tether length)=1 km. h (boom length)=80 m.
AE (tether axial stiffness)= 61645 N.

The deformations of several modes are shown in Fig.2, and the results of calculations for a few generic modes is shown in Table 1.

n	(p, j)	λ	ω_n	A_{pj}	C_{pj}	D_{pj}	$I_1^{(n)}$
1	(0, 1)	3.012	1.02778	2.1979	0	-.08381	2875.55
2	(0, 2)	6.206	1.02946	3.1389	0	3.119e-3	-322.84
3	(0, 3)	9.371	1.03692	3.8468	0	-1.28e-4	93.44
4	(0, 4)	12.53	1.05696	4.4425	0	5.368e-6	-38.73
5	(1, 1)	4.530	1.02821	3.8359	0	-.01901	0
6	(1, 2)	7.737	1.03198	4.9627	0	7.045e-4	0
7	(1, 3)	10.91	1.04459	5.8752	0	-2.845e-5	0
8	(2, 0)	2.292	0.00867	3.6597	-3.47e-6	0.2240	0

Table 1. The Results of Calculations for a Few Generic Modes of the Shell

Point Actuator Placement and Model

To control the shape and attitude of the shell and the tether, tether tension alone is not sufficient, so that a few point actuators are added. The concept of the degree of controllability has been used for determining the placement of the actuators on the shell[4]. The degree of controllability is the scalar measure of system controllability and its reciprocal indicates the effort to control the system. The values of the degree of controllability for some actuator placement designs are listed in Table 2. It is assumed that the thrusters at the shell's edge have two jet directions: i) tangent to the edge; ii) normal to the shell surface. Each of the other thrusters has

Case	Number of Act.	Locations of Actuators	Degree of Controllability
1	6		0.0
2	6		$1.457*10^{-11}$
3	6		0.0
4	12	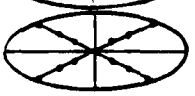	0.0
5	12	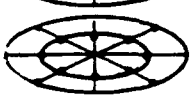	$5.893*10^{-11}$
6	12	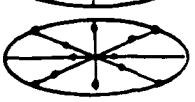	$5.443*10^{-9}$
7	12	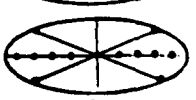	$5.443*10^{-9}$
8	8		$4.987*10^{-9}$

Table 2. The Degree of Controllability for a Few Actuator Designs

only one jet direction, i.e. normal to the shell surface. In case 8 only eight actuators are used, and the degree of controllability is satisfactory, so this actuator location design is recommended.

For an actuator which can generate a force $\mathbf{f}_i=(f_x \quad f_y \quad f_z)^T$ and is placed at a location $\mathbf{r}_i=(x_i \quad y_i \quad z_i)^T$ the control torque is given by $\mathbf{r}_i \times \mathbf{f}_i$, so in eqs. (1)-(3)

$$(L_{epx} \quad L_{epy} \quad L_{epz})^T = \Sigma \mathbf{r}_i \times \mathbf{f}_i \qquad (11)$$

$$(L_{Epx} \quad L_{Epy} \quad L_{Epz})^T = (0 \quad C_d E_{pz} \quad C_d E_{py})^T \qquad (12)$$

where C_d is the distance between the mass centers of the shell and the tethered shell system. In the remaining equations

$$L_{ey} \approx -I_x E_{pz} / m_\Sigma \qquad (13)$$

$$L_{ez} \approx I_{py} E_{py} / m_\Sigma \qquad (14)$$

$$H_{ex}^{(n)} = -I_{\phi_n} E_{px} / m_\Sigma \qquad (15)$$

$$H_{ey}^{(n)} = -I_{\phi_n} E_{py} / m_\Sigma \qquad (16)$$

$$H_{ez}^{(n)} = -I_{\phi_n} E_{pz} / m_\Sigma \qquad (17)$$

$$E_n = \sum_{i=1}^{8} \phi_{p_n}(y_i, z_i) f_i \qquad (18)$$

(each jet is along the shell's x axis)

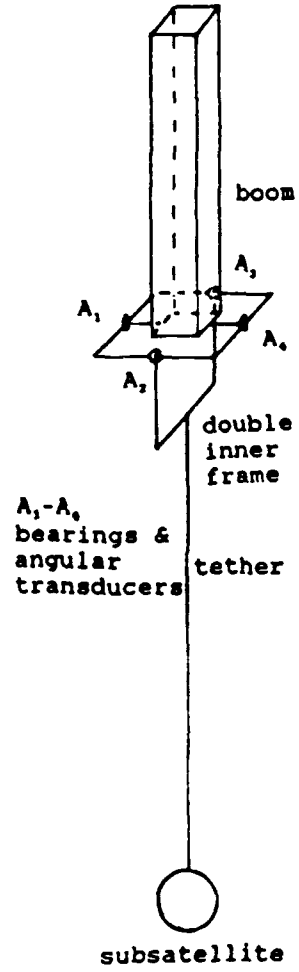

Fig.3a. A Design for Measurement of Transverse Motion of the Tether

Sensors and Observational Model

The system will be unobservable if tether transverse motion (swing and vibration) is not measured. A new method to measure the motion is shown in Fig.3a. The accuracy of angular transducer can be very high (e.g. the ones used on inertial platforms) during station keeping (i.e. the error angle is very small). The subsatellite is quite heavy, so that an inner framed structure is adopted. Since the tether can bear only the longitudinal tension, the position of the frame should coincide with the tangent direction of the tether at the attachment point

(Fig.3b). The displacement of the tether in-plane vibration is approximated by

$$W=\sum_{n=1}^{\infty} C_n(t)\ \sin(n\pi x/L) \qquad \text{then}$$

$$\alpha_1 \sim \tan\alpha_1 = dW/dx|_{x=0} = \sum_{n=1}^{\infty} C_n(t)\ (n\pi/L)\cos(n\pi x/L)\,|_{x=0} = \sum_{n=1}^{\infty} C_n(t)\ (n\pi/L)$$

The angular transducer A_2 is assumed to measure the in-plane displacement between the shell reference axis and the tether line

$$y_1 = K_\alpha(\alpha+\alpha_1) = K_\alpha[\alpha+\sum_{n=1}^{\infty} C_n(t)\ (n\pi/L)] \qquad (19)$$

Similarly for out-of-plane case, the value obtained from transducer A_1 is

$$y_2 = K_\gamma[\gamma+\sum_{n=1}^{\infty} B_n(t)\ (n\pi/L)] \qquad (20)$$

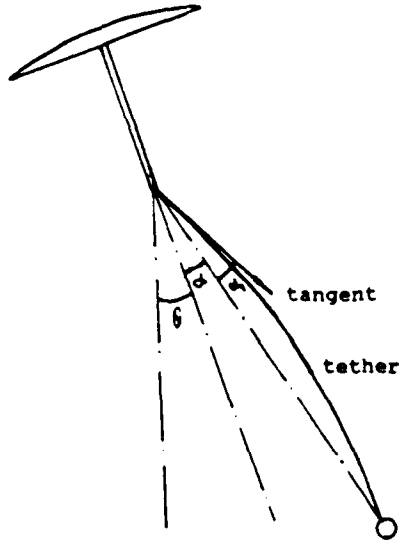

Fig.3b. The In-plane Angle Between the Deformed Tether and the Shell Reference

A dial with magnetic encoder is assumed to be used to measure tether length and its changing rate. The dial is fixed to the reel from which the tether is retrieved or deployed. When the dial turns it produce a series of impulses. The sum of the impulse number represents tether length, and the reciprocal of impulse interval represents the rate of tether change.

$$y_3 = K_e e \qquad (21) \qquad y_4 = K_e e' \qquad (22)$$

where $\epsilon=(L-L_c)/L_c$
L_c is the commanded length of the tether.

The shell attitude is assumed to be measured by an inertial platform based on gyroscopes. The advantage of the inertial platform is that it produces signals, for both the attitude and angular velocities, with a high signal:noise ratio. The drift of the inertial devices is then modified by two infra-red horizon sensors of the Earth and two sun sensors[5]. The reason why an inertial platform is used is that

the infra-red and sun sensors give signals with low ratios of signal to noise, and in the dark part of the orbit the sun sensor can not give any signal at all. So the measurement equations for the shell attitude are:

$$y_5=K_\theta\,\theta \quad (23) \qquad y_6=K_\psi\,\psi \quad (24) \qquad y_7=K_\phi\,\phi \quad (25)$$

$$y_8=K_{\theta'}\theta' \quad (26) \qquad y_9=K_{\psi'}\psi' \quad (27) \qquad y_{10}=K_{\psi'}\phi' \quad (28)$$

It is assumed that four displacement sensors, which are collocated with the actuators in the first and second quadrants, are used to measure the shell vibration:

$$y_i=K_i a\sum_{j=1}^{\infty}\Phi_{pj}^{(j)}(\xi_i\,\zeta_i)\,e_{pj}(t) \qquad (i=11,12,13,14) \qquad (29)$$

Eqs.(19)-(29) consist of the measurement equations, for which the system is completely observable.

The State Equations and LQG Regulators and Observers

After substituting Eqs. (11)-(15n) into Eqs. (1)-(10n), and after some algebraic manipulations, the system equations can be written in the state vector form:

$$x' = A\,x + B\,u \qquad (30)$$

$$where \quad u=(f_1, f_2, \ldots\ldots f_8, \Delta f)^T$$

$$x=(\theta,\alpha,e,e_{p_1},e_{p_2},\ldots\ldots,e_{p_8},c_1,c_2,c_3,\psi,\phi,\gamma,b_1,b_2,b_3,$$
$$\theta',\alpha',e',e'_{p_1},e'_{p_2},\ldots\ldots,e_{p_8},c_1',c_2',c_3',\psi',\phi',\gamma',b_1',b_2',b_3')^T$$

$$c_i=C_i/L_c \qquad b_i=B_i/L_c \qquad \Delta f=F_{tx}/(\omega_c^2 m_{st}^* L_c)+3\left[(m_s+m_t/2)/m_{st}+h/L_c\right]$$

In fact, dynamic systems are driven not only by their own control input, but also by disturbances which we can neither control nor model deterministically. Sensors generally do not provide exact readings of desired quantities, but introduce their own system dynamics and distortions as well. Furthermore these devices are also noise corrupted. In order to solve these difficulties, the LQG techniques (design of the optimal stochastic controller for a problem described in terms of linear system models, quadratic cost criteria, and Gaussian noise models) are effective. In this section the LQG theory is

applied to the design of suboptimal regulators and estimators for the tethered shell system.

For the infinite-time optimal regulator, given the system represented by Eqs.(30), the task is to find the optimal control such that the performance index

$$J=\frac{1}{2}\int_o^\infty (x^T Q_c x+u^T R_c u)\,dt \qquad (31)$$

is minimized. In Eq.(31) Q_c is a symmetric positive semidefinite matrix; R_c is a symmetric positive definite matrix. After discretization and consideration of noise, Eq.(30) becomes[6]

$$x(k+1)=\tilde{A}(T)\,x(k)+\tilde{B}(T)\,u(k)+w(k) \qquad (32)$$

$$y(k)=C\,x(k)+v(k) \qquad (33)$$

$$\text{where}\quad \tilde{A}(T)=e^{AT} \qquad \tilde{B}(T)=\int_o^T e^{AT}\,B\,dt$$

and Eq.(33) is the state vector form of Eqs.(19)-(28). w(k) and v(k) are the n-dimension and m-dimensional white Gaussian discrete time noise with

$$E[w(i)\;w^T(j)]=Q\delta_{ij} \qquad E[v(i)\;v^T(j)]=R\delta_{ij}$$

respectively, and assumed to be independent of each other and the initial conditions. The initial condition x(0) is modelled as a Gaussian random vector with mean, x_o and covariance, P_o.

From Eq.(31), the discretized performance index is

$$J=\frac{1}{2}\sum_{k=0}^{\infty}[x^T(k)\tilde{Q}x(k)+2x^T(k)\tilde{W}u(k)+u^T(k)\tilde{R}u(k)] \qquad (34)$$

$$\text{where}\ \tilde{Q}=\int_o^T e^{A^T t}\,Q_c\,e^{At}\,dt \qquad \tilde{W}=\int_o^T e^{A^T t}\,Q_c\,g(t,0)\,dt$$

$$\tilde{R}=\int_o^T [R_c+g^T(t,0)\,Q_c\,g(t,0)\,dt \qquad g(t,0)=\int_o^t e^{As}\,B\,ds$$

The problem now is to find the control u(k), so that the performance index in Eq.(34) is minimized. If the system represented by Eq.(32) is controllable (or stabilizable) and

observable (detectable), the LQG solution is[7,8]

$$u(k) = -G\,\hat{x}(k) \tag{33}$$

$$G=(\tilde{R}+\tilde{B}^T P\tilde{B})^{-1}(\tilde{B}^T P\tilde{A}+\tilde{W}^T) \tag{34}$$

where P satisfies the algebraic Ricatti equation

$$P=\tilde{A}^T P\tilde{A}+\tilde{Q}-(\tilde{A}^T P\tilde{B}+\tilde{W})(\tilde{R}+\tilde{B}^T P\tilde{B})^{-1}(\tilde{B}^T P\tilde{A}+\tilde{W}^T) \tag{35}$$

The state estimate at the k^{th} interval can be related to its predicted value based on information from the $(k-1)^{st}$ interval; together with the measurement vector at the k^{th} interval, as

$$\hat{x}(k)=\hat{x}(k/k-1)+K[y(k)-C\hat{x}(k/k-1)] \tag{36}$$

$$\text{where} \quad \hat{x}(k/k-1)=\tilde{A}\,\hat{x}(k-1)+\tilde{B}\,u(k-1) \tag{37}$$

$$K = P_e\,C^T\,(\,C\,P_e\,C^T + R\,)^{-1} \tag{38}$$

The covariance of the state estimate, P_e, satisfies the algebraic Ricatti equation

$$P_e=(\tilde{A}-K^*C)\,P_e(\tilde{A}-K^*C)^T+K^*RK^{*T}+Q \quad (\text{ where } K^*=\tilde{A}K\,) \tag{39}$$

Due to computational delay, what is often considered for implementation is not the control law given by Eq.(33), but a suboptimal control

$$u\,(\,k\,) = -\,G\;\hat{x}\,(\,k\,/\,k-1\,) \qquad \text{where}$$

$$\hat{x}(k+1/k)=\tilde{A}\hat{x}(k/k-1)+\tilde{B}u(k)+K^*[y(k)-C\hat{x}(k/k-1)] \tag{40}$$

It is wise to seek the possibility of a separate determination of the state estimate and the controller. The error of the predicted estimate of the state is defined as

$$\Delta X(k/k-1)=x(k)-\hat{x}(k/k-1) \tag{41}$$

the x(k+1) and Δx(k+1/k) may be combined into a simple system described by the state equations[9]

$$\begin{bmatrix} x(k+1) \\ \Delta x(k+1)/k) \end{bmatrix} = \begin{bmatrix} \tilde{A}-\tilde{B}G & \tilde{B}G \\ 0 & \tilde{A}-K^*C \end{bmatrix} \begin{bmatrix} x(k) \\ \Delta x(k/k-1) \end{bmatrix} + \begin{bmatrix} I & 0 \\ I & -K^* \end{bmatrix} \begin{bmatrix} w(k) \\ v(k) \end{bmatrix} \tag{42}$$

From Eq.(42), the LQG suboptimal control dynamics consist of

two parts: the dynamics of the plant with a feedback controller and the dynamics of the estimator feedback loop. The matrices describing the dynamics of the closed loop controller and the closed loop estimator are

$$A_c^*=\bar{A}-\bar{B}G \qquad (43) \qquad \text{and} \qquad A_e^*=\bar{A}-K^*C \qquad (44)$$

respectively. The eigenvalues of A_c^* and A_e^* are independent of each other. In the synthesis it is, therefore, possible to arrange the poles of the estimators and controllers separately.

It is well known that if and only if the open loop system model is both stabilizable with respect to u(k) and detectable with respect to y(k), there do exist gains G and K^* that can provide asymptotic closed loop stability. Furthermore, under the stronger assumptions of complete controllability and complete observability (as in the designs of the actuators and measurements for the tethered shell system, here), we can place both the regulator and observer poles arbitrarily (within the restriction of the complex conjugate pairs).

It should be noted that in Eq.(30) the differentials are respect to the orbit time, i.e.

$$x_i'=dx_i/d\omega_c t=(1/\omega_c)dx_i/dt$$

If the noise added to dx_i/dt is w_i, the noise added to x_i' should be $(1/\omega_c)w_i$. So the covariance matrixes should be[10]:

$$Q=\mu_Q\begin{bmatrix} I_{20} & 0 \\ 0 & (1/\omega_c^2)\,I_{20}\end{bmatrix} \qquad R=\mu_R\begin{bmatrix} I_{10} & 0 \\ 0 & (1/\omega_c^2)\,I_4\end{bmatrix} \qquad (45)$$

For the control loop let the weighting matrices

$$Q_c=C^T\,C \qquad R_c=\mu_c I$$

In order to find the appropriate arrangement of the observer and controller poles it is necessary to study the loci of the eigenvalues of A_e^* and A_c^* with μ_Q, μ_R and μ_c, respectively. The maximum and minimum moduli of the eigenvalues of A_e^* and A_c^* vs. the different parameters μ_Q, μ_R and μ_c are listed in Table

3 and 4, respectively.

Based on these data in Tables 3 and 4 we can arrange the position of the controller and observer poles.

Table 3. Max. & Min. Moduli of Eigenvalues of A_e^* vs. μ_Q ($\mu_R=10^{-8}$)

μ_Q	min.	max.
10^{-11}	6.3514e-4	0.96714
10^{-12}	1.6817e-2	0.97003
10^{-14}	0.11649	0.97714
10^{-16}	0.55691	0.98687

Table 4. Max. & Min. Moduli of Eigenvalues of A_c^* vs. μ_c

μ_c	min.	max.
10^{-3}	0.88481	0.99948
10^{-4}	0.83930	0.99943
10^{-6}	0.73230	0.99850
10^{-7}	0.57579	0.99701

4.3 SIMULATIONS

It is assumed that the accuracy of the displacement sensors is about 1 cm. for the shell deflection, the angular sensor accuracy is about 10^{-4} rad., and the modelling error for the dynamical system is less than the error of the measurement sensors. In Eq.(45) the parameters of the covariance matrices used for simulation are $\mu_R=10^{-8}$ and $\mu_Q=10^{-16}$ It is also assumed that both the measurement and the plant noises are Gaussian white noises with zero mean.

In general, as for the design of the Kalman filter, the considered covariances of the measurement and plant noises should be greater than or equal to the actual ones. After these conditions have been satisfied the location of the observer poles may be changed by means of the variation of the parameters μ_R and μ_Q. When $\mu_R=10^{-8}$, $\mu_Q=10^{-16}$ the minimum and maximum moduli of the eigenvalues of A_e^* (observer) are 0.55691 and 0.98687.

As we know the minimum and maximum moduli of the observer closed-loop eigenvalues should be less than those of the controller closed-loop eigenvalues, so that the estimator can provide accurate timely state information for the controller. Based on this principle, the possible appropriate minimum and maximum controller eigenvalues are 0.57579 and 0.99701.

The initial state is also assumed to be noise-corrupted

$$\mathbf{x}(0)=\mathbf{x}_o+\mathbf{w}_o \qquad \mathbf{x}_o=E\{\mathbf{x}(0)\} \qquad P_o=E\{\mathbf{w}_o\,\mathbf{w}_o^T\}$$

The initial conditions are assumed as:

$x_1(0)=\theta(0)=0.1\ rad.$ $x_2(0)=\alpha(0)=0.1\ rad$ $x_3(0)=e(0)=0.001$

$x_4(0)=\dot{e}(0)=0.001$ $x_{12}(0)=c_1(0)=0.001$ $x_{15}(0)=\psi(0)=0.1\ rad.$

$x_{16}(0)=\phi(0)=0.1\ rad.$ $x_{17}(0)=\gamma(0)=0.1\ rad.$ $x_{18}(0)=b_1(0)=0.001$

and the rest of the initial conditions are taken to be zero. The initial values of the estimated state are assumed to be zero, i.e.,

$$x_i(0/-1)=0.0 \qquad (i=1, 2, \ldots\ldots, 40)$$

The strategy of choosing the sampling time, T, should be to select the sampling time as long as possible after the performance of the sampled-data system meets the requirements of the design. Generally speaking, too long a sampling interval tends to deteriorate the performance of a sampled data system (increase the sensitivity, decrease stability, loss of controllability etc.)[10] On the other hand, the implementation of a very short sampling interval may be limited by computer operation times and the expense of fast A/D and D/A devices. The choice of the sampling time, T, will also be constrained by the capability to restore the signal which comes from observational data, i.e. T meets Shannon's theorem, $t<\pi/\omega_m$, where ω_m is the maximum frequency of the input signal. In the simulation here T=5 sec.

The result of the simulations are shown in Figs.4-6. Fig.4 is for the in-plane motion, Fig.5 for the out-of-plane motion, and Fig.6 for each actuator force needed during the regulating process. Since the tether can not support compressive forces and a large tension force should be avoided, the tether tension boundary is set: $0<F_{tx}<$ 5 newton (Fig.4 c). The result of the simulation is satisfactory. The initial errors are converging smoothly, the required forces for each actuator are reasonable. After 5 minutes we can hardly see any difference between the actual value of each state variable and its estimate.

4.4 CONCLUSIONS

1) The actuator placement design used here is satisfactory. The degree of controllability is quite high considering only eight point actuators are applied. This design can control elastic vibrations and orientations of a flexible shell and a flexible tether, and it has been verified by simulations.

2) The system is not observable if the tether transverse motions are not directly measured. A new method of measuring tether transverse motion presented here can be applied not only to tethered shell systems, but also to any system with a tether. This design is easy to implement in engineering practice and of high accuracy of measurement.

3) The discrete time data system is more practical for a controller based on an on-board computer system. The sampling time, T=5 sec. is a good compromise between the performance of the system and the capacity of the on-board computer.

4) For a dynamic system with plant and measurement noises, the LQG technique is effective. As for the placement of the controller and observer poles, the minimum and the maximum moduli of the eigenvalues of the closed-loop observer must be less than the minimum and maximum moduli of the eigenvalues of the closed-loop controller, respectively, so that the observer can provide the timely and accurate estimate of the state variables for the controller. We should also ensure that the ratio μ_R/μ_Q can not be too small, otherwise the Kalman filter may become too sensitive to the observational noise.

5) Since the tethered shell system consists of a flexible shell and flexible tether, the dimensionality of the state vector is as high as 40. Because of the practical possibility of on-board computational implementation, it is suggested for further work to design low-order controllers based on robustness theory.

REFERENCES

1. L. Liu and P. M. Bainum, "Dynamics and Control of Tethered Antennas/Reflectors in Orbit", Presented at the Third International Conference on Tethers in Space, San Francisco, CA, May 17-19, 1989. Also in The Journal of the Astronautical Sciences, Vol.38, No.3 July-Sept. 1990, pp.247-268

2. Z. Tan and P. M. Bainum, "Minimum-Time Large Angle Slew of an Orbiting Flexible Shallow Spherical Shell System", Presented at the first Annual AAS/AIAA Space Flight Mechanics Conference, Houston, Texas, Feb. 11-13, 1991.

3. L. Liu and P. M. Bainum, "Effect of Tether Flexibility on Tethered Shuttle Subsatellite Stability and Control", PSN/NASA/AIDAA Second International Conference on Tethers in Space Venice, Italy, Oct. 4-8, 1987; also, Journal of Guidance, Control, and Dynamics, Vol.12, No.6, Nov.-Dec., 1989, pp 866-873.

4. G. Xing and P. M. Bainum, "Some Definitions of Degree of Controllability (Observability) for Discrete-Time System and their Applications", The 12th Biennial ASME Conference on Mechanical Vibrations and Noise, Sept. 17-20, 1989, Montreal, Canada.

5. G. Xing and P. M. Bainum, "The Optimal LQG Digital Shape and Orientation Control of an Orbiting Shallow Spherical shell system", 40th Congress of the International Astronautical Federation, Beijing, China, Oct. 7-12, 1989. Also in Acta Astronatica, Vol.21, No.10, 1990, pp. 719-731.

6. B. C. Kuo, "Design of Digital Control Systems with State Feedback and Dynamics Output Feedback", The Journal of the Astronautical Sciences, Vol.27, No.2, April-June, 1979, pp.207-214.

7. H. Kwakernaak and R. Sivan, Linear Optimal Control System, John Wiley and Sons Inc., New York, 1982.

8. P. S. Mybeck, Stochastic Models, Estimation and Control,

Vol.3, Academic Press, New York, 1982.

9. G. Xing and P. M. Bainum, "The Optimal LQG Control of Orbiting Large Flexible Beams", The Journal of the Astronautical Sciences, Vol.37, No.1, January-March 1989, pp. 59-78

10. Z. Tan and P. M. Bainum, "The Optimal LQG Digital Control of An Orbiting Large Flexible Platform" Presented at the International Conference on Dynamics, Vibration and Control, Beijing, China, July 3-7, 1990.

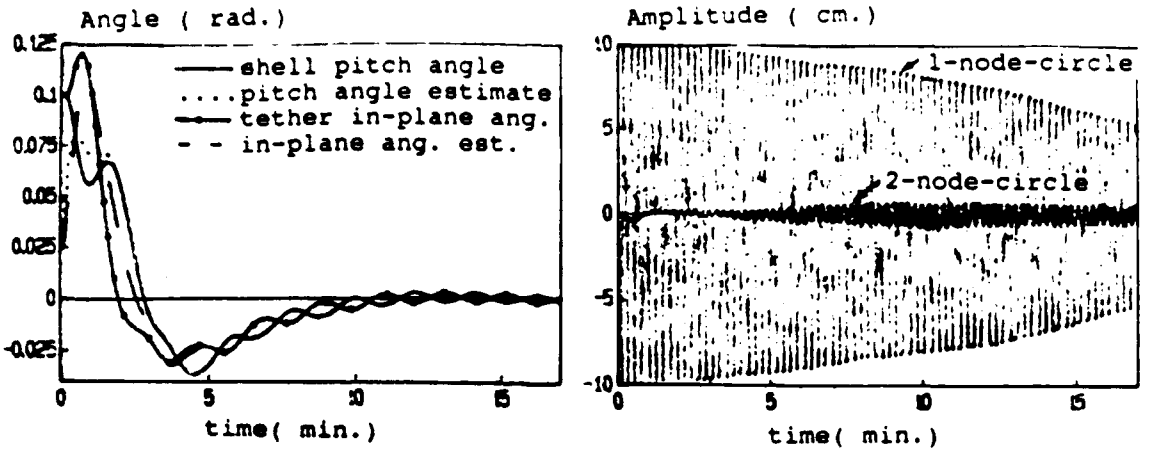

a. The shell pitch & tether swing

d.shell axisymmetric modes

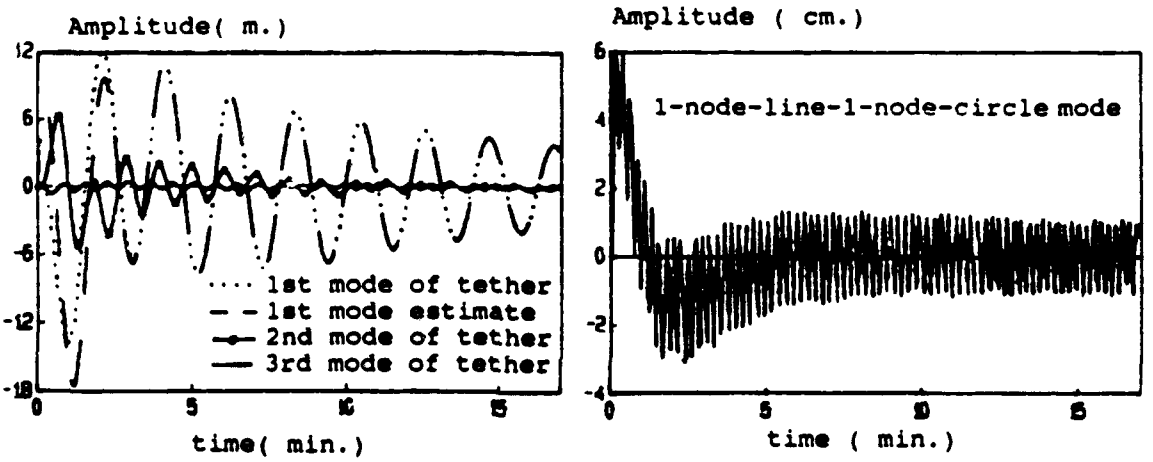

b. The tether in-plane vibration

e. shell non-axisymmetric-mode

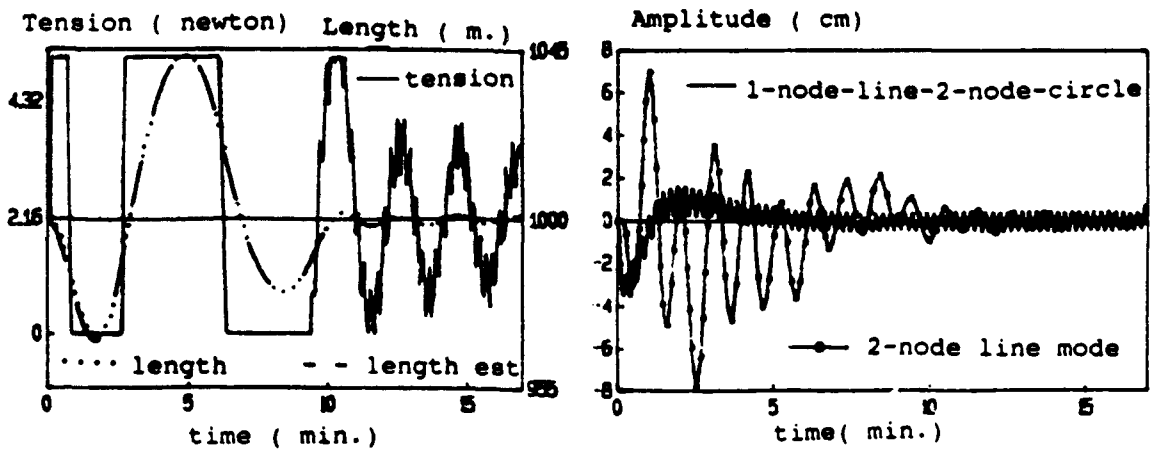

c. Tether tension & length

f. shell non-axisymmetric-modes

Fig.4.The transient response of the in-plane motion of a tethered shell system

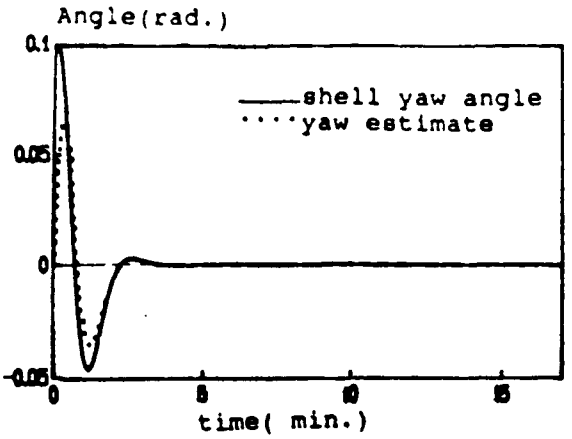

a.The shell yaw angle

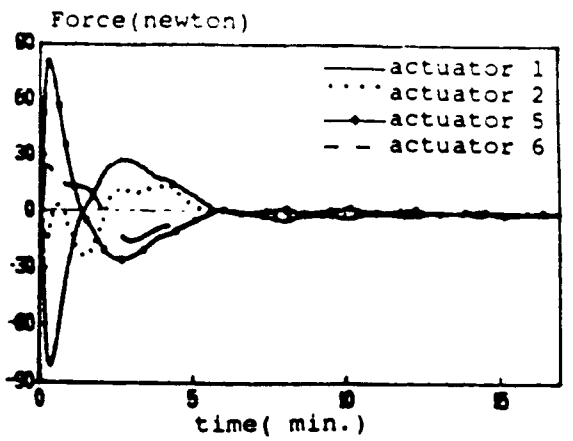

a. The actuators 1, 2, 5 & 6 (jets normal to shell)

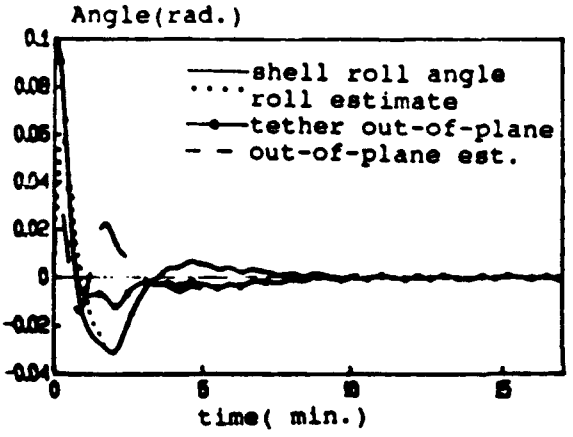

b.The shell roll & tether swing

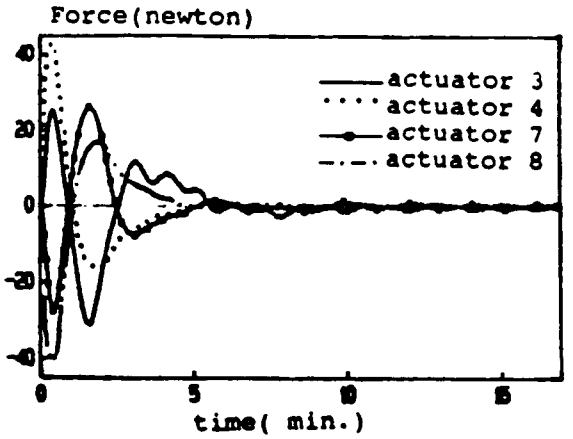

b. The actuators 3, 4, 7 & 8 (jets normal to shell)

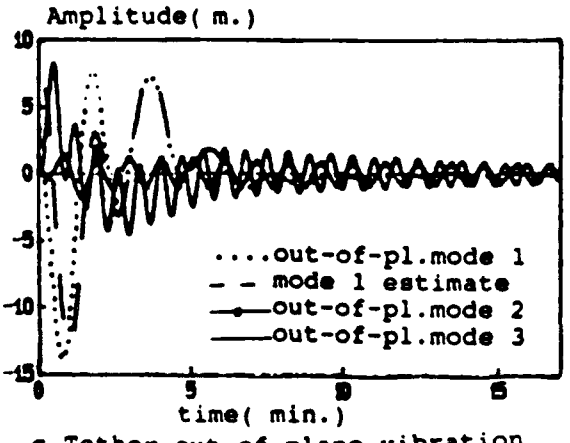

c.Tether out-of-plane vibration

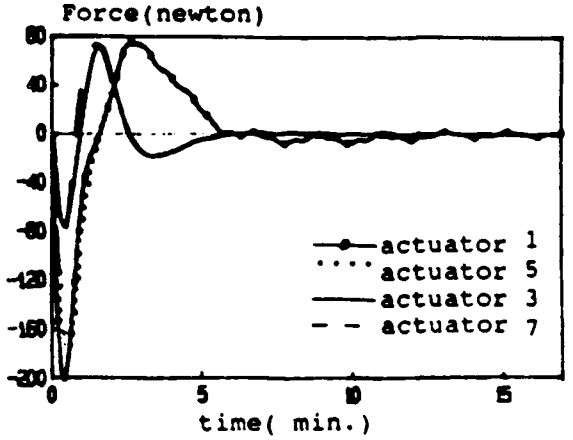

c. The actuators 1, 5, 3, 7 (jets tangent to the edge)

Fig.5.The transient response of the out-of-plane motion

Fig.6 The transient response of the actuators

5. EFFECTS OF SOLAR RADIATION PRESSURE ON THE TETHERED ANTENNA/REFLECTOR SUBSATELLITE SYSTEM

5.1 Introduction

Since the initial proposal of the tethered subsatellite system, the dynamics and control of the tethered subsatellite systems have been investigated by a host of investigators. A comprehensive survey article was given by **Misra** and **Modi** [1] recently. Sources of applications of tethers in space have been proposed for different purposes. For example, a number of very large space antenna and reflector types of orbiting structures have been proposed for power transmission, astronautical research and communications.

A tether tension control law based on the tether length and length rate for in-plane control was formulated by **Rupp** [2] and represented a pioneering effort in establishing the feasibility of control by using tether tension control modulation. Recently, **Bainum** and **Liu** [3] developed a system mathematical model of a class of large antenna and reflector orbiting structures which has an articulated tether connected supporting mechanism to provide the favorable moment of inertia distribution for over-all gravitational stabilization and controllable tether tension used for producing restoring torques on the shallow shell reflector. The optimal control law for tether tension control has been suggested and evaluated. The numerical results show that the in-plane motion of the tether could be asymptotically stable with Rupp's tension law; and the transient response can be improved significantly by carefully selecting optimal control gains with suitable state penalty and control penalty matrices.

As the different control laws are being developed, a question arises that if some environmental disturbances are considered, will the tension control laws still be suitable for maintaining the required pointing accuracy of the antenna/reflector subsatellite

system ?

It is known that the solar radiation pressure is one of the dominant environmental disturbances, especially in higher orbits. An overview about the environmental torques was given by **Shrivastava** and **Modi.**[4] The tension control is based on utilizing the gravity-gradient and centrifugal forces; therefore, the capability of the tension control will be decreased as the altitude level is increased. On the other hand, the solar radiation disturbance will be augmented because of less oxygen, nitrogen and ozone at the higher altitude.

In general, the disturbance forces and torques induced by solar radiation pressure vary with the illuminated area, the characteristics of the illuminated surface of the orbiting structure, and the offset of the center of solar radiation pressure from the center of mass of the system. The general formulations for evaluating the solar radiation pressure forces and torques are as follows: [5]

$$\underline{F_a} = -w\int_s (\hat{n}\cdot\hat{\theta})\,\hat{\theta}\,ds \tag{5.1}$$

$$\underline{F_f} = -2w\int_s (\hat{n}\cdot\hat{\theta})^2\,\hat{n}\,ds \tag{5.2}$$

$$\underline{F} = (1-\epsilon)\,\underline{F_a} + \epsilon\underline{F_f} \tag{5.3}$$

$$\underline{N_a} = -w\int_s (\hat{n}\cdot\hat{\theta})\,\underline{r}\times\hat{\theta}\,ds \tag{5.4}$$

$$\underline{N_f} = -2w\int_s (\hat{n}\cdot\hat{\theta})^2\,\underline{r}\times\hat{n}\,ds \tag{5.5}$$

$$\underline{N} = (1-\epsilon)\,\underline{N_a} + \epsilon\underline{N_f} \tag{5.6}$$

where $\underline{F}_a$: resultant solar radiation pressure force on a completely absorbing surface

$\underline{F}_f$: resultant solar radiation pressure force on a completely reflecting surface

$\underline{F}$: resultant solar radiation pressure force on a general surface with arbitrary reflectivity

$\underline{N}_a$: resultant solar radiation pressure torque on a completely absorbing surface

$\underline{N}_f$: resultant solar radiation pressure torque on a completely reflecting surface

$\underline{N}$: resultant solar radiation pressure torque on a general surface with arbitrary reflectivity

ϵ: reflection coefficient i.e. the ratio of the energy density of the reflected light flux to the energy density of the incident light flux

s: illuminated part of the surface

But there is a major difficulty in determining the boundary of the illuminated area on the surface of the orbiting structure. The illuminated area is affected by the position of the orbiting structure in the orbit, the attitude and the shape of the structure. Sometimes it is extremely difficult to obtain an exact analytical formulation for the solar radiation disturbance. **Bainum** and **Krishna** [6] used a numerical method to approximate the force and moment induced by the solar radiation pressure on an orbiting flexible beam and plate, because of the complicated vibrational modes and the time varying shadow attributed to each of those modes.

One of the objectives of the study is to develop the analytical formulations for the modelling of the solar radiation disturbance on a class of large tethered antenna/reflector types of orbiting structures. The other is to evaluate the effects of these disturbances in the case of station-keeping and to determine at which altitude level the tension control law is still able to maintain the satisfactory pointing accuracy of the tethered

antenna/reflector subsatellite system by numerical simulation.

5.2 Modelling of the Solar Radiation Disturbance Torques

The system discussed here is composed of a spherical shallow shell reflector, a boom attached at the apex of the shell reflector, an articulated tether connected at the end of the boom and a spherical subsatellite.(Fig. 5.1) For mathematical modelling of the solar radiation disturbance, the following assumptions are made:

1) The shell reflector, boom and the subsatellite are assumed to be rigid bodies, and the tether is compressible but considered as a straight line (neglecting the transverse deformation) during the swing motion. The surfaces of these bodies are characterized by isotropical reflectivity properties.
2) The spherical shallow shell is totally illuminated either on the inner shell surface or outer shell surface, since the ratio of the height of the shell to the radius of the base of the shell is far less than unity.
3) Local shadowing on the tether and the boom is considered. There are two phenomena; one is that some sections of the tether or the boom will not be illuminated in certain positions of the orbit due to the shadowing of the reflector; the other is that the boom or the tether is considered as a cylindrical column; therefore, at any instant of time the tether or the boom can only be illuminated on one side when the emission of the sun light and the reflected sun light from the Earth or other space objects are neglected. In addition, the shadow of the Earth on the orbit has been taken into account during the numerical simulation.
4) The solar incidence vector in the orbital coordinate reference system is treated as a time varying parameter. It varies with the inclination of the orbit and the position of the space structure in the orbit. A circular and equatorial orbit is

assumed in the numerical simulation without losing generality.

The coordinate systems used in the development of the system equations of motion are shown in Fig. 5.2; $OX_oY_oZ_o$ is an orbital reference system centered at the center of mass of the shell reflector with OX_o along the local vertical, OY_o along the normal to the orbit plane and OZ_o along the orbital tangent velocity direction. $OX_rY_rZ_r$ is a shell body reference frame, the axes OX_r, OY_r and OZ_r are principal axes of the shell reflector. $O_tX_tY_tZ_t$ is the tether reference frame with O_tX_t along the undeformed tether, where O_t is the point from which the tether is deployed or retrieved. The coordinates of O_t in the shell reference are $(h_x,0,0)$.

The yaw, pitch and roll angles of the shell are denoted by ψ, θ and ϕ, respectively. An Euler angle rotation sequence is assumed as: (1)ψ, (2)θ and (3)ϕ. Therefore the transformation from $OX_oY_oZ_o$ to $OX_rY_rZ_r$ is assumed to be given by:

$$\begin{bmatrix} X_r \\ Y_r \\ Z_r \end{bmatrix} = Q_r \begin{bmatrix} X_o \\ Y_o \\ Z_o \end{bmatrix} \tag{5.7}$$

where

$$Q_r = \begin{bmatrix} c\phi c\theta & s\phi c\psi + c\phi s\theta s\psi & s\phi s\psi - c\phi s\theta c\psi \\ -s\phi c\theta & c\phi c\psi - s\phi s\theta s\psi & c\phi s\psi + s\phi s\theta c\psi \\ s\theta & -c\theta s\psi & c\theta c\psi \end{bmatrix} \tag{5.8}$$

The in-plane swing angle of the tether, α, depicts the angle between the projection of the non-deformed tether in the orbit plane and the OX_r axis; and the out-of-plane swing angle of the tether, γ, indicates the angle between the projection of the undeformed tether in the OX_rY_r plane and the OX_r axis. The

transformation from $O_tX_tY_tZ_t$ to $OX_rY_rZ_r$ can be derived by:

$$\begin{bmatrix} X_r \\ Y_r \\ Z_r \end{bmatrix} = Q_t^{-1} \begin{bmatrix} X_t \\ Y_t \\ Z_t \end{bmatrix} + \begin{bmatrix} h_x \\ 0 \\ 0 \end{bmatrix} \tag{5.9}$$

where

$$Q_t = \begin{bmatrix} -c\gamma c\alpha & s\gamma & s\alpha c\gamma \\ s\gamma c\alpha & c\gamma & -s\alpha s\gamma \\ -s\alpha & 0 & -c\alpha \end{bmatrix} \tag{5.10}$$

The unit solar incidence vector can be formed in the orbital reference system:

$$\hat{\partial}_o = [a_o,\ b_o,\ c_o]^T \tag{5.11}$$

where a_o, b_o and c_o are components along the OX_o, OY_o and OZ_o axes, respectively. Furthermore, the unit solar incidence vector can be transformed into the shell reference system:

$$\hat{\partial}_r = \begin{bmatrix} a_r \\ b_r \\ c_r \end{bmatrix} = Q_r \begin{bmatrix} a_o \\ b_o \\ c_o \end{bmatrix} \tag{5.12}$$

here a_r, b_r and c_r represent the components along the OX_r, OY_r and OZ_r axes, respectively. Similarly, the unit solar incidence vector in the tether reference system can be written as:

$$\hat{\partial}_t = \begin{bmatrix} a_t \\ b_t \\ c_t \end{bmatrix} = Q_t \begin{bmatrix} a_r \\ b_r \\ c_r \end{bmatrix} \tag{5.13}$$

a_t, b_t and c_t are the components of the unit solar incidence vector along O_tX_t, O_tY_t and O_tZ_t axes, respectively.

The disturbance torque induced by the solar radiation pressure on the antenna/reflector can be expressed:

1) for completely absorbing shell surface

$$\underline{N_{ra}} = \begin{bmatrix} N_{rax} \\ N_{ray} \\ N_{raz} \end{bmatrix} = R_a \begin{bmatrix} 0 \\ c_r \\ -b_r \end{bmatrix}, \qquad (5.14)$$

2) for completely reflecting shell surface

$$\underline{N_{rf}} = \begin{bmatrix} N_{rfx} \\ N_{rfy} \\ N_{rfz} \end{bmatrix} = R_f \begin{bmatrix} 0 \\ c_r \\ -b_r \end{bmatrix}, \qquad (5.15)$$

3) for general shell surface with arbitrary reflectivity properties

$$\underline{N_r} = \begin{bmatrix} N_{rx} \\ N_{ry} \\ N_{rz} \end{bmatrix} = (1-\epsilon)\,\underline{N_{ra}} + \epsilon \underline{N_{rf}}, \qquad (5.16)$$

where

$$R_a = -\pi w R^3 c_r \sin^2\beta_0 \left(1 - \cos\beta_0 - \frac{r_0}{R}\right)$$

$$R_f = -\pi w R^3 c_r \sin^4\beta_0 \left(1 - \frac{r_0}{R}\right)$$

w: solar constant

β_0: cone angle of the spherical shell reflector

R: radius of the spherical shell reflector

r_0: distance from the apex of the shell to the center of mass of the shell

The disturbance torque induced by the solar radiation pressure on the boom has the form:

1) for completely absorbing boom surface

$$\underline{N_{ba}} = \begin{bmatrix} N_{bax} \\ N_{bay} \\ N_{baz} \end{bmatrix} = B_a \begin{bmatrix} 0 \\ -c_r \\ b_r \end{bmatrix}, \tag{5.17}$$

2) for completely reflecting boom surface

$$\underline{N_{bf}} = \begin{bmatrix} N_{bfx} \\ N_{bfy} \\ N_{bfz} \end{bmatrix} = B_f \begin{bmatrix} 0 \\ -\frac{b_r^2}{3}\sin^3\lambda_b - \frac{2}{3}b_r c_r \cos^3\lambda_b - c_r^2(\sin\lambda_b - \frac{\sin^3\lambda_b}{3}) \\ b_r^2(\cos\lambda_b - \frac{\cos^3\lambda_b}{3}) + \frac{2}{3}b_r c_r \sin^3\lambda_b + \frac{c_r^2}{3}\cos^3\lambda_b \end{bmatrix}$$

(5.18)

3) for general boom surface with arbitrary reflectivity properties

$$\underline{N_b} = \begin{bmatrix} N_{bx} \\ N_{by} \\ N_{bz} \end{bmatrix} = (1-\epsilon)\,\underline{N_{ba}} + \epsilon \underline{N_{bf}}, \tag{5.19}$$

where

$$B_a=-wr_b(b_r\cos\lambda_b+c_r\sin\lambda_b)\,(l_b^2-l_{bo}^2)$$

$$B_f=-2wr_b(l_b^2-l_{bo}^2)$$

r_b: radius of the cylindrical column boom
l_b: length of the boom
l_{bo}: length of the shadowed boom

$$\lambda_b=\begin{cases}\tan^{-1}\dfrac{c_r}{b_r} & (b_r>0)\\ \tan^{-1}\dfrac{c_r}{b_r}+\pi & (b_r<0)\end{cases}$$

The disturbance force induced by the solar radiation pressure on the subsatellite is written:

1) for both absorbing and reflecting subsatellite surface

$$\underline{F_{sa}}=\begin{bmatrix}F_{sax}\\F_{say}\\F_{saz}\end{bmatrix}=\pi wr_s^2\begin{bmatrix}a_t\\b_t\\c_t\end{bmatrix}=\underline{F_{sf}}=\begin{bmatrix}F_{sfx}\\F_{sfy}\\F_{sfz}\end{bmatrix}, \qquad (5.20)$$

2) for general subsatellite surface with arbitrary reflectivity properties

$$\underline{F_s}=\begin{bmatrix}F_{sx}\\F_{sy}\\F_{sz}\end{bmatrix}=(1-e)\,\underline{F_{sa}}+e\underline{F_{sf}}\,, \qquad (5.21)$$

here r_s is the radius of the spherical subsatellite.

The disturbance torque induced by the solar radiation pressure on the subsatellite about the point O_t is written:

1) for both completely absorbing and reflecting subsatellite surface

$$\underline{N_{sa}} = \begin{bmatrix} N_{sax} \\ N_{say} \\ N_{saz} \end{bmatrix} = l_t w \pi r_s^2 \begin{bmatrix} 0 \\ -c_t \\ b_t \end{bmatrix} = \underline{N_{sf}} = \begin{bmatrix} N_{sfx} \\ N_{sfy} \\ N_{sfz} \end{bmatrix}, \qquad (5.22)$$

2) for general subsatellite surface with arbitrary reflectivity properties

$$\underline{N_s} = \begin{bmatrix} N_{sx} \\ N_{sy} \\ N_{sz} \end{bmatrix} = (1-e)\underline{N_{sa}} + e\underline{N_{sf}}, \qquad (5.23)$$

where l_t: the instantaneous length of the tether

The disturbance force induced by the solar radiation pressure on the tether is:

1) for completely absorbing tether surface

$$\underline{F_{ta}} = \begin{bmatrix} F_{tax} \\ F_{tay} \\ F_{taz} \end{bmatrix} = 2wr_t(b_t\cos\lambda_t + c_t\sin\lambda_t)(l_t - l_{t0}) \begin{bmatrix} a_t \\ b_t \\ c_t \end{bmatrix}, \qquad (5.24)$$

2) for completely reflecting tether surface

$$\underline{F_{tf}} = \begin{bmatrix} F_{tfx} \\ F_{tfy} \\ F_{tfz} \end{bmatrix} = 4w\pi(l_t - l_{t0}) \begin{bmatrix} 0 \\ b_t^2(\cos\lambda_t - \frac{\cos^3\lambda_t}{3}) + \frac{c_t^2}{3}\cos^3\lambda_t + \frac{2}{3}b_t c_t \sin^3\lambda_t \\ \frac{b_t^2}{3}\sin^3\lambda_t + c_t^2(\sin\lambda_t - \frac{\sin^3\lambda_t}{3}) + \frac{2}{3}b_t c_t \cos^3\lambda_t \end{bmatrix}, \qquad (5.25)$$

3) for general tether surface with arbitrary reflectivity properties

$$\underline{F_t} = \begin{bmatrix} F_{tx} \\ F_{ty} \\ F_{tz} \end{bmatrix} = (1-e)\,\underline{F_{ta}} + e\underline{F_{tf}} \,, \tag{5.26}$$

where r_t: the radius of the tether

l_{t0}: the length of the shadowed tether

$$\lambda_t = \begin{cases} \tan^{-1}\dfrac{c_t}{b_t} & (b_t>0) \\ \tan^{-1}\dfrac{c_t}{b_t} + \pi & (b_t<0) \end{cases}$$

The disturbance torque induced by solar radiation pressure on the tether about the point O_t is given by:

1) for completely absorbing tether surface

$$\underline{N_{ta}} = \begin{bmatrix} N_{tax} \\ N_{tay} \\ N_{taz} \end{bmatrix} = 2wr_t(b_t\cos\lambda_t + c_t\sin\lambda_t)(l_t^2 - l_{t0}^2)\begin{bmatrix} 0 \\ -c_t \\ b_t \end{bmatrix} , \tag{5.27}$$

2) for completely reflecting tether surface

$$\underline{N_{tf}} = \begin{bmatrix} N_{tfx} \\ N_{tfy} \\ N_{tfz} \end{bmatrix} = 2wr_t(l_t^2 - l_{t0}^2)\begin{bmatrix} 0 \\ -\dfrac{b_t^2}{3}\sin^3\lambda_t - c_t^2(\sin\lambda_t - \dfrac{\sin^3\lambda_t}{3}) - \dfrac{2}{3}b_tc_t\cos^3\lambda_t \\ b_t^2(\cos\lambda_t - \dfrac{\cos^3\lambda_t}{3}) + \dfrac{c_t^2}{3}\cos^3\lambda_t + \dfrac{2}{3}b_tc_t\sin^3\lambda_t \end{bmatrix}$$

(5.28)

3) for general tether surface with arbitrary reflectivity properties

$$\underline{N_t} = \begin{bmatrix} N_{tx} \\ N_{ty} \\ N_{tz} \end{bmatrix} = (1-\epsilon)\,\underline{N_{ta}} + \epsilon \underline{N_{tf}} \ , \tag{5.29}$$

5.3 Modelling of the System Equations of Motion

Since the above analytical models of the solar radiation disturbance are derived without taking the vibrations of the tether and the shell into consideration, the system equations of motion must also be developed based on this assumption.

Besides, it is known that the roll and yaw motion of the shell as well as the out-of-plane swing motion of the tether are decoupled from the pitch motion of the shell and the in-plane swing motion of the tether in the linear range. [3] Thus, after placing the solar radiation disturbances derived previously into the right hand side of the equation of motion and proceeding with a series of complicated algebraic manipulations, the linear non-dimensional equations for in-plane motion are obtained:

$$\theta'' + K_2\alpha'' - 3\Omega_y^*\theta - k_5 e'_t = \frac{N_{py} + N_{by} + h_x[F_{sv} + F_{tv} - \alpha(F_{sx} + F_{tx})]}{\omega_c^2 J_y^*} \tag{5.30}$$

$$k_1\alpha'' + \theta'' + 3\theta + 3\alpha - k_4 e'_t = \frac{N_{tv} + N_{sv}}{\omega_c^2 (H_{xx} - h_x I_x)} \tag{5.31}$$

$$e''_t + 2(k+\beta_x)\theta' - 3k e_t + 2k\alpha' = 3(k+\beta_x) + \frac{T_x}{l_{tc}\omega_c^2 m_{st}} + \frac{F_{sx} + F_{tx}}{l_{tc}\omega_c^2 m_{st}} \tag{5.32}$$

where

$$m_{st}=m_s+m_t\ ,\qquad k=\frac{m_s+\frac{m_t}{2}}{m_{st}}\ ,\qquad k_1=\frac{H_{xx}}{H_{xx}-I_x h_x}$$

$$k_2=-I_x\frac{h_x}{J_x^*}\ ,\qquad k_4=\frac{2I_x l_{tc}}{H_{xx}-h_x I_x}\ ,\qquad k_5=-2m_{st}h_x\frac{l_{tc}}{J_y^*}$$

$$I_x=\int_{s.t}x\,dm\ ,\qquad H_{xx}=\int_{s.t}x^2\,dm\ ,\qquad J_x^*=J_x$$

$$J_y^*=J_y+h_x^2m_{st}-I_x h_x\ ,\qquad J_z^*=J_z+h_x^2m_{st}-I_x h_x$$

$$\beta_x=-\frac{h_x}{l_{tc}}\ ,\qquad \Omega_y^*=\frac{J_x^*-J_z^*}{J_x^*}$$

and $(\ )'=d(\ )/d\tau$, $(\ )''=d(\ )'/d\tau$, $\tau=\omega t$; $\epsilon_t=\Delta l_t/l_{tc}$, $\Delta l_t=l_t-l_{tc}$

T_x: the tension of the tether

ω_c: the orbital angular velocity

m_s: the mass of the subsatellite

m_t: the mass of the tether

l_{tc}: the command length of the tether

m_{st}: the total mass of the subsatellite and the tether

h_x: coordinate of the length of the boom in the shell reference system

J_x, J_y and J_z are principal moments of inertia of the shell

If we let

$$\Delta f=3\,(k+\beta_x)+\frac{T_x}{l_{tc}\omega_c^2 m_{st}}$$

$$D_\theta = \frac{N_{py} + N_{by} + h_x [F_{sv} + F_{tv} - \alpha (F_{sx} + F_{tx})]}{\omega_c^2 J_y^*}$$

$$D_\alpha = \frac{N_{tv} + N_{sv}}{\omega_c^2 (H_{xx} - h_x I_x)}$$

$$D_e = \frac{F_{sx} + F_{tx}}{l_{tc} \omega_c^2 m_{st}}$$

then the equations of in-plane motion become:

$$k_2 \alpha'' + \theta'' - 3\Omega_y^* \theta - k_5 e'_t = D_\theta \qquad (5.33)$$

$$k_1 \alpha'' + \theta'' + 3\alpha + 3\theta - k_4 e'_t = D_\alpha \qquad (5.34)$$

$$e''_t + 2(k + \beta_x)\theta' + 2k\alpha' - 3k e_t = \Delta f + D_e \qquad (5.35)$$

The system equations of motion can be written in matrix form as:

$$\underline{x}' = A\underline{x} + B\underline{u} + C\underline{D} \qquad (5.36)$$

where

$$\underline{x} = [\theta, \alpha, e, \theta', \alpha', e']^T$$

and

$$A = \begin{bmatrix} O & I \\ A_1 & A_2 \end{bmatrix}, \qquad B = \begin{bmatrix} O \\ B_1 \end{bmatrix}, \qquad B_1 = \begin{bmatrix} 0 \\ 0 \\ 1 \end{bmatrix}$$

It is obvious that if we consider:

$$\underline{u} = \underline{u}_o + \underline{u}_c \,, \qquad \underline{u}_o = \Delta f_o \,, \qquad \underline{u}_c = \Delta f_c \,,$$

and if $\underline{u}_c$ can be found such that

$$B\underline{u}_c+C\underline{D}=O$$

then the system equation (5.36) becomes

$$\underline{x}'=A\underline{x}+B\underline{u}_o=A\underline{x}+B\Delta f_o\ , \tag{5.37}$$

and an all state feedback control law can be constructed:

$$\Delta f_o=-K\underline{x} \tag{5.38}$$

For the system parameters: m_r=10,000 kg, m_s=500 kg, m_t=8.35, l_{tc}=1,000 m, and 80 meter boom, an optimal control $\underline{u}_o$ which minimizes the performance index

$$J=\int_0^{\infty}(\underline{x}^TQ\underline{x}+\underline{u}_o^TR\underline{u}_o)\,dt \tag{5.39}$$

can be found by carefully selecting Q and R.

here $\underline{x}$: state variable

Q: positive semi-definite state penalty matrix

R: positive definite control penalty matrix

Some typical simulation results demonstrate that the transient response with the optimal gains obtained by suitable Q and R has low overshoots, short settling times and rising times.

But the optimal control based only on the use of tether tension can not realize $B\underline{u}_c+C\underline{D}=0$, since only one control exists. Thus, the best way to proceed is to form an optimal compensator:

$$\Delta f_c=-(B^TB)^{-1}B^TC\underline{D} \tag{5.40}$$

Nevertheless, the disturbance D_θ and D_α can not be totally

compensated in this way. Fortunately, the effects of D_θ and D_α are not significant in lower orbit. On the other hand, the in-plane motion of the shell and the tether are coupled with the longitudinal motion of the tether. The system still can be controlled to a satisfactory degree in lower orbit, which can be demonstrated by some numerical simulation results (Fig. 5.7). If the altitude level is increased to approximately 8600 km, it is difficult to maintain the satisfactory pointing accuracy of the shell reflector because of the significant effects of the uncompensated disturbances. Therefore, in order to still control the system in higher orbit with the presence of the solar radiation disturbances, a hybrid control system, i.e. introducing some other kind of actuator on the shell or on the subsatellite, is necessary.

5.4 Numerical Simulations

The numerical simulations are conducted based on the previous assumptions. Since the solar incidence vector expressed in the orbital reference system is a function of the orbital period and the motions of the tethered system are varied periodically for the most part, the disturbance torques induced by the solar radiation pressure are periodic functions; and the period is close to the orbital period, which is demonstrated by the numerical simulation results (see Figs. 5.3, 5.4, 5.5 and 5.6). Comparing Figs. 5.3, 5.4, 5.5 and 5.6, we can easily see that the magnitude of in-plane torques are much larger than those of out-of-plane torques, and the maximum amplitude of the in-plane torques in the completely reflecting case is greater than that in the completely absorbing case. In the completely absorbing case, the torque acting on the subsatellite about the Y_t axis is larger than the torque acting on the shell about the Y_r axis, but vice versa in the completely reflecting case. Therefore, if the solar radiation disturbances are considered, the major disturbances are the in-plane torques acting on the shell and the subsatellite because of the large illuminated

area on the shell and the long moment arm from the center of mass of the whole system to the subsatellite.

From Fig. 5.7, it is noticed that the effects of the solar radiation disturbances are small in the low earth orbit (L.E.O), since the steady state performance of the tethered system controlled by the tether tension with the solar radiation disturbances is almost the same as that without the solar radiation disturbances. But in the high earth orbit (H.E.O), the higher the altitude level is, the worse the performance of the steady state of the tether system (see Fig. 5.8); therefore, the effects can not be neglected, especially, when the altitude level is higher than about 8600 km. This suggests that the attitude and dynamic control law for such a system in a high earth orbit or geosynchronous orbit (G.E.O) should involve some kind of active (actuator) control on the shell or subsatellite.

5.5 Conclusions

Several conclusions can be obtained from the numerical simulation results:

1. The effects of the solar radiation disturbance in lower orbit can be neglected but they are more significant in higher orbits.
2. The tension control law with optimal control gains which are obtained by carefully selecting the state penalty matrix Q and control penalty matrix R is able to maintain the satisfactory pointing accuracy when the altitude is lower than about 8634 km, for a 100 m diameter shell reflector connected to a 1 km tether at the end of an 80 m boom.
3. The maximum magnitude of the solar radiation disturbance torque which disturbs the in-plane motion of the system is larger than that which disturbs the out-of-plane motion of the system.
4. The dominant contribution to the solar disturbance torque is

induced by the solar radiation pressure on the shell reflector or the subsatellite.

5. In the case of a completely absorbing surface, i.e. $\epsilon=0$, the magnitude of the disturbance torque is smaller than that in the case of a completely reflecting surface, i.e. $\epsilon=1$.
6. In the case of a completely absorbing surface, the solar radiation disturbance torque contributed by the subsatellite is greater than that contributed by the reflector shell; and vice versa in the case of a completely reflecting surface.
7. In order to control such a system to a satisfactory degree, a hybrid control law based on both tension modulation and some kind active (actuator) is needed.

References

1. **Misra, A.K.** and **Modi, V.J.**, A Survey on the Dynamics and Control of Tethered Satellite Systems, Tethers in Space, Advances in the Astronautical Sciences, Vol. 62, American Astronautical Society, San Diego, CA 1987, pp.667-719
2. **Rupp, C.C.**, A Tether Tension Control Law for Tethered Subsatellites Deployed Along the Local Vertical, NASA TMX-64963, Sept. 1975.
3. **Liu, L.** and **Bainum, P.M.** Effect of Tether Flexibility on the Tethered Shuttle Subsatellite Stability and Control, Journal of Guidance, Control and Dynamics, Vol. 12, No. 6, Nov.-Dec. 1989, pp.866-873.
4. **Shrivastava, S.K. and Modi, V.J.**, Satellite Attitude Dynamics and Control in the Presence of Environmental Torques --- A Brief Survey, Journal of Guidance, Control and Dynamics, Vol. 6, No. 6, Nov.-Dec. 1983, pp.461-471.
5. **Karymov, A.A.**, Determination of Forces and Moments due to Light Pressure Acting on A body in Motion in Cosmic Space, PMM Vol. 26, No. 5, 1962, pp.867-876.
6. **Bainum, P.M.** and **Krishna, R.**, Control of an Orbiting Flexible Square Platform in the Presence of Solar Radiation, Acta Astronautica, Vol. 12, No. 9, 1985, pp.699-704.

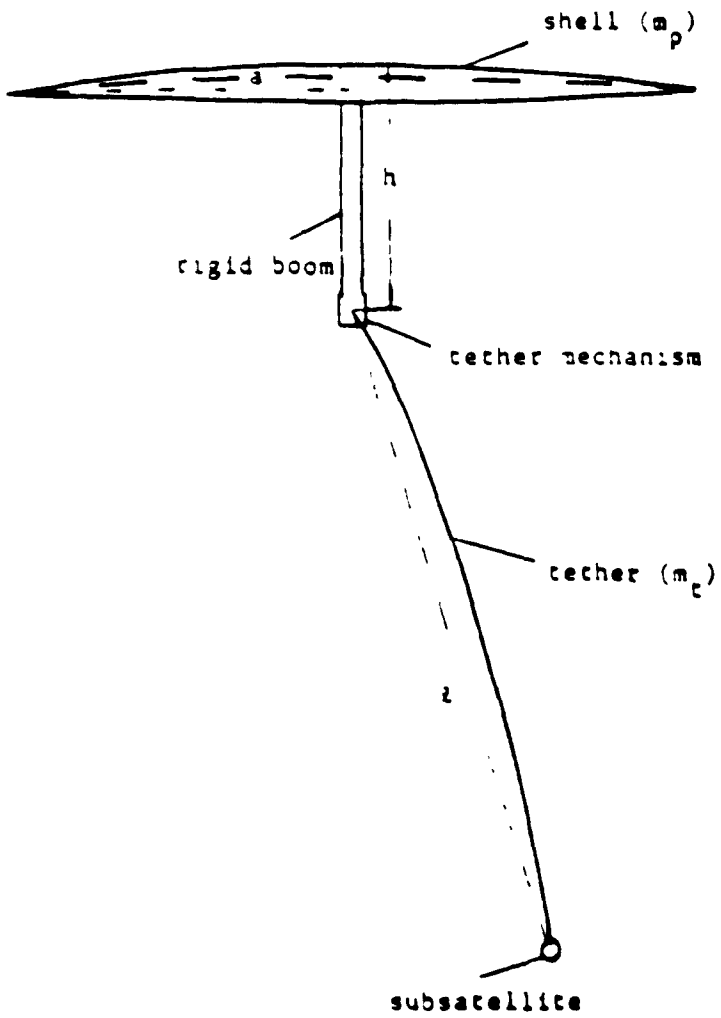

Fig. 5.1 Tethered Antenna/Reflector System

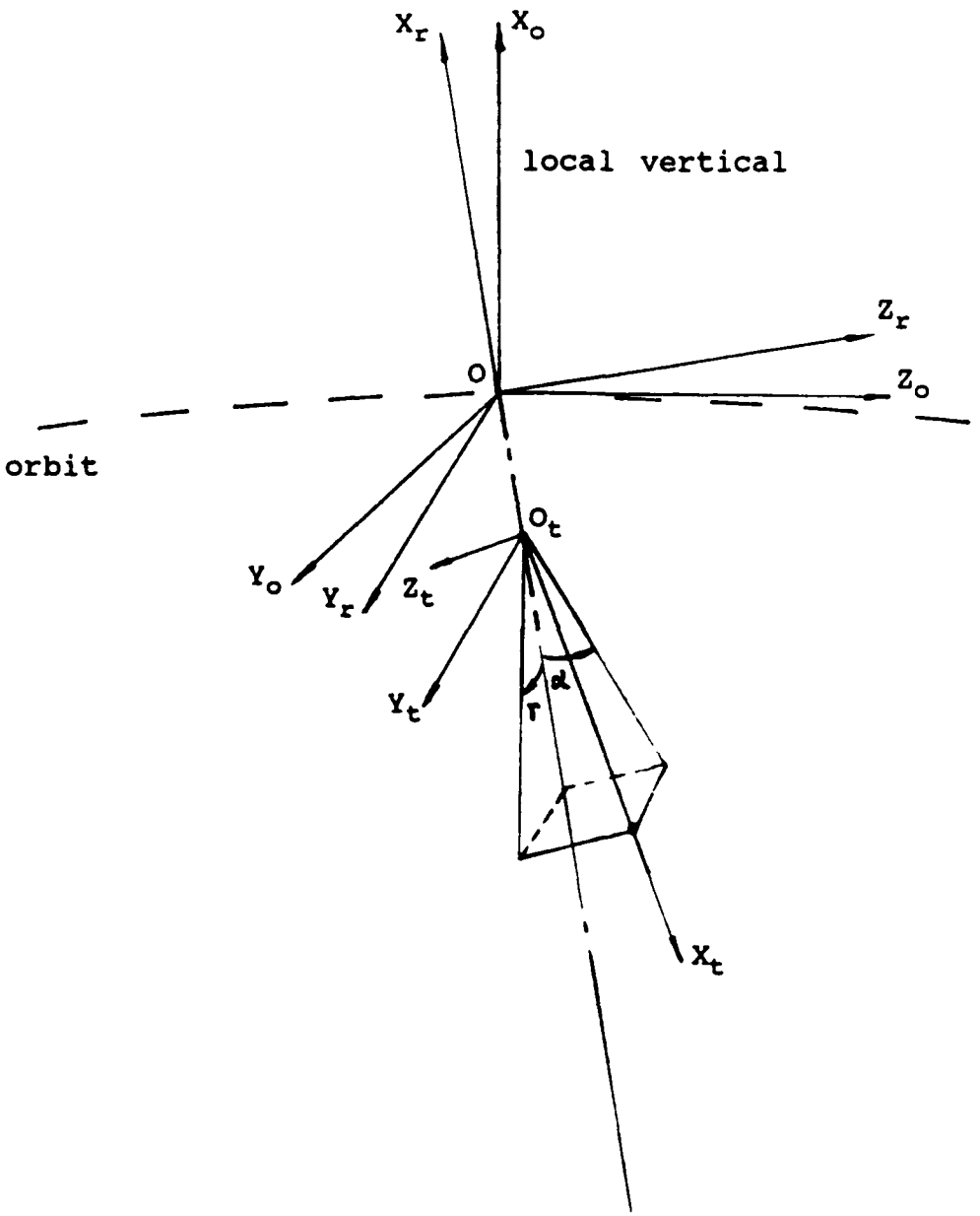

Fig. 5.2 The Coordinate Reference Systems

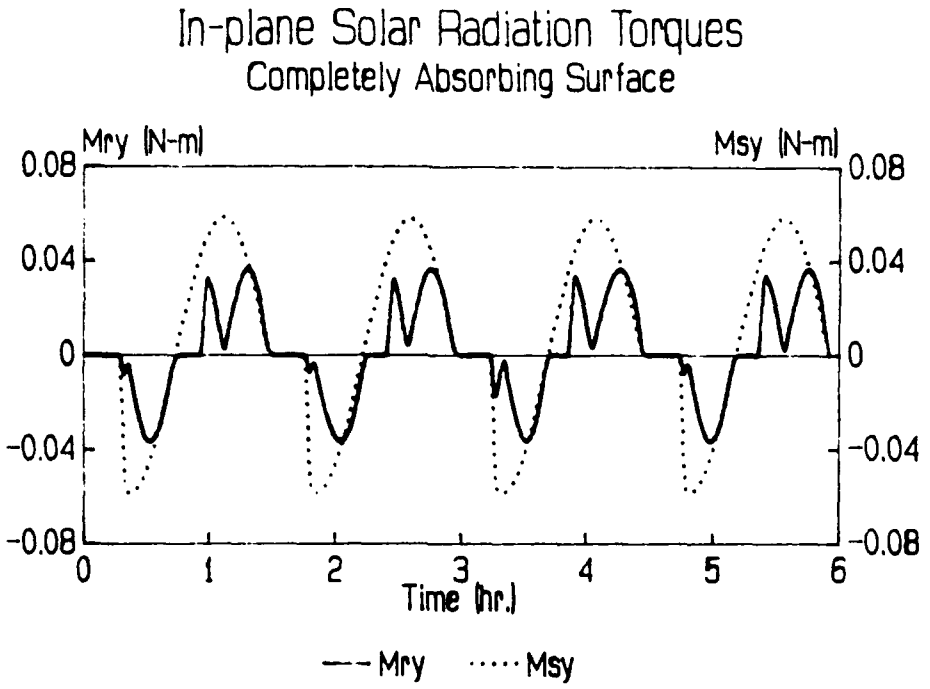

Mry: Torque on Shell about Yr Axis
Msy: Torque on Subsat. about Yt Axis

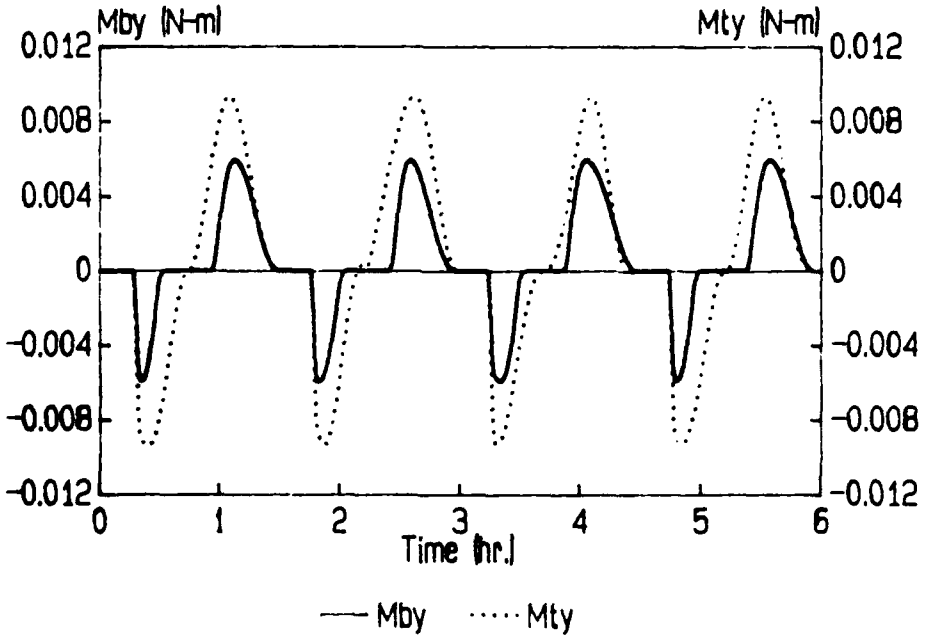

Mby: Torque on Boom about Yr Axis
Mty: Torque on Tether about Yt Axis

Fig. 5.3

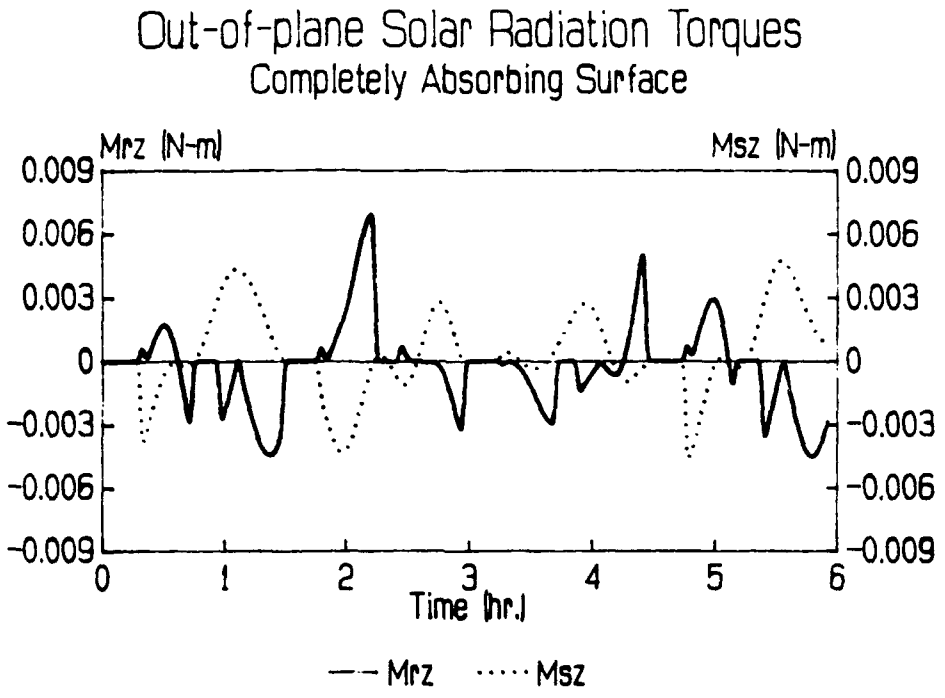

Mrz: Torque on Shell about Zr Axis
Msz: Torque on Subsat. about Yt Axis

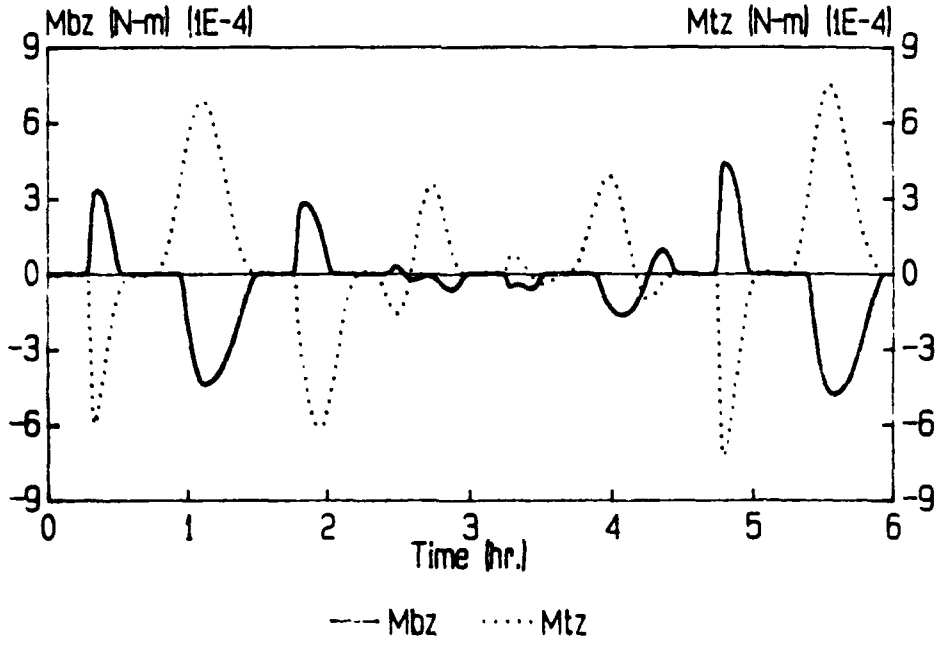

Mbz: Torque on Boom about Zr Axis
Mtz: Torque on Tether about Zt Axis

Fig. 5.4

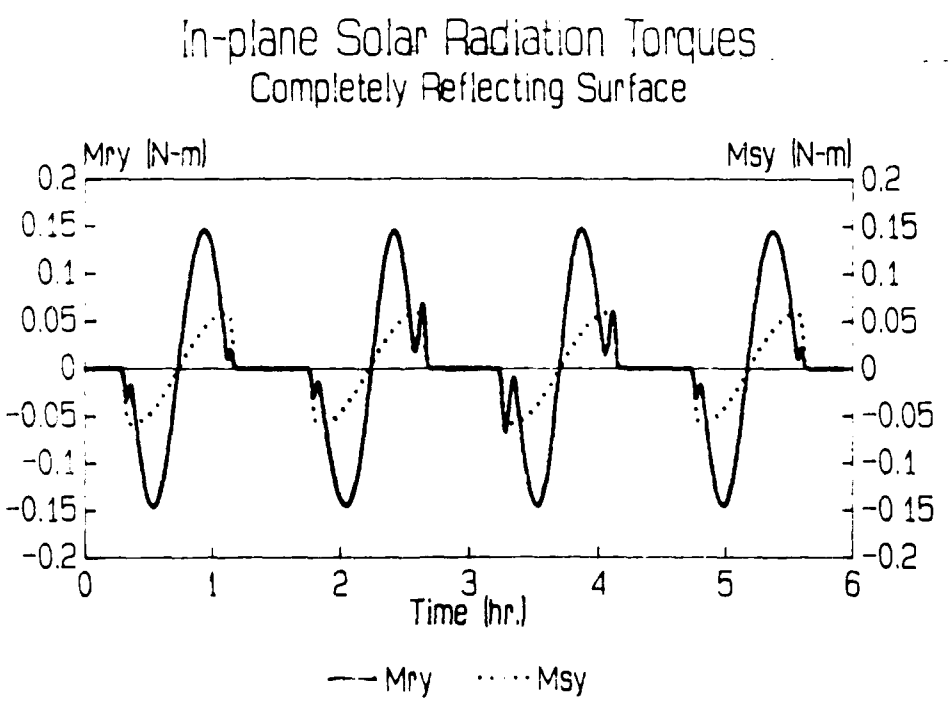

Mry: Torque on Shell about Yr Axis
Msy: Torque on Subsat. about Yt Axis

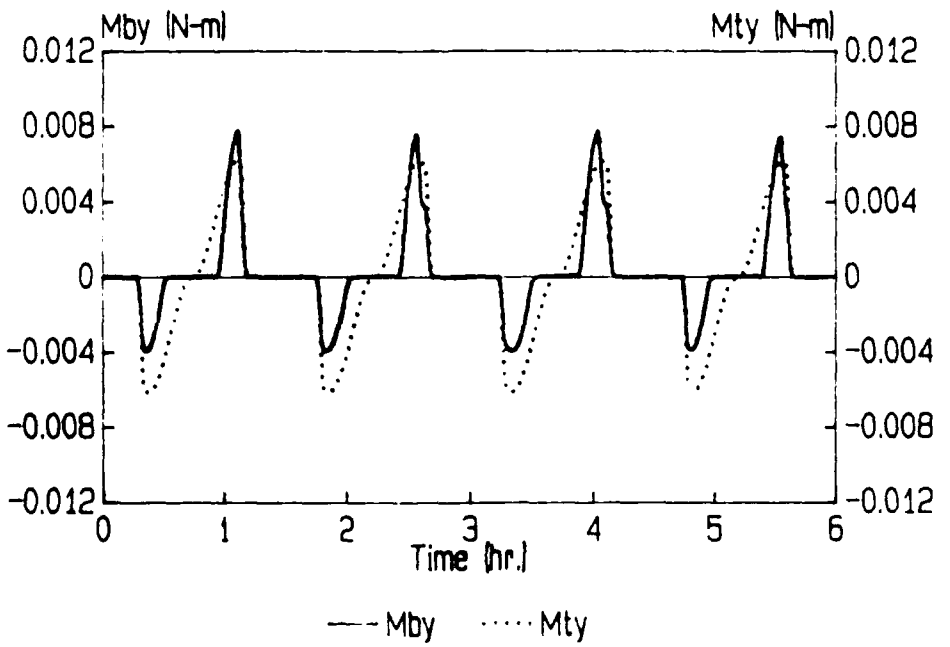

Mby: Torque on Boom about Yr Axis
Mty: Torque on Tether about Yt Axis

Fig. 5.5

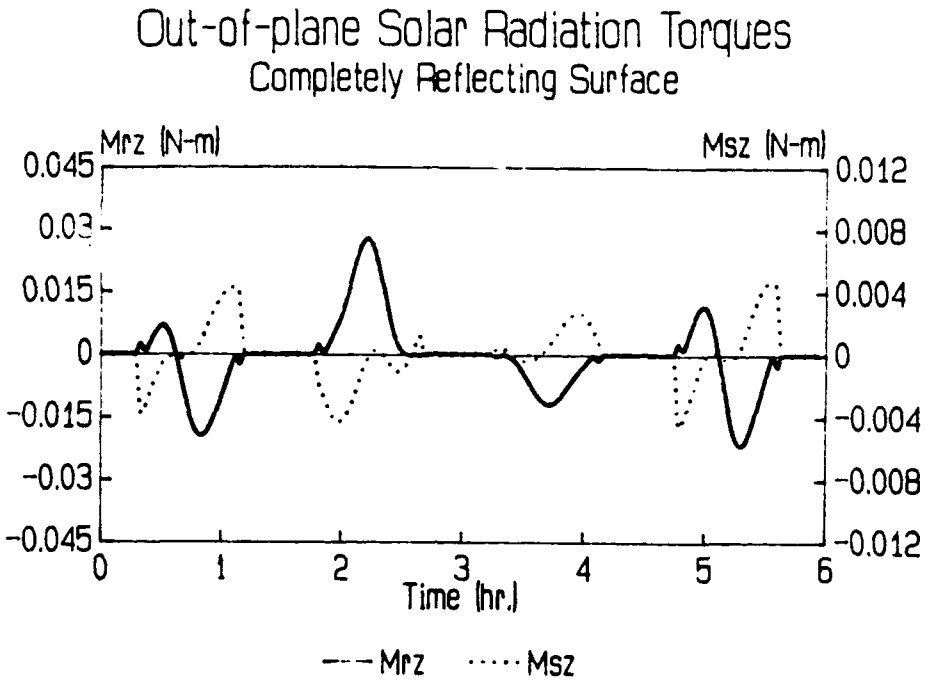

MrZ: Torque on Shell about Zr Axis
Msz: Torque on Subsat. about Zt Axis

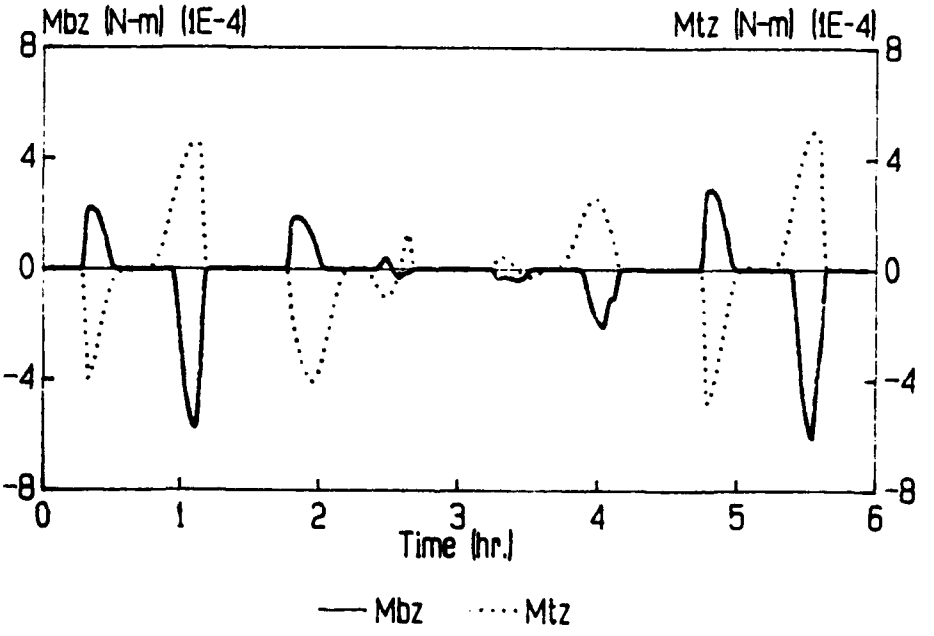

Mbz: Torque on Boom about Zr Axis
Mtz: Torque on Tether about Zt Axis

Fig. 5.6

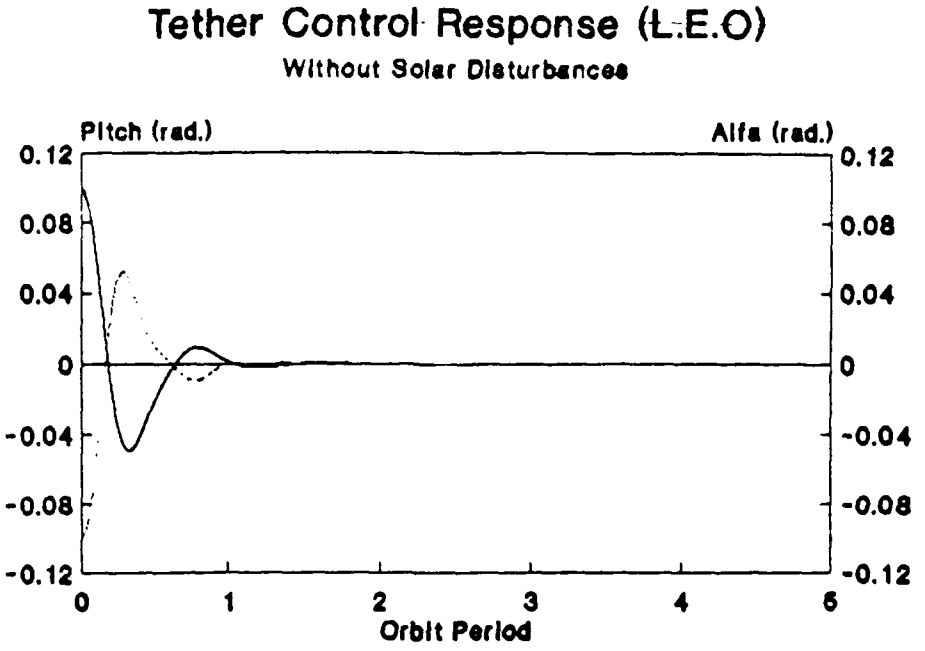

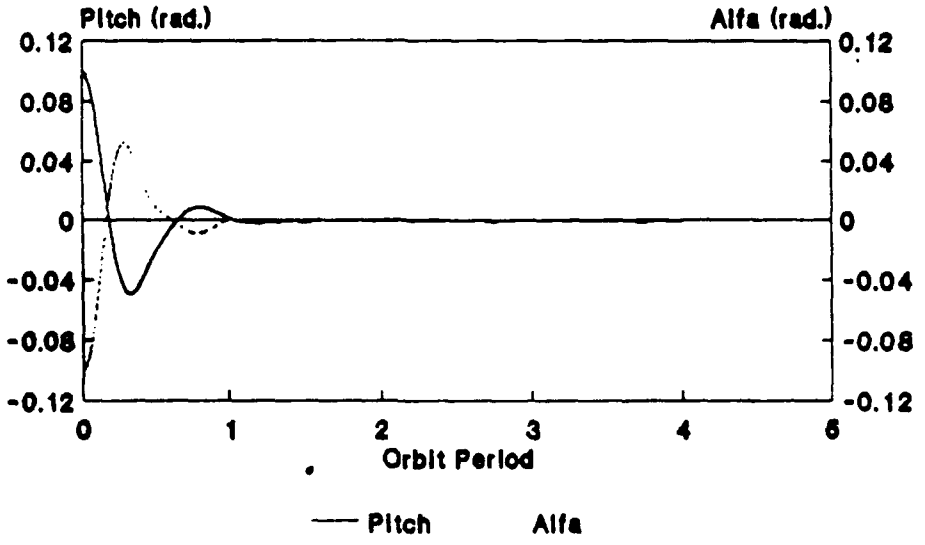

Pitch: In-plane Motion of Shell
Alfa: In-plane Swing Motion of Tether

Fig. 5.7

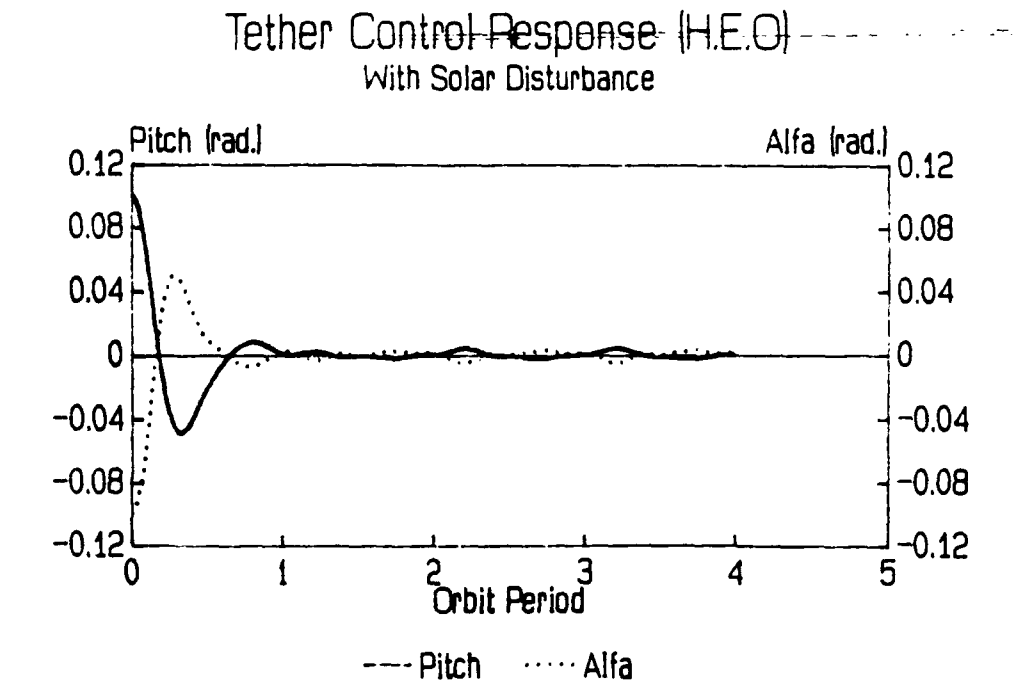

Altitude: 8634.0 km
P=1

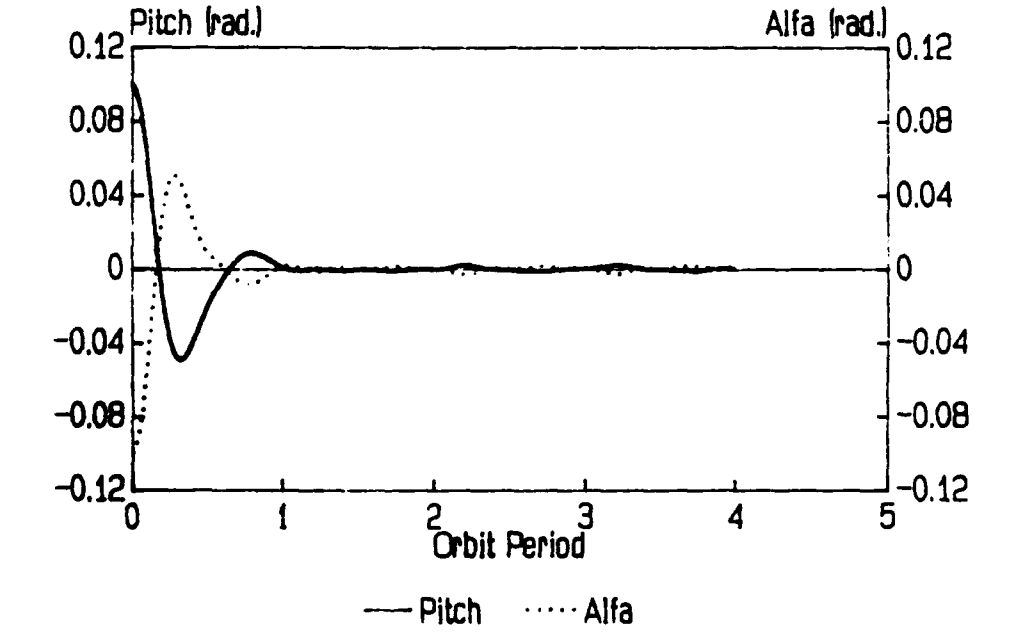

Altitude: 5421.8 km
P=1

Fig. 5.8

6. CONCLUSIONS AND RECOMMENDATIONS

A momentum exchange controller which utilizes the time rate of change of the flexible momentum relative to the rigid body motion as a part of a feedback control law for maneuvering and vibration suppression is proposed and analyzed. For this initial application a model of a rigid hub (base) with cantilevered flexible appendages undergoing a single-axis maneuver is examined. The lower and upper bounds of the control gains for system stability are obtained based on Lyapunov methods. For further vibration suppression an additional independent flexible control system activing on the flexible appendages can be included.

This momentum exchange control technique has also been incorporated in an adaptive feedback control concept for the retrieval of the subsatellite in the orbiting tethered antenna/reflector system. The time rate of change of that part of the angular momentum attributed to the tether motion from the local vertical is used as a part of the feedback law in the antenna attitude control system. This is used in conjunction with an open-loop exponentially decreasing commanded length during retrieval. Numerical simulation results verify the effectiveness of this approach for the suppression of both the antenna and tether in-plane motions at quick retrieval rates.

The optimal linear quadratic Gaussian (LQG) digital control of the orbiting tethered antenna/reflector system is analyzed. In this high order system (up to 40 state components) model the flexibility of both the antenna and the tether are included. With eight point actuators optimally positioned together with tether

tension modulation it is seen that the degree of controllability is very high. A method of measuring tether transverse motions is proposed and is required to guarantee system observability. For such a dynamic system with plant and measurement noises, the LQG technique is effective for designing the best combinations of controller and observer pole locations for the control and estimation processes. The discrete time data system is more practical for the design of a controller based on an on-board computer system.

An analytical formulation of the modelling of the solar radiation disturbance on a class of large tethered antenna/reflector types of orbiting structures has been completed. The effects of this disturbance during station keeping operations have been evaluated based on numerical simulation of the equations of motion. For the large orbiting 100 m. diameter reflector considered and connected to a 1 km. long tether at the end of an 80 m boom, it is seen that the effects of solar radiation in the lower orbits can be neglected. A tether tension modulation control law where the gains are based on the liner quadratic regulator theory is able to maintain satisfactory pointing accuracy when the altitude is lower than 8634 km. The dominant contribution to the solar disturbance torque is induced by the solar radiation pressure acting on the (shell) reflector or on the subsatellite. For the higher altitudes a combination of tether tension modulation together with active (actuator) control will be required.

It is suggested that further research needs to be conducted on the application of the new momentum exchange and compensation

control technique to flexible and telerobotic systems, beginning with a simple two-link manipulator system in two dimensions, followed by an extension to the three dimensional model. As a further application of this concept, the use of a movable rigid boom connected to the Shuttle (or reflector) and through which the tether would be deployed/retrieved should be studied. In order to prove the feasibility of the tethered antenna/reflector subsatellite system, test scale models for in-orbit experiments need to be further studied. The incorporation of the momentum exchange and compensation control technique with the test scale model should be emphasized.

In order to fully implement a control system for the tethered antenna/reflector, the design of a reduced order controller is suggested. Both direct and indirect methods for designing a low order controller which still achieve satisfactory performance and robustness should be considered.

Further investigation of the effects of solar radiation on the tethered antenna/reflector system should concentrate on the related effects of solar heating and the practical implementation of the required control/measurement systems. Measurement of in-plane and out-of-plane angular displacements as well as the relatively small levels of the differential tension required present challenges to the current state-of-the-art capability.

Finally, questions related to the validation of the defensive rapid retargeting results for the reflector system as a three dimensional maneuver can be addressed by disigning some experiments using the ASTREX facility at the Phillips Laboratory as a 3-D

experimental test bed. These experiments would be based on mathematical studies of rapid retargeting slews of the ASTREX configuration, first based on a suitable reduced order model of the flexible ASTREX and an implementation of the application of Pontryagin's maximum principle based on the quasilinearization method for solving the associated two point boundary value problem.